Journal of Sound and Vibration 326 (2009) 1–49

Contents lists available at ScienceDirect

Journal of Sound and Vibration

journal homepage: www.elsevier.com/locate/jsvi

Review

Experimental identification and analytical modelling of human walking forces: Literature review

V. Racic *, A. Pavic [1], J.M.W. Brownjohn [2]

Department of Civil & Structural Engineering, University of Sheffield, Sir Frederick Mappin Building, Sheffield S1 3JD, UK

ARTICLE INFO

Article history:
Received 26 November 2008
Received in revised form
1 April 2009
Accepted 8 April 2009
Handling Editor: C.L. Morfey
Available online 14 May 2009

ABSTRACT

Dynamic forces induced by humans walking change simultaneously in time and space, being random in nature and varying considerably not only between different people but also for a single individual who cannot repeat two identical steps. Since these important aspects of walking forces have not been adequately researched in the past, the corresponding lack of knowledge has reflected badly on the quality of their mathematical models used in vibration assessments of pedestrian structures such as footbridges, staircases and floors. To develop better force models which can be used with more confidence in the structural design, an adequate experimental and analytical approach must be taken to account for their complexity. This paper is the most comprehensive review published to date, of 270 references dealing with different experimental and analytical characterizations of human walking loading.

The source of dynamic human-induced forces is in fact in the body motion. To date, human motion has attracted a lot of interest in many scientific branches, particularly in medical and sports science, bioengineering, robotics, and space flight programs. Other fields include biologists of various kinds, physiologists, anthropologists, computer scientists (graphics and animation), human factors and ergonomists, etc. It resulted in technologically advanced tools that can help understanding the human movement in more detail. Therefore, in addition to traditional direct force measurements utilizing a force plate and an instrumented treadmill, this review also introduces methods for indirect measurement of time-varying records of walking forces via combination of visual motion tracking (imaging) data and known body mass distribution. The review is therefore an interdisciplinary article that bridges the gaps between biomechanics of human gait and civil engineering dynamics.

Finally, the key reason for undertaking this review is the fact that human–structure dynamic interaction and pedestrian synchronization when walking on more or less perceptibly moving structures are increasingly giving serious cause for concern in vibration serviceability design. There is a considerable uncertainty about how excessive structural vibrations modify walking and hence affect pedestrian-induced forces, significantly in many cases. Modelling of this delicate mechanism is one of the challenges that the international civil structural engineering community face nowadays and this review thus provides a step toward understanding better the problem.

* Corresponding author. Tel.: +44 114 222 5727; fax: +44 114 222 5700.
E-mail addresses: v.racic@sheffield.ac.uk (V. Racic), a.pavic@sheffield.ac.uk (A. Pavic), james.brownjohn@sheffield.ac.uk (J.M.W. Brownjohn).
[1] Tel.: +44 114 222 5721; fax: +44 114 222 5700.
[2] Tel.: +44 114 222 5771; fax: +44 114 222 5700.

0022-460X/$ - see front matter © 2009 Elsevier Ltd. All rights reserved.
doi:10.1016/j.jsv.2009.04.020

Contents

1. Introduction

Human-induced vibrations are an increasingly important serviceability and safety issue in modern structural design. Over the past decade, there has been growing interest in the subject, since a number of newly built structures have had difficulties in satisfying vibration serviceability criteria when occupied and dynamically excited by humans, such as footbridges [1], grandstands [2], staircases [3] and open-plan floors [4]. The problems have been caused typically by human occupants performing normal daily activities such as walking, running, jumping, bouncing/bobbing and dancing. The vast majority of the reports on these problems stated that the excessive vibrations were caused by a near resonance of one or more modes of vibration. The reason for this is that the range of natural frequencies of light and slender structures often matches the dominant frequencies of the human-induced dynamic load [5–7]. However, excessive structural vibrations are not necessarily resonant. For instance, in the case of high-frequency floors used to accommodate vibration sensitive facilities, strong vibration response due to people walking typically shows a transient character [8,9]. Such response is induced by high-frequency components of pedestrian dynamic loading generated every time the heel strikes the walking surface [10]. Although generally stiff and massive, high-frequency floors may fail to satisfy stringent vibration serviceability criteria imposed by presence of sensitive equipment such as medical lasers in operation theatres and precision manufacturing facilities.

To this end, there have been numerous attempts to provide reliable and practical descriptions of pedestrian-induced forces by measuring the contact forces between the ground and pedestrian. These are generally known as ground reaction forces (GRFs). Present state-of-the-art GRF measurement facilities typically comprise equipment for direct force measurement, such as a force plate and an instrumented treadmill, mounted on rigid laboratory floor. It has been demonstrated recently that using these measurements to calculate directly structural response under walking humans is justifiable in the case of civil engineering structures which do not vibrate perceptibly under pedestrian-induced excitation [11]. However, when predicting the response of perceptibly vibrating structures, it can (in the majority of cases) be significantly overestimated yielding the predicted degree of liveliness which is unrealistic [11]. This is because the human body is a very sensitive vibration receiver characterized by the innate ability to adapt quickly to almost any type and level of vibration which normally occurs in nature [12]. Moreover, this effective self-adapting mechanism may trigger pedestrians to start changing their way of walking when sensing strong structural vibrations, in order to prevent losing the body balance. The balance control mechanism affects further GRFs [13] leading to the force patterns significantly different from the corresponding rigid-ground measurements [14]. This interdependency between movement of pedestrians and the vibration response of the structure whose motion is perceived is usually referred to as human–structure synchronization. However, as noted by Sachse et al. [15], human–structure synchronization is only one small aspect of a more complex phenomenon of human–structure dynamic interaction influencing human-induced forces. In the context of this review, the human–structure dynamic interaction is associated not only with the forces that excite the structure, but also with the corresponding influence of humans on the dynamic properties of the structure they occupy (i.e. modal mass, damping and stiffness).

The issue of human–structure dynamic interaction is complicated even more by the fact that humans are characterized by huge inter- and intra-subject diversity to induce dynamic loads on structures [16,17]. Inter-subject variability means that differences exist between different people, whereas intra-subject variability applies to the same person performing the same activity at different times (e.g. the difference between two subsequent steps during walking). Although the concept of variability and uncertainty is well developed in structural dynamics disciplines such as wind, wave and earthquake engineering, the stochastic concept is surprisingly underdeveloped in the area of human–structure dynamic interaction where there is a considerable randomness of the key design parameters related to the human-induced dynamic loads and structural dynamic properties. The main reason for this is the sheer complexity of the human-induced loading accompanied by the inability of the state-of-the-art technology to provide their realistic time-varying records under a wide range of conditions. Therefore, the way forward is an alternative experimental approach to studying pedestrian-induced GRFs to account for their complexity.

Human motion and associated internal forces that cause this motion are in fact the key generator of human-induced dynamic forces on structures occupied and dynamically excited by people performing activities such as walking, running, jumping, bouncing, etc. This literature survey reveals that mechanics of human locomotion has been the subject of comprehensive research in the biomechanical community. The heavy investment in such research has resulted in technologically advanced motion tracking systems, such as VICON [18] and CODA [19], that can provide a different approach to the study of human movement and assist in understanding the subject in detail. Moreover, interdisciplinary research has become more popular over recent years, with application of these innovative technologies wherever the human motion analysis has been concerned. Typical examples are the new generation of human gait animations, video game design, aerospace engineering and robotics [18]. Bearing this in mind, this review aims to provide a reader, interested in vibration serviceability problems of civil engineering structures, with a solid theoretical and practical grounding in human movement analysis. In this way, this review forms a basis for discussion of a novel method to utilize 'free field' measurement of human walking forces continuously in time using motion capturing technology. Here, the free field measurement applies the method to examine experimentally walking forces in the real world (i.e. naturally occurring environments) rather than in a constrained laboratory setting, which was the case in vast majority of studies so far.

The literature review contains nine parts. After this foreword, Section 2 aims to introduce basic concepts and terminology in human gait analysis. Sections 3 and 4 present an overview of the current state-of the-art experimental and analytical characterization, respectively, of the dynamic forces induced by humans walking. Section 5 presents the synchronization phenomenon as one of the most important attributes of the human–structure dynamic interaction. Section 6 provides a solid grounding in the basics of techniques to study human bodies in motion. Section 7 describes how the physical parameters of various body parts, such as segmental mass and centre of the mass, can be estimated effectively among the human population. Section 8 integrates knowledge from previous sections to provide a methodology for indirect measurements of the human-induced loading via combination of motion tracking data presented in Section 6 and known mass distribution given in Section 7. Finally, Section 9 summarize the key findings of this review.

2. Basic concepts and terminology in human gait analysis

Gait analysis is a branch of biomechanics that is concerned with the study of locomotion from mechanical perspective [20]. The study includes systematic measurement, description and assessment of quantities that are representative of human motion [21].

Professional organizations, such as the American Academy of Orthotists and Prosthetists Gait Society [22,23] and the North American Society of Gait and Clinical Movement Analysis [24], made first attempts to introduce and define contemporary gait terminology commonly used among investigators. Since the target readers for this review are mainly civil structural engineers, who might not be familiar with such terms and phrases, this section defines terminology essential for understanding biomechanical concepts outlined in the text. For more information, the reader is referred to more detailed texts, such as Inman et al. [25], Perry [26], Rose and Gamble [27] and Whittle [28].

2.1. Walking and gait

Normal human walking can be defined as a gait that humans use at low speeds [28]. A less formal definition is given by the Oxford dictionary, where the gait is defined as a 'way of walking'. Whittle [28] emphasized that the vast majority of investigators, including himself, tend to use the words gait and walking interchangeably. However, the word gait in the literature normally describes the *manner* or style of locomotion, rather than the process of locomotion itself. Therefore, it makes more sense to discuss difference in gait between two individuals than a difference in walking.

2.2. Gait cycle

The gait cycle is the period of time between any two nominally identical events in the walking process [22]. In this review, the term 'cycle duration' or 'cycle time' stands for the length of time that the complete gait cycle lasts. Any event could be marked as the beginning since the gait has to be performed in a particular sequence where cycles follow each other continuously and smoothly. Therefore, the instant at which one foot hits the ground has been generally selected as starting (and completing) event.

The duration of a complete gait cycle is divided into two periods: stance and swing phase (Fig. 1). For each foot, the stance phase, also called the support or contact phase, is when the foot is on the ground. It is initiated with 'heel strike' and ends with 'toe off' of the same foot, constituting approximately 60 percent of the gait cycle. Heel strike (also known as heel contact) is a distinct impact between the heel and the ground at initial contact. Toe off is an event in the gait cycle when the foot leaves the ground. The swing phase lasts from toe off to the next initial contact, constituting approximately the remaining 40 percent of the gait cycle. It denotes the time in which the foot is off the ground, moving through the air when all parts of the foot are in forward progression.

There is a period of time when both feet are in contact with the ground, thus right foot initial contact occurs while the left foot is still on the ground, and vice versa (Fig. 1). This period is known as double support or double limb stance and occurs twice in the gait cycle—at the beginning and end of the stance phase [29]. Both the initial double limb support and the terminal double limb support take up about 10 percent of the gait cycle, or about 20 percent all together. However, this varies with the speed of walking. The duration of double support becomes proportionally shorter as the speed increases [30]. Finally, single support is the period of time when only one foot is in contact with the ground and when the opposite limb is simultaneously in its swing phase.

The stance period can be further divided into five functional sub-phases occurring in the following sequences: initial contact (IC), loading response (LR), midstance (MSt), terminal stance (TSt) and preswing (PSw). Similarly, the swing phase

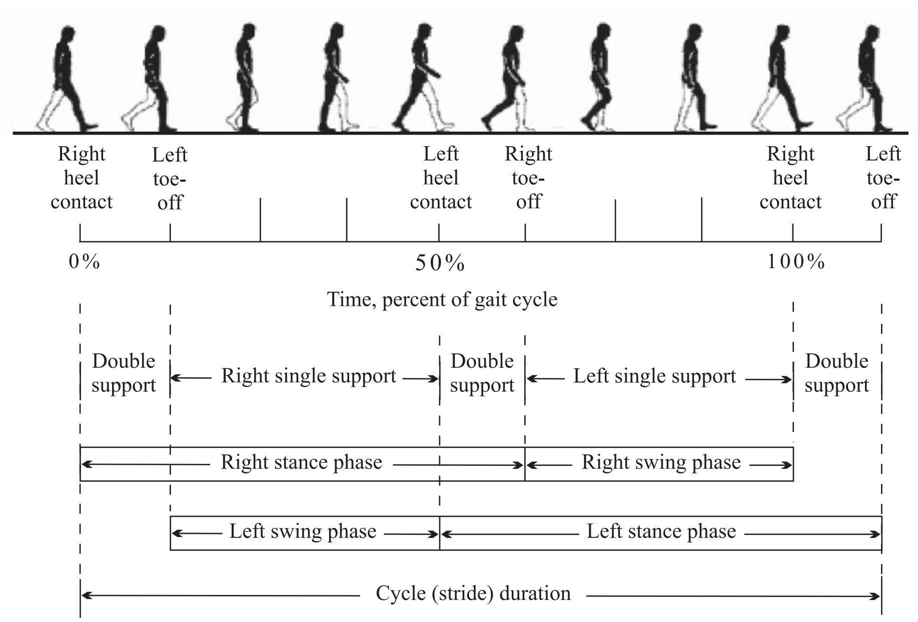

Fig. 1. Gait cycle (after Inman et al. [25]).

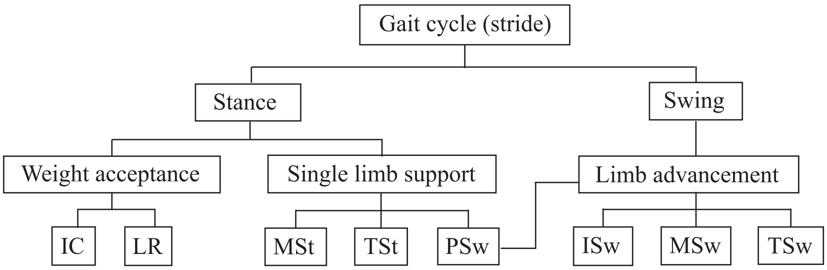

Fig. 2. functional tasks and phases of gait (after Perry [26]).

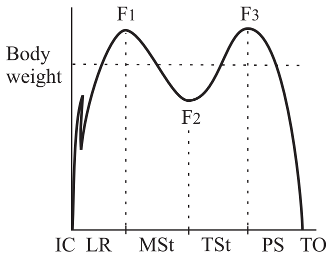

Fig. 3. The vertical force graph can identify with precision all five phases of gait occurring during stance (after Ayyappa [29]).

is broken down into three sub-phases occurring in the following order: initial swing (ISw), mid-swing (MSw) and terminal swing (TSw). An overview of the phases of the gait cycle is given in Fig. 2. Although the PSw is the final stage of the stance, it can be also regarded as preparatory phase for the swing period. Therefore, it is usually considered as an intermediate phase between the stance and swing. Each of these sub-phases enables lower limbs to accomplish the three basic functional tasks of gait: weight acceptance, single-limb support and limb advancement [26]. In the context of this review, the functional tasks of lover limbs during walking are associated with generation of contact forces exerted by pedestrians against the ground i.e. GRFs.

2.3. Generation of ground reaction forces

Initial contact (IC) refers to an instantaneous point in time when the foot hits the ground at the beginning of the contact phase (Fig. 3). Abrupt transfer of body weight to the supporting structure as soon as the heel strikes the ground is the most demanding task in the gait cycle. This causes the foot and leg to act together as shock absorbers [26]. Consequently, the impact force is followed quickly by loading response (LR in Fig. 3). During this phase the foot is in the full contact with the surface and vertical GRF increases to the first maximum F_1 (Fig. 3). Descending the peak of the vertical force–time history reveals the period of midstance (MSt). During midstance the opposite foot is in the mid-swing phase (MSw), so all the body weight is supported by the stance limb alone. It is the period when the foot and relatively straight leg provide a stable platform to vaults over the rest of the body, like an inverted pendulum [29]. It begins when the opposite foot leaves the ground (previously defined as toe off) and continues until body weight is aligned over the ankle, just before heel rise. Heel rise, also known as heel off, is a phase when the heel lifts away from the supporting surface, so the GRF starts increasing once again. The ascending second peak (F_3) of the vertical ground reaction pattern refers to the period of terminal stance (TSt). It begins with heel rise and continues until opposite foot strikes the ground. Finally, the vertical force pattern starts descending to zero in parallel with the preswing (PS) phase and drops to zero at the end of toe off (TO) phase (Fig. 3).

During limb advancement, the stance limb leaves the ground and swings through the air while passing forward ready for the next initial contact. Since swing limb is in the aerial phase, it will affect the GRF indirectly through acceleration of its mass [31]. Section 8 illustrates how this information can be used to provide indirect measurements of human-induced loading on civil engineering structures.

2.4. Spatial and temporal parameters of gait

Parameters used in gait analysis and related to time and space are known as temporal and spatial parameters, respectively. Sometimes, both terms are referred together as time–distance parameters. Typically measured spatial parameters are stride length, step length, and step width, while temporal parameters commonly in use are walking speed and cadence (also known as step frequency).

Stride length is a distance between two successive placements of the same foot in direction of progression during one gait cycle. It is commonly studied as the distance from heel strike of one foot to heel strike of the same foot (Fig. 4). Since stride length is sometimes referred to as cycle length, stride period is actually the same as previously defined the cycle duration or cycle time.

Stride length consists of two step lengths, left and right. Therefore, the step length is the distance between the feet in direction of progression during one step. It is usually measured between two consecutive heel strikes (Fig. 4).

Step width, also known as the stride width, walking base or base of support, is side-to-side distance between the paths taken by the two feet. It is commonly measured at the mid-point of the heels (Fig. 4).

Cadence denotes the number of steps taken in a given time, commonly expressed in steps per minute. In biomechanics, natural or free cadence describes a self selected walking rhythm. Since measurement in steps per minute has not been in accordance with the SI (Sistemé International) units, there is a tendency to replace cadence entirely by the cycle time expressed in seconds. Civil engineers instead of cadence prefer to use the terms pacing rate, and step or walking frequency expressed in Hz.

Walking speed is the rate of motion typically measured in metres per second and is a scalar quantity. When coupled with the information on the direction of walking, a term walking velocity is used [28]. The term free-walking speed describes the normal self-selected walking speed [32]. Moreover, fast walking refers to increased free walking speed. On the other hand, slow walking refers to speeds below the self-selected speed.

2.5. Human motion in 3D space

Descriptions of human motion in space and the relationships between different parts of the body are associated with the standardized anatomical position (Fig. 5), in which a person is standing upright with the feet together and the arms by the side of the body, with the palms facing forward [28].

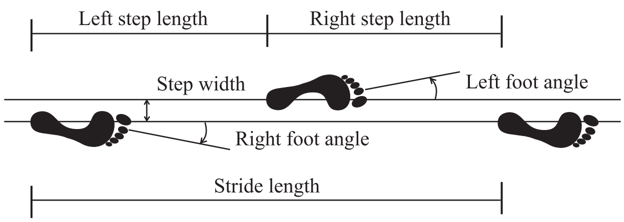

Fig. 4. Spatial parameters of gait (after Vaughan et al. [237]).

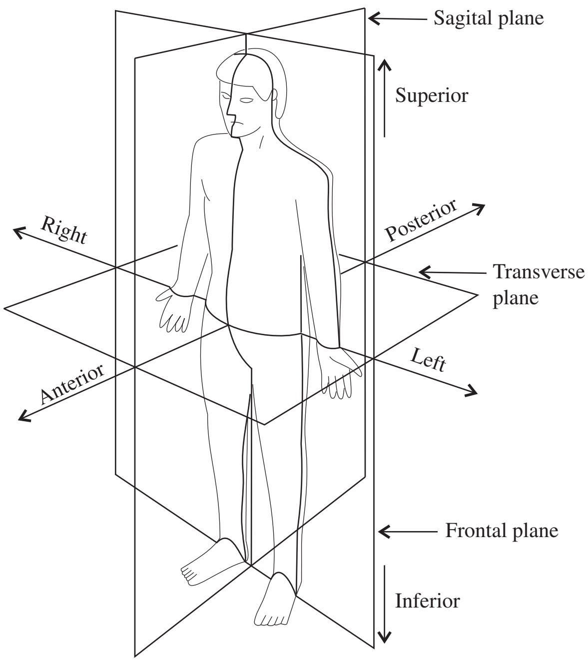

Fig. 5. Anatomical position with three reference planes and six fundamental directions (after Whittle [28]).

When in the anatomical position, the body can be divided by three naturally imposed reference planes, as illustrated in Fig. 5. A sagittal section is any plane corresponding to a side view. Moreover, a midsagittal or median plane divides body into right and left halves. Similarly, the frontal plane, also called the coronal plane, divides a body into front and back portions. A plane which divides a body into upper and lower portions is known as the transverse plane.

Six terms are used to describe the six direction of movement relatively to the body centre (Fig. 5): anterior, posterior, superior, inferior, right and left.

Similarly, four terms are used to explain relations within a single part of the body. 'Medial' defines positions towards, whereas lateral defines positions away from the midsagittal plane. For example, the big toe is on the medial side of the foot and the little toe is on the lateral side of the foot [28]. Proximal means closer to torso (e.g. the shoulder is the proximal part of the arm). Distal denotes further away from the torso (e.g. the elbow is the distal part of the arm). In this way, each body part can be defined with a proximal and distal end.

3. Kinetics

Kinetics is the study of forces that cause motion of objects and systems [28,33]. When investigating issues such as the human–structure dynamic interaction, civil structural engineers are particularly interested in the GRFs. From the civil engineering point of view, these are the forces with which humans dynamically excite structures. On the other hand, equal in magnitude but opposite in direction forces act externally on human bodies. For human movement, biomechanics consider GRFs arguably as the most significant external forces acting on human bodies, which cause the initiation and modification of the movement of the body parts and thus of the whole body [34]. In this context, valuable biomechanical knowledge about kinetics of human motion can contribute significantly to better understanding of the human-induced forces on civil engineering structures.

This section includes discussions of qualitative and quantitative analysis of GRFs through both biomechanical and civil engineering studies. The qualitative analysis provides a detailed description of GRFs, whereas the quantitative analysis refers to technology and procedures for the force data collection.

3.1. Direct force measurements

Early attempts at measuring the load distribution under the feet were mainly qualitative. Beely [35] analysed impressions of feet in plaster during standing, whereas Morton [36] used a kinetograph (an inked fabric and a layer of paper) to display pressure patterns during walking. Inspired by the work of Marey [37] and Amar [38], Fenn [39] invented the first mechanical force plate which could measure walking forces in only anterior–posterior direction. Modern force plates are electronic and, in addition to mechanical, can record amplitudes of the three-component GRF as a subject steps onto the plate during locomotion [40]. Typical shapes of vertical, medial–lateral and anterior posterior projections of walking force vector due to a single footstep are presented in Fig. 6.

One of the first measurements of pedestrian-induced loading by means of a force plate was conducted by Harper et al. [41] with the aim to investigate the friction and slipperiness of a floor surface. Similar single-step force measurements were carried out by other researchers such as Galbraith and Barton [42], Ohlsson [43] and Kerr [44]. Concerning the effect of the contact forces on structures, a comprehensive research relevant to footbridge dynamic excitation was conducted by Wheeler [45] who systematized the work of other researchers related to different modes of human moving from slow walking to running (Fig. 7). He presented dependence of many gait parameters defined in Section 2, such as step length, walking velocity, contact time and peak force as functions of the walking frequency (Fig. 8). Wheeler also noted considerable inter-subject variation of all these parameters. This issue will be discussed more in Section 3.5.

Much research into walking forces has been in the domain of biomechanics as GRF patterns provide useful diagnostics in medical and sports applications [25,26,46]. For this purpose, GRF patterns in all three directions can be characterized by nine distinct points on the force time histories (F_1-F_9), also called force parameters, and their chronological incidences of occurrence (T_1-T_9), as illustrated in Fig. 6. To allow comparison between different individuals, these parameters should be normalized with respect to body weight, and their durations expressed as percentages of the stance phase [47]. Although the mathematical criterion for finding extreme values is applied to determine the force parameters, each point has a physical interpretation in the gait cycle. As explained in Section 2.3, parameters F_1 and F_3 correspond to the absolute maximum force during weight acceptance and push-off phase, respectively, and F_2 refers to the absolute minimum force recorded during the midstance.

Every time the heel hits the ground, a transient impulsive load beneath the foot, generally referred to as a 'shock-wave', is seen as a short spike superimposed on the upslope of the GRF [10], as shown in Fig. 9. Often in gait analysis this peak in vertical GRF pattern is not seen due to low-pass filtering or a small sampling rate [48]. Keeping in mind that this force spike typically lasts 10–20 ms, the sampling rate needs to be high enough (at least 1000 Hz) to record the actual GRF waveform accurately. The magnitude of this impulse typically varies from 0.5 to 1.25 times body weight (BW) and has energy in the frequency range from 10 to 75 Hz [49]. In general, the peak depends on the walking speed, angle at which the foot meets the ground, type of footwear, mechanical properties of the ground surface and even mood of test subject [10]. Since the

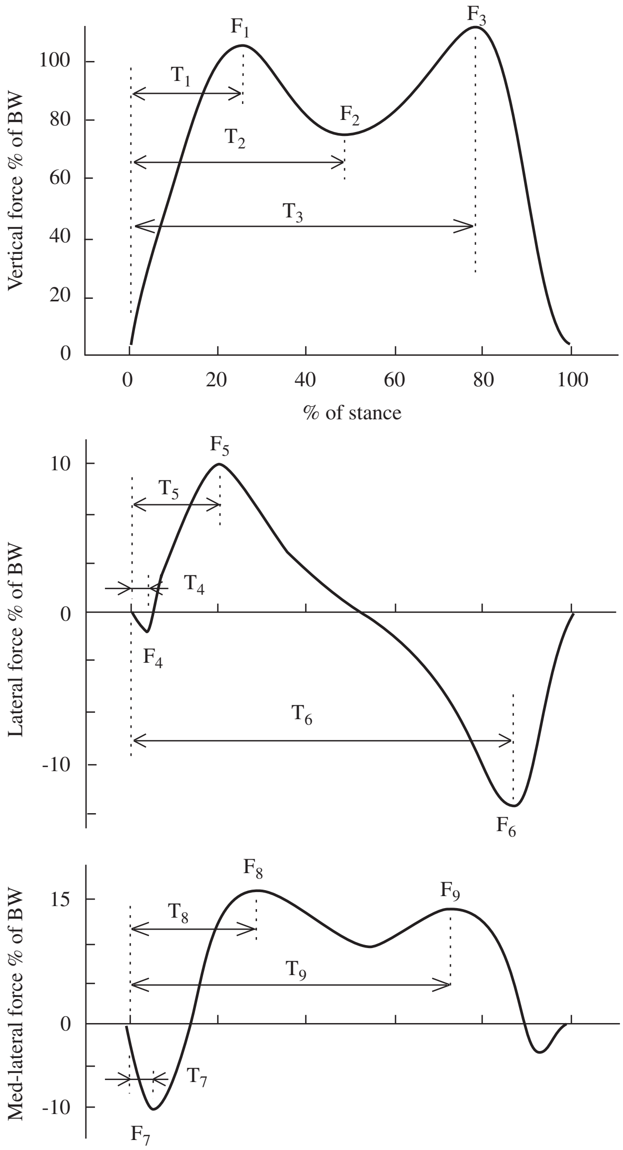

Fig. 6. Typical shapes of walking force in vertical, antero-posterior and medial–lateral direction.

magnitude of heel impact can be significant, its broad frequency content may certainly affect vibration serviceability of high frequency floors [8,9].

As interest in the research of human-induced excitation broadened, measurements of individual step forces were followed by more advanced assessments of continuous walking time histories comprising several consecutive steps. For this purpose Blanchard et al. [50] designed a 'gait machine', whereas Rainer et al. [51] used a continuously measured reaction of a floor strip having known its dynamic properties. More recently, Gard et al. [52] used six individual force plates arranged along the short walkway as illustrated in Fig. 10, which enabled a minimum of three foot strikes (i.e. one stride) to be captured at the fastest walking speeds. However, the assessment of GRF data using floor-mounted force plates is usually time consuming and not best representing the reality. This is because the subjects must control and target their footsteps to land at particular locations so as to allow adequate recordings. This usually means to step only by one foot onto each individual plate [53]. As a result, targeting can affect ability to walk naturally and therefore alter GRF patterns [26]. The multi-unit arrangement also requires considerable laboratory space.

One solution to overcome these drawbacks is to use an instrumented force measuring treadmill (IFMT). It requires less laboratory space and enables quick collection of GRFs during a large number of successive cycles and over a wide range of

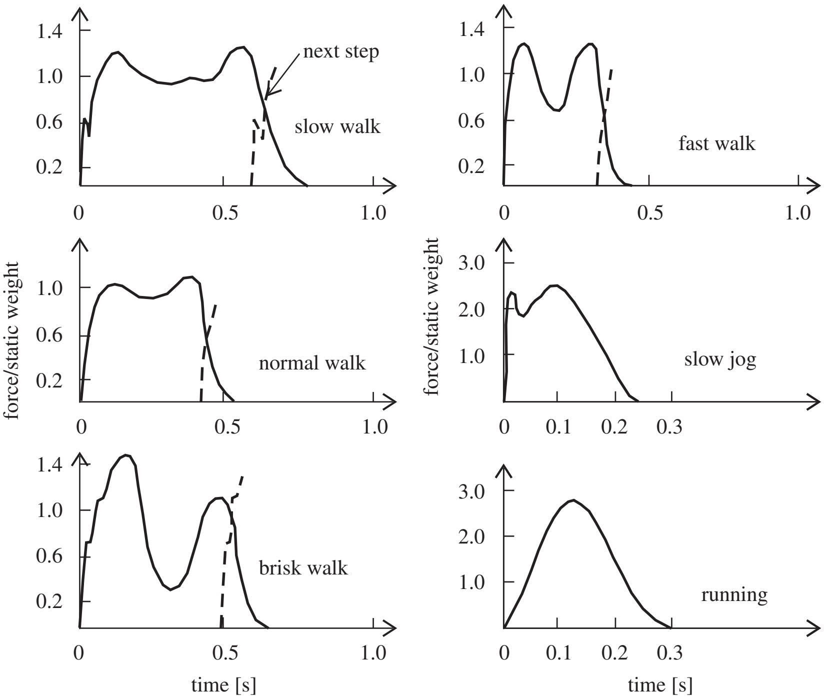

Fig. 7. Typical vertical force patterns for different types of human activities (after Wheeler [45]).

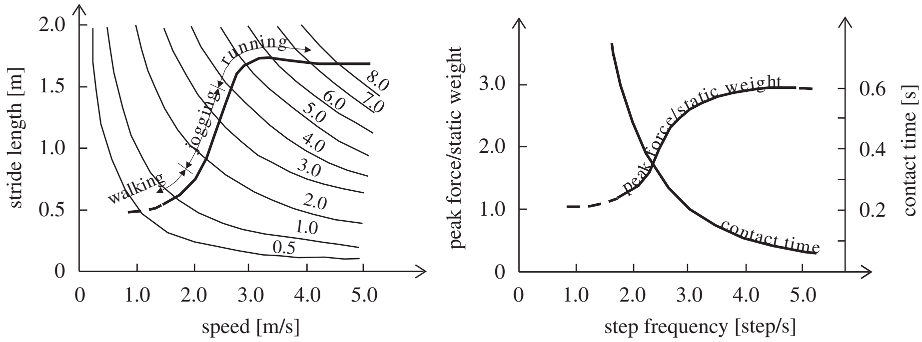

Fig. 8. Dependence of stride length, velocity, peak force and contact time on different pacing rates (after Wheeler [45]).

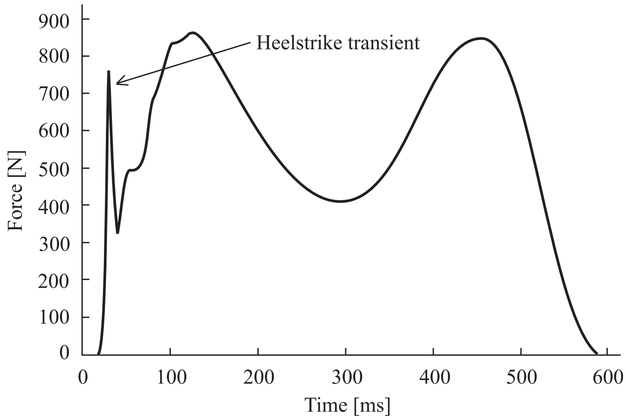

Fig. 9. Vertical component of GRF from normal subject walking barefoot (after Whittle [10]).

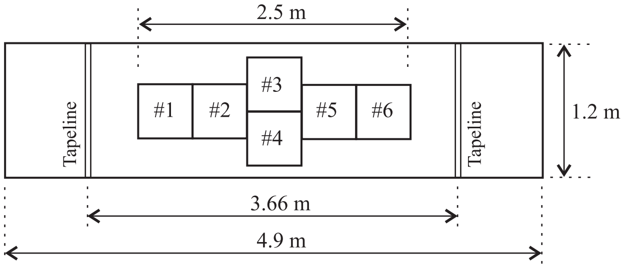

Fig. 10. A combination of six force plates, numbered 1–6, arranged along the walkway to measure several consecutive footsteps (after Grad et al. [52]).

steady-state gait speeds [53]. With such a system, even high-speed running studies can be carried out in very small laboratories [54]. Various designs for IFMT were proposed including mounting a single force plate inside a treadmill [54,55], building a treadmill around multi-plate system [56,57], and mounting a treadmill on top of multiple force transducers [58,59].

Notwithstanding a number of advantages, the treadmill technology has several shortcomings. Although there is no theoretical difference in the physics of treadmill and overground locomotion [60], some experimental studies reported discrepancies between overground and by treadmill measured GRFs [61], as well as with temporal and spatial parameters of gait such as step length and step frequency [62]. In general, treadmill locomotion was found to be less variable [61,62]. The reason for this is constrained speed of movement, controlled by the rotation of the treadmill belt, as opposed to the overground locomotion when the gait speed has no similar control [63]. Interestingly, Van de Putte et al. [64] reported that these differences vanished after only 10 min of practice of treadmill walking by inexperienced treadmill users. The reports on continuous walking forces measured by means of an instrumented treadmill for an application in the civil engineering context are, however, rare and generally incomplete. The most comprehensive data set to-date was collected and presented by Brownjohn et al. [16] to analyse the effect of the force random imperfections on structural response. Unfortunately, their treadmill could measure only vertical GRFs.

Using their advanced treadmill design [57], Riley et al. [65] performed recently a series of experiments to permit more accurate comparisons between treadmill versus overground walking. Contrary to the common belief, they reported that analysis of gait using their treadmill was functionally equivalent to evaluating overground gait. Although it was possible to detect subtle differences in kinematics and kinetics, such differences were generally within the normal variability of the gait and force parameters (see Section 3.5). Differences in the medial–lateral GRF component were attributed to a constraint on foot placement imposed by the narrow treadmill belts, whereas in the anterior–posterior direction discrepancies were associated to small changes in the belt speed. The same authors thereupon emphasized that maintenance of constant belt speed is crucial for reliability of experimental data of this kind.

Other direct methods used by biomechanics researchers to recover GRFs include pressure insoles or instrumented shoes [66,67]. For a subject in locomotion, a number of force sensors fixed to the sole inside a shoe can measure the pressure distributed over a contact area between the shoe's sole and feet at any time during stance phase [40]. A typical shape of the pressure distribution for a subject running is given in Fig. 11. Amplitude of GRF can thus be calculated as area integral of the distributed pressure. Typically, only vertical GRF is reported [68], although several researchers proposed algorithms to determine horizontal forces having measured the vertical pressure distribution [66,67]. The main advantage of pressure insoles is the ability to record GRFs for consecutive steps without imposing constraints on foot placement, such as targeting the footsteps in the case of a force plate or constrained walking speed in the case of a treadmill. However, when compared with a force plate and treadmill data, pressure insoles data universally lack accuracy [69]. To the best knowledge of the authors of this review, the only attempt ever made involving pressure insoles in civil engineering context to measure pedestrian dynamic loads was made during the Millennium Bridge investigation. Unfortunately, it was never publicized in more detail, so it is not clear how successful it was.

For the case of multiple pedestrians, Eriksson [70] tried to measure indirectly the effect of a group of people during walking on low-frequency floors by measuring response of a structure with known dynamic properties. Similarly, Pimentel [71] estimated walking forces due to three uncorrelated people on two lively footbridges in the UK, whereas Fujino et al. [72], Dallard et al. [73] and Dziuba et al. [74] did the same analysis for a pedestrian crowd on the T-bridge in Tokyo, the Millennium Bridge in London and Solferino Bridge in Paris, respectively. Nevertheless, because of difficulties in practical implementation, the procedure has not been further developed. The only known attempt to measure physically dynamic loads from more realistic larger groups of pedestrians walking together was by Ebrahimpour et al. [75,76] who used no more than four test subjects in experiments.

The measured continuous force patterns were invariably near-periodic, indicating their narrow-band nature [16]. However, to simplify analysis and utilization of the measured force–time histories, individual foot-fall traces were often in the past assumed to be identical. This implies that the forces due to continuous walking can be obtained as a succession of these identical single foot traces, resulting in periodic force–time history as illustrated in Fig. 12. However, only by chance a single footfall trial can represent an average performance, but it also might be atypical [77].

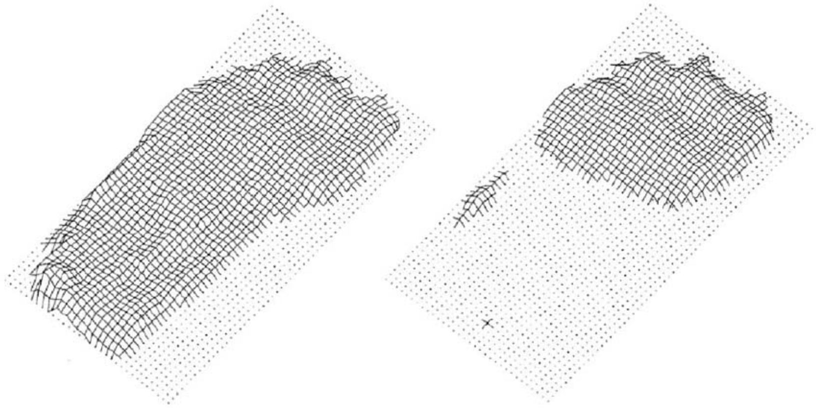

Fig. 11. Pressure patterns from the left foot at different times in the stance phase of running (after Caldwell et al. [40]).

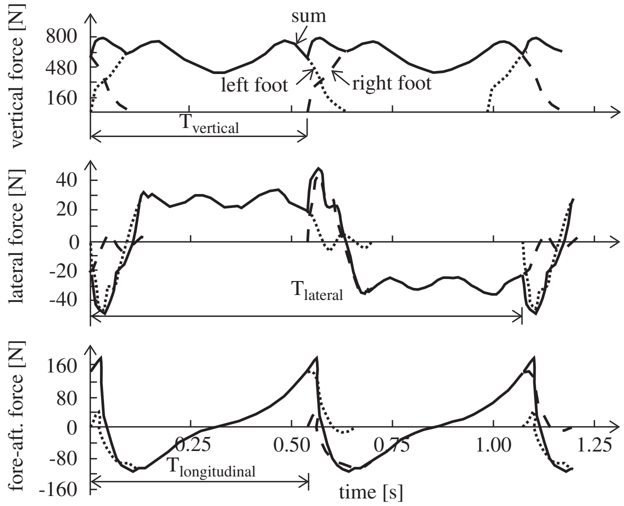

Fig. 12. Periodic walking time histories for GRF patterns in three directions (after Zivanovic et al. [1]).

Here, it should be noticed that the period of medial–lateral force is two times longer than its vertical and anterior–posterior counterparts (Fig. 12). This is because a body makes one full up-and-down cycle during one stride and it takes two strides to make one full left-and-right cycle.

Apart from the lack of the original time-varying force data, the vast majority of studies mentioned so far were carried out using very limited samples of pedestrians and therefore have limited statistical reliability. Recent examples of good quality data indicating clear randomness in the gait parameters data were presented by Pachi and Ji [78], Sahnaci and Kasperski [79], and Zivanovic et al. [80]. Stochastic nature of human walking forces will be discussed in Section 3.5.

3.2. Forces induced on stairs and inclined surfaces

Although the majority of researchers in human-induced forces have investigated GRFs during level walking, only a few studies reported GRF measurements while ascending and descending stairs [44,81–84]. Riener et al. [85] developed a unique instrumented staircase design that allowed collection of three-component GRF data for multiple steps at different staircase inclination. The characteristic double-wave shape of vertical GRF curve was found to change slightly from level walking to climbing the stair, but significantly during the stair descent (Fig. 13). In the latter case, the first maximum produced at the beginning of the loading response (F_1 in Fig. 6) was dominant while the second peak (F_3 in Fig. 6) often was not present [85]. The influence of staircase inclination was, however, relatively small. These findings have been later confirmed in a similar study by Stacoff et al. [86]. When compared with level walking, the amplitudes of the

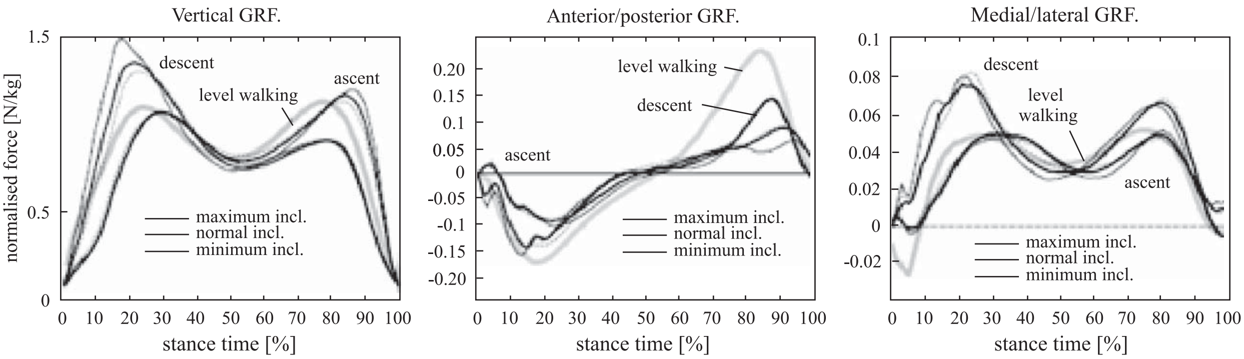

Fig. 13. GRF during accent and descent at minimum, normal and maximum inclinations and during level walking averaged over 10 subjects. Curves are normalized to 100 percent of stance time and force amplitudes to body weight (after Riener et al. [85]).

anterior–posterior forces were considerably smaller during stair walking (Fig. 13). Conversely, forces in medial–lateral direction exhibited higher amplitudes during stair descent, and only slight changes during stair accent.

Further, Stacoff et al. [86] found age to be an important factor which should be considered when analysing human loading on staircases. In his experiments the young age group walked faster and produced larger vertical GRF maxima during level walking and on stair ascent than the middle and old age group.

Studies on slope walking reported that GRF pattern during ascent and descent preserved most of the features observed during level walking. However, surface inclination affected significantly amplitudes of the force parameters in Fig. 6 [87,88]. These changes were unlike those for ascending and descending stairs previously discussed [44,81–84]. When compared with level walking, the magnitude of the first peak in the vertical direction (F_1 in Fig. 6) increased as the angle of incline increased for both up and down walking [88]. There was little change in the magnitude of the second peak (F_3 in Fig. 6) while walking downhill, but there was a significant increase while walking uphill. Medial–lateral force amplitudes were considerably higher for inclined surfaces. When compared with the changes in the other two directions, the anterior–posterior component increased most markedly from the horizontal to slope walking. This was independent from walking direction and walkway inclination. The higher force magnitudes parallel to the direction of walking may be perhaps attributed to the friction of the shoe-ground interface needed to prevent slipping [88].

3.3. Forces induced on flexible structures

All measurements of the walking forces mentioned so far were obtained on rigid surfaces, such as a floor-mounted force plate, the gait machine or an instrumented treadmill. To study lateral pedestrian loads on perceptibly moving footbridges, Pizzimenti and Ricciardelli [89] used an instrumented treadmill device vibrating in the lateral direction with prescribed amplitude and frequency. Similarly, in his doctoral thesis Rönnquist [90] measured lateral walking forces induced by people walking across a suspended platform. Both studies observed that the amplitude of the horizontal walking force remained unchanged in the case of small vibration amplitude, indicating weak interaction between pedestrian and the structure. However, for larger amplitudes of vibration, they observed that when the frequency of lateral vibrations of the structure approached the pacing rate, much stronger interaction took place. Thereupon, amplitudes of the horizontal walking force increased. Unfortunately, current understanding of the human–structure dynamic interaction phenomenon is insufficient to clarify the issue. More examples of actual measurements of lateral walking forces generated on slender structures prone to human-induced vibrations will be given later in Section 5.

Experimental studies on the vertical walking forces induced on flexible structures are very rare and limited. However, McMahon and Greene [91] investigated the effect of surface stiffness on mechanics of running. Their work showed that decrease in surface stiffness resulted in decrease in a runner's metabolic rate and decrease in the vertical GRF, but without affecting running support mechanics. These results indicated that flexible surfaces enhanced a runner's performance, hence made running easier. On the other hand, observations of pedestrian behaviour while crossing real full-scaled footbridges suggested that perceptible vertical movements of the deck made walking very difficult [11,71]. However, this suggestion was made without much justification. Yao et al. [92] also found it impossible to jump at (or very near) the natural frequency of a structure that moves significantly. As the human-induced vibrations increased, feet–structure contact time simultaneously increased, so the body motion became more bouncing-like than jumping. Moreover, the directly measured force magnitude experienced a drop around the regions in which significant resonant, or near resonant, excitation occurred. Biomechanical research on jumping provided a further proof of higher human-induced forces on stiffer structures [93]. However, similar tests on the vertical walking force are not known. Alternatively, Ohlsson [43] was interested more in the frequency content than in the exact time history of the pedestrian loading. He compared the spectra of vertical walking forces measured on a rigid surface and measured on a flexible timber floor. The force amplitude spectra reduced significantly around the natural frequency of the structure, showing the same feature as the time history of resonant jumping force reported by Yao et al. [92]. This significant drop in the force amplitude might have also been caused by the human–structure dynamic interaction, however, no evidence was presented to support this idea.

3.4. Ground reaction forces under various conditions

Numerous studies have demonstrated the complex nature of human-induced dynamic forces and their dependence of many external factors, such as a subject body mass [94], mechanical properties of surface [95], foot-ground contact area and foot landing position [96], texture and stiffness of footwear [97–99], gait style [100], and variations in the temporal and spatial parameters of gait [101]. Of the many factors that influence GRF, gait speed was the central focus of many investigations [102,103]. For instance, Galbraith and Barton [42] measured a single step vertical force on a floor-mounted force plate, ranging from slow walking to running. GRF records showed that the shape of running force had one peak and therefore differed from the characteristic double-peak shape of the walking force (Fig. 14). They also noticed that increasing subject weight and step frequency led to higher peak amplitudes of the force. However, the force was not dependant on type of the footwear and walking surface. Further, Galbraith and Barton [42] shifted individual foot forces in time, assumed to be identical, to obtain artificially continuous walking or running force–time history (Fig. 14). As explained in Section 2.2, during double support phase, walking forces under the left and right foot overlap (Fig. 14-right). On the other hand, when increasing walking speed, the double support period steadily decreases and finally disappears when the subject starts jogging or running (Fig. 14-left). As a result, the load–time record changes into a series of single-peak pulses in quick succession, separated by zero-force periods which correspond to the aerial (i.e. ‘flying’) phase.

Although all mentioned studies claimed consistently that the amplitude of the vertical GRF increases for greater gait speed, they were generally limited to a narrow range of examined walking or running speeds and/or small number of male subjects. Conversely, Keller et al. [104] made an exception and collected over 1100 vertical GRF–time histories for walking, slow jogging and running over a wide range of speeds from 1.5 to 8 m/s. The results of this study on 13 men and 10 women indicated that the maximum vertical GRF (F_z) increased linearly with gait speed up to about 3.5 m/s (Fig. 15), which is approximately 60 percent of the subjects’ maximum speed [104]. Moreover, they developed a linear regression equation for F_z normalized by body weight and expressed as a function of walking and running speed v (m/s) over the range of 1.5–3.5 m/s:

$$F_z = 0.614v + 0.208 \tag{1}$$

At higher walking speeds ($v > 3.5$ m/s), maximum vertical forces were constant at approximately 2.5 times body weight. Male and female subjects had similar values for the F_z at all the speeds examined (Fig. 15), so the linear regression was established for both groups together. Moreover, slow jogging, characterized by more bouncy running style, produced vertical forces as much as 1.6 times greater than normal walking at the same speed or running at higher speeds [104]. Gait style, therefore, appears to be a particularly important determinant of the peak amplitude of vertical GRF.

Due to the intra-subject variability, the walking force parameters (Fig. 6) are not constants but fluctuate with time and change from one stride to the next [16]. Following section therefore reviews studies on the appropriate number of trials (i.e. records) to establish a stable mean and reliability of these parameters.

3.5. Variability and stability of ground reaction forces

By the very nature of human beings who come in all shape and sizes, variability is associated with all types of human activities across repeated trials, such as walking, running, bouncing/bobbing and jumping [105]. Broadly speaking, the

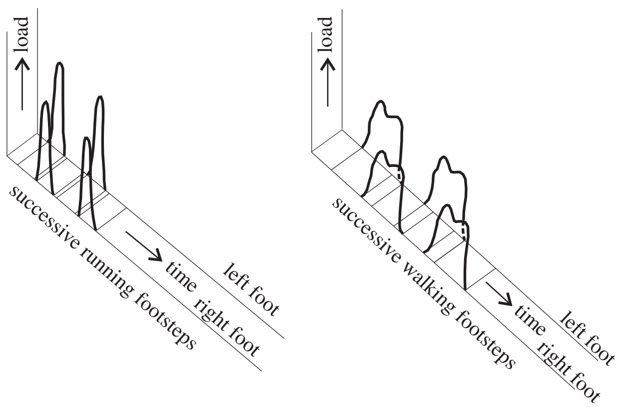

Fig. 14. 3D vertical GRF patterns for walking and running (after Galbraith and Barton [42]).

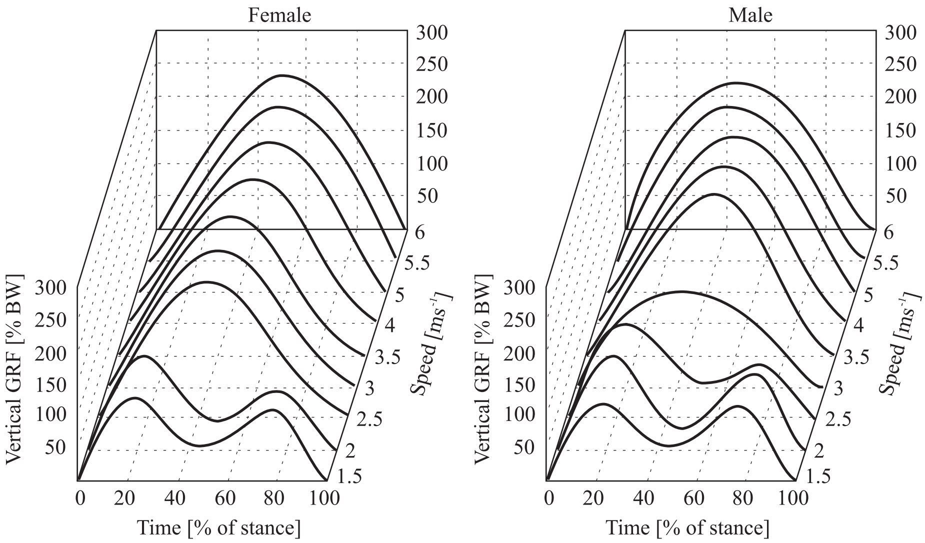

Fig. 15. Vertical GRF patterns as function of gait speed, expressed in percent of stance time (after Keller et al. [104]).

study of walking force variability is the analysis of fluctuations in GRF parameters, such as peak amplitudes and timing [106]. On the other hand, the study of stability of a force variable examines the repeatability of that variable across multiple trials i.e. observed performances over time [77]. Finally, the degree of the stability and consistency of data measured is usually referred to as reliability [103].

Past investigators have used a number of methods to quantify and report on the variability, stability and reliability of the gait data both within a single day and between several days [58,107–109], and for consecutive [58,109] and non-consecutive trials [107,108]. Because of its simplicity, a coefficient of variation CoV (standard deviation divided by mean) is widely accepted in the biomechanical community when estimating variability of GRF data. A value for the CoV of <12.5 percent is usually considered as acceptable level of variability for experimental data of this type [110]. Some researchers [111] prefer a more conservative value of 10 percent. However, the CoV cannot separate the contribution of two or more factors to the variability in GRFs, such as pacing rates and force peak amplitudes. To accomplish this, n-way ANOVA statistical analysis can be used [112], where n represents the number of the factors. On the other hand, stability of a force variable (also called repeatability) can be evaluated using test–retest reliability methods, such as the sequential averaging technique [103] and a more traditional intra-class correlation [113].

The repeatability of a variable across trials influences the stability of the mean value of the group of trials. When the mean value is not stable, both the reliability of the mean and its ability to represent a more generalized performance are limited [77]. The number of trials obtained from an individual in an experiment is thought to influence stability of the mean [114] and therefore is an important methodological consideration in the design of walking loading experiments. The next two sections review this subject in more detail.

3.5.1. Force plate measurements

In the case of force plate measurements, GRF data assessment typically requires a subject to step on a force plate whilst walking, providing only a single footfall record [115]. There is thus concern regarding the ability of a force plate to detect natural variability of human-induced forces and represent the individual's long-term performance [77]. Greater gait variability results in greater likelihood of sampling an atypical GRF pattern from the population of all possible patterns. Except for unique circumstances (e.g. a single trial is the subject of interest) several trials are thought to provide a more stable and representative mean value [77]. A sample size must be large enough to estimate reliably the subject's true performance within acceptable limits [105]. While increasing the number of trials is commonly thought to increase performance stability [114], there is a question of how many trials are necessary to provide stable data [109]. Previous investigations of the variability suggested the use of a mean value calculated from three trials per block [110] to 20 trials per block [102]. Winter [107] estimated the variability of the vertical and anterior–posterior force components for a test subject over three days. The CoV over nine trials was 7 and 20 percent for the vertical and anterior–posterior force, respectively. Kadaba et al. [108] assessed 40 adult subjects walking at self-selected speeds and tested three times on each of three separate days. They showed that the vertical and anterior–posterior reaction force were more repeatable than the medial–lateral force. In a comprehensive study of 20 subjects (10 males and 10 females), Hamill and McNiven [103] examined reliability and stability of the walking force parameters (Fig. 6) over 20 trials carried out during a single and over several days. They found that an adequate protocol for the investigation of GRF parameters during walking should include at least 10 trials per block of measurements with several preliminary trials prior to the actual data collection. The lack of statistically significant differences between blocks carried out on the same day or on different days indicated intraday and interday consistency of the GRF data. Therefore, the GRF parameters may be collected at different times during one day or over several days and remain stable. By comparison, De Vita and Bates [105] revealed that tests may have to be repeated 25 times to ensure reproducibility of running forces, whereas Rodano and Squadrone [116] stated that at least 12 trials are needed to establish stable data in jumping.

Using harmonic analysis, Giakas and Baltzopoulos [111] showed that frequency content of walking loading measured over 10 trials has acceptable limits of variability. CoV for all amplitudes in the force spectra was <10 percent. Their results in the time domain were generally in agreement with the studies mentioned above, but they observed less variation in the medial–lateral force. However, different studies have used either different criteria or different methods for determining stability of GRF data, making comparisons between studies difficult.

Finally, Grabiner et al. [117] investigated the effect of visual guidance on GRF variability and reported some unexpected results. They observed that targeting the force plate does not reflect on the GRF variability, although it can alter the overall GRF pattern as shown previously in Section 3.1.

3.5.2. *Instrumented treadmill measurements*

Compared to a single force plate, treadmill technology allows analysis of stride-to-stride variations for many consecutive cycles over a long period of time. The test protocol usually requires 1 or 2 min of walking measurements depending on the aims of the experiment. Typically between 20 and 120 successful steps can be recorded, making any statistical comparison powerful [118]. In the study by Riley et al. [65], test subjects were first allowed to adjust themselves to the treadmill walking and then only 30 s trials were captured. However, this protocol was repeated three times for each subject in order to assess the repeatability of measurements. Moreover, each of the 26 participants considered themselves to be experienced treadmill users. As already mentioned in Section 3.1, for inexperienced test subjects a maximum 10 min 'warm-up' is enough for pre-test habituation to treadmill walking [64]. For running speeds, Belli et al. [58] reported that treadmill measurements should be performed on at least 32–64 consecutive steps, which corresponds to about 15–20 s of running necessary to reach a stable mean data.

There are few studies that have addressed the minimization of variability in the spatial and temporal parameters of gait. This is generally known as optimization [119]. Yamasaki et al. [120] reported that the variability of step length was minimum at the self-selected (also called usual, preferable or comfortable) walking speeds during the treadmill locomotion. The same result was later confirmed by Sekiya et al. [121] who studied over-ground walking. However, similar research on human-induced loading is found to be quite limited. Masani et al. [122] found a speed dependency for GRF variability during treadmill walking in relation to different constant speeds. For vertical (F_z) and medial–lateral direction (F_x), there was an increasing trend in variability with increasing the speed from 3 to 8 km/h (Fig. 16). On the other hand,

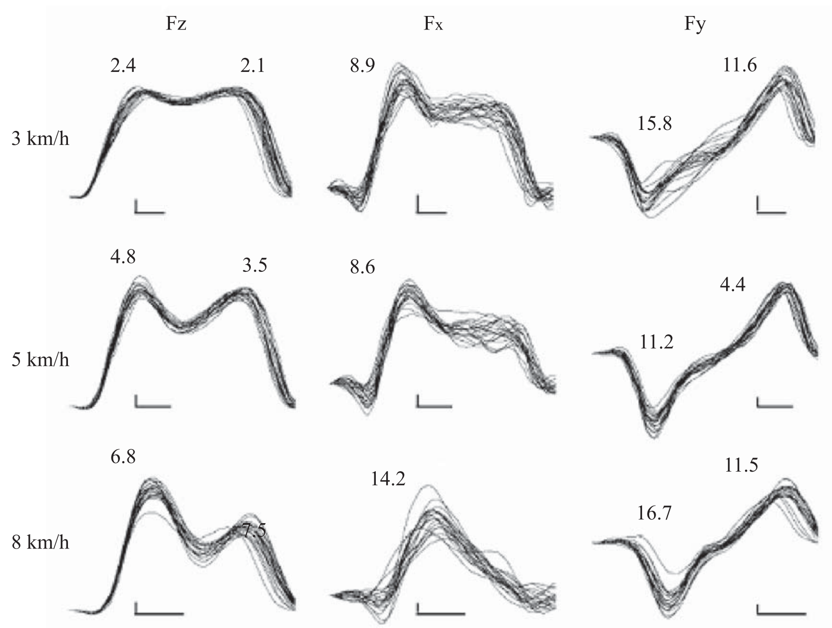

Fig. 16. Qualitative visualization of GRF variability. Twenty GRF curves from one subject for right leg at three different speeds are superimposed on each graph. Numbers near each peak indicate the coefficient of variation (CV) in percent for corresponding force parameter (after Masani et al. [122]).

there was a speed at which the variability of GRF was minimum for anterior–posterior direction (F_y). It is interesting to note that this minimum variability speed was in the range of 5.5–5.8 km/h, i.e. within the limits of the usual self-selected walking speeds [120,123,124]. Moreover, this result is similar to those of previous studies which revealed that the self-selected speeds are optimal in terms of energy consumption of walking [120,125]. This optimization phenomenon thus suggests that humans unconsciously choose the energetically most efficient walking speed (i.e. for which minimum energy is expended), and that at this speed gait data is most stable [122].

4. Modelling of human walking force

In order to satisfy specified vibration serviceability criteria under footfall excitation it is crucial to predict (as accurately as possible) at the design stage how a structure will vibrate when occupied and dynamically excited by pedestrians. Accuracy of prediction relies mostly on adequate mathematical representation of human-induced loading. In general, two types of mathematical models have been proposed to date: time- and frequency-domain force models. These will be described in the next two sections. The last section then critically reviews design codes and guidelines dealing with walking loads.

4.1. Time-domain force models

In general, there are two types of time-domain models: deterministic and probabilistic. The former takes no account of random variation among human population and therefore suggests a uniform walking force model for each individual pedestrian. The latter type considers all people as individuals with distinctive gait parameters which influence human-induced forces, such as the body weight, step frequency, etc. Therefore, there is a need for taking into account these natural diversities (i.e. inter-subject variability) via their probabilities of occurrence, best described via their probability density functions.

4.1.1. Deterministic force models

The ratio between the pedestrian pacing rate and natural frequencies of a structure is a key design parameter in determining the extent to which the structure vibrates when occupied and dynamically excited by humans walking [126]. Based on many years of expertise in field testing of structures subjected to moving people, a number of researchers have distinguished between so-called 'low-' and 'high-frequency' structural responses [126,127]. The former occurs typically if a vibrating structure has energy in the frequency range below approximately 10 Hz. Therefore, if the natural frequencies are close to the pacing rate (for normal humans between 1.5 and 2.5 Hz according to Kerr [44]), the vibration generated by one footfall is reinforced by the response to following footfalls leading to a build-up of resonance. Resonant vibration can also be developed in structures having the natural frequencies that are an integer multiple of the pacing rate, known as the harmonics of the walking force [131]. Open-plan floors, staircases and footbridges are generally low frequency structures. On the other hand, if the natural frequencies of a structure are high compared to the pacing rate (approximately 10 Hz or higher) then the vibration generated is a transient impulsive response to each following heel strike [128]. Rather than shoving a resonant build-up, the transient response is characterized by decaying amplitudes after separate footfalls. The rate of decay is determined by the structural damping. Facilities designed to accommodate vibration sensitive equipment, such as laboratories and operating theatres, must have high natural frequencies to avoid generating resonant vibrations.

The difference in the nature of resonant and transient vibration responses led further to the need for two conceptually distinct walking force models for low- and high-frequency structures [128]. These will be elaborated in the next two sections. However, this distinction is created artificially since there is so far no uniform walking force model, which can generate both resonant build-up and transient decay.

4.1.1.1. Force models for low-frequency structures. Walking forces on low-frequency structures might depend on how a structure responds to pedestrians and the pedestrians in turn respond to the structure they occupy and dynamically excite. In Section 3.3 this has been defined as one aspect of the human–structure dynamic interaction. However, models presented in this section are all obtained from walking force measurements conducted on various forms of rigid surface, such as a built-in force plate on stiff ground. This leaves a possibility that they might not be appropriate for vibration assessment of low-frequency structures that move perceptibly under pedestrian action. For example, Baumann and Bachmann [129] reported that vertical walking load was up to 10 percent higher if measured on stiff ground in comparison to measurements on a flexible pre-stressed concrete beam. Similarly, Pimentel [71] showed that in the case of flexible footbridges walking forces were considerably lower than those previously reported on solid surfaces. Walking force models which account for the human–structure dynamic interaction will be reviewed in Section 5.

Under the assumption that an individual generates identical and therefore perfectly repeatable footfalls with the period T, the vertical walking force $F_p(t)$ can be represented in time domain as a sum of Fourier harmonic components [130]:

$$F_p(t) = G + \sum_{i=1}^{n} G\lambda_i \sin(2\pi f_p t - \phi_i) \tag{2}$$

where G is the subject's static weight (N), i the order number of the harmonic, n the total number of contributing harmonics, λ_i the Fourier coefficient of the ith harmonic generally known as dynamic loading factor (DLF), f_p the activity rate (Hz) and φ_i the phase shift of the i-th harmonic (rad).

DLFs have been reported in a number of publications [44,131] and incorporated worldwide into contemporary design guidelines on vibration performance of civil engineering structures when subjected to pedestrian movement [9,132]. One of the first such guidelines was published by Blanchard et al. [50] who proposed a simple walking force model relevant to footbridge dynamic excitation. The model describes a single pedestrian loading as a sinusoidal force assumed to be in resonance with the first vertical vibration mode of the structure. For footbridges with a vertical fundamental frequency up to 4 Hz, the resonance would be developed due to the first harmonic with DLF equal to 0.257 and pedestrian weight $G = 700$ N. However, for fundamental frequencies between 4 and 5 Hz it was assumed that this frequency range could not be excited by the first harmonic of walking force, so some reduction in the DLF was applied to account for the lower amplitude of the second harmonic.

Bachmann and Ammann [7] went further and reported values of the first five harmonics for the vertical, and several harmonics and sub-harmonics for medial–lateral and anterior–posterior walking force (Fig. 17). The same authors pointed out that dynamic-induced load was primarily determined by the pacing frequency. They quoted an example for a subject walking at 2 Hz producing vertical dynamic loading 37 percent of static weight for dominant first harmonic. They also reported that the first and third harmonics (at 1 and 3 Hz, respectively) were dominant in the medial–lateral direction, whereas the first and the second harmonic (at 2 and 4 Hz, respectively) were the most significant in the case of longitudinal force. Interestingly, in the lateral case they found that third harmonic for some pedestrians might exceed the fundamental in amplitude. An extended discussion on more recent research on lateral pedestrian excitation will continue in Section 5.

As the scope of the research in human-induced excitation broadened to include different modes of locomotion, Rainer et al. [51] conducted a study designed to provide measurement and analysis of continuous force due to a single-person walking, running and jumping. It was confirmed that DLFs strongly depend on the frequency of the activity. The maximum dynamic loads for walking were found to be nearly twice as large as those recommended previously by current design codes [133,134]. The same authors suggested that the loading function should include up to four harmonic components with frequencies of integer multiples of the pacing rate and decreasing amplitudes for the higher harmonics (Fig. 18). Unfortunately, the study included only three test subjects and therefore lacks statistical rigour.

Probably the most comprehensive research to date relevant to walking forces was carried out by Kerr [44] as a part of his doctoral thesis. He collected approximately 1000 vertical GRF records of a single footfall force. These were generated by 40 individuals as they walked over a force plate making a single step on it. All trials covered a range of walking frequencies from a very slow 1 Hz to a very fast 3 Hz. Kerr reported large scatter in the DLF values and only the first harmonic (out of the four considered) showed a clear trend to increase with increasing the step rate (Fig. 19). This work created currently the most comprehensive database on pedestrian loading available worldwide, however, apart from the limited number of test subjects, the key problem with this data set is that it cannot represent the variability of real walking between subsequent steps of the same pedestrian during one walking exercise (i.e. intra-subject variability).

Young [131] carried out a further study to develop more accurate design guidelines on pedestrian-induced vibrations of civil engineering structures such as floors and footbridges. He systematized data published by Kerr [44] and others (Fig. 20) and proposed DLFs for the first four harmonics of walking force as a function of pacing rate assumed to be in the range of 1–2.8 Hz. This assumption was supported by the fact that walking frequencies out of the given range would be physically meaningless i.e. they would be either too slow or too fast, hence hardly likely to happen in reality. Design values were

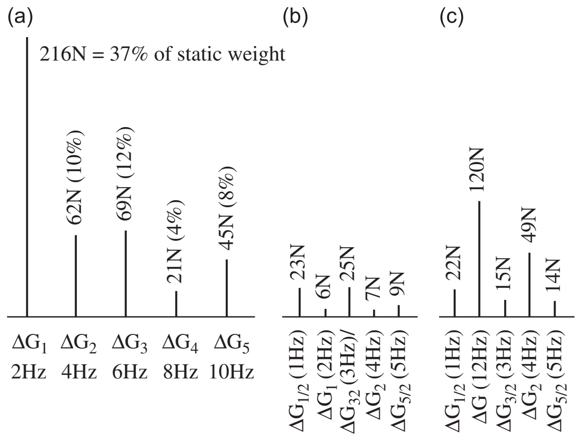

Fig. 17. Harmonic components of the walking force in: (a) vertical, (b) lateral and (c) longitudinal directions (after Bachmann and Ammann [7]).

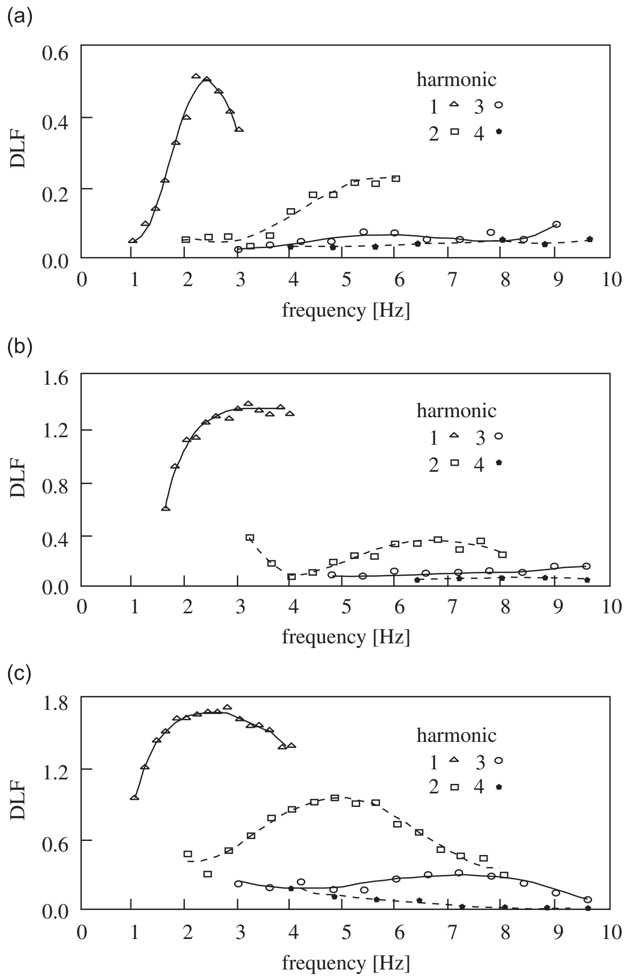

Fig. 18. DLFs for the first four harmonics for: (a) walking, (b) running and (c) jumping force (after Rainer et al. [51]).

presented as regression equations [131]:

$$\begin{aligned} \alpha_1 &= 0.41(f-0.95)\leqslant 0.56 && f=1\text{–}2.8\,\text{Hz} \\ \alpha_2 &= 0.069+0.056f && f=2\text{–}5.6\,\text{Hz} \\ \alpha_3 &= 0.033+0.0064f && f=3\text{–}8.4\,\text{Hz} \\ \alpha_4 &= 0.013+0.0065f && f=4\text{–}11.2\,\text{Hz} \end{aligned} \tag{3}$$

where f is the frequency of an appropriate harmonic. These values were selected so that there is 25 percent chance of them being exceeded, assuming that they represent entire population. This is a rudimentary attempt, probably the first of its kind, to take into account the stochastic nature of pedestrian excitation.

The overview of DLFs for vertical footfall loading reported by different authors (Table 1) is given in a comprehensive literature review by Zivanovic et al. [1] related to vibration serviceability of footbridges under human-induced excitation.

Similar studies on groups of walking people are rare. Ellis [135,136] measured the structural response (i.e. acceleration) induced by individuals and groups of up to 32 people walking across a floor structure. Although there was a significant difference in acceleration levels for resonant and off resonant loading for individuals, this was not always the case for the larger groups. Ellis also noticed that any given group size walking at a controlled pacing rate to generate resonance did not always produce the largest response. Moreover, the DLFs of the group loads decrease with increasing group size, with the rate of attenuation being greater for the higher harmonics. Earlier, Pernica [137] reported similar results for a wide range of activities. He observed that individuals performing walking, running and jumping in groups generated on average lower DLFs than when acting alone. This supported the work on jumping forces by Rainer et al. [51] who reported that the reduction in dynamic loading for groups of people was greater for the higher harmonics, while the DLF for the fundamental harmonic remained approximately the same.

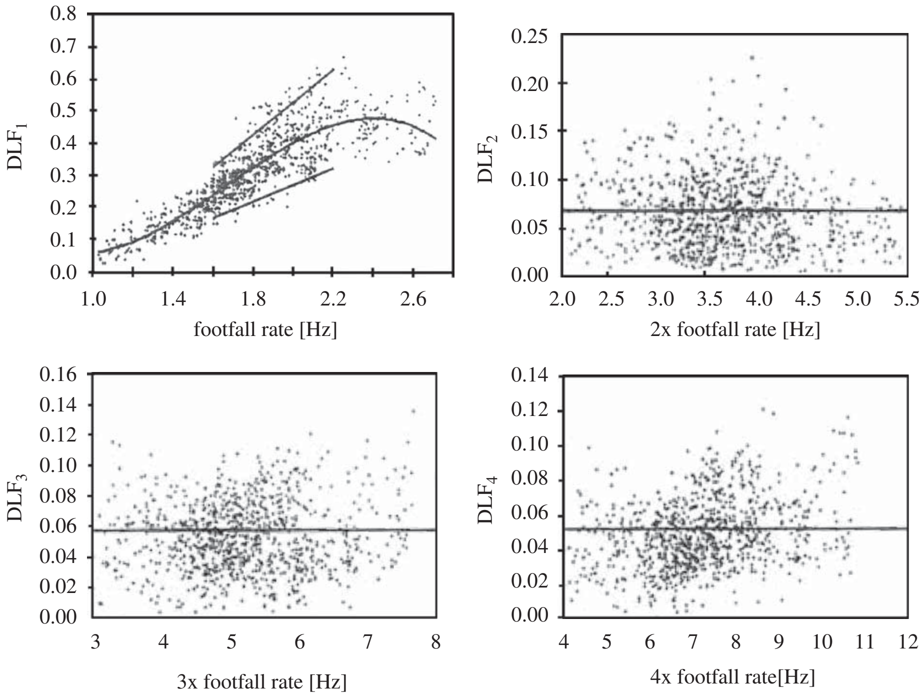

Fig. 19. DLFs of walking force for the first four harmonics (after Kerr [44]).

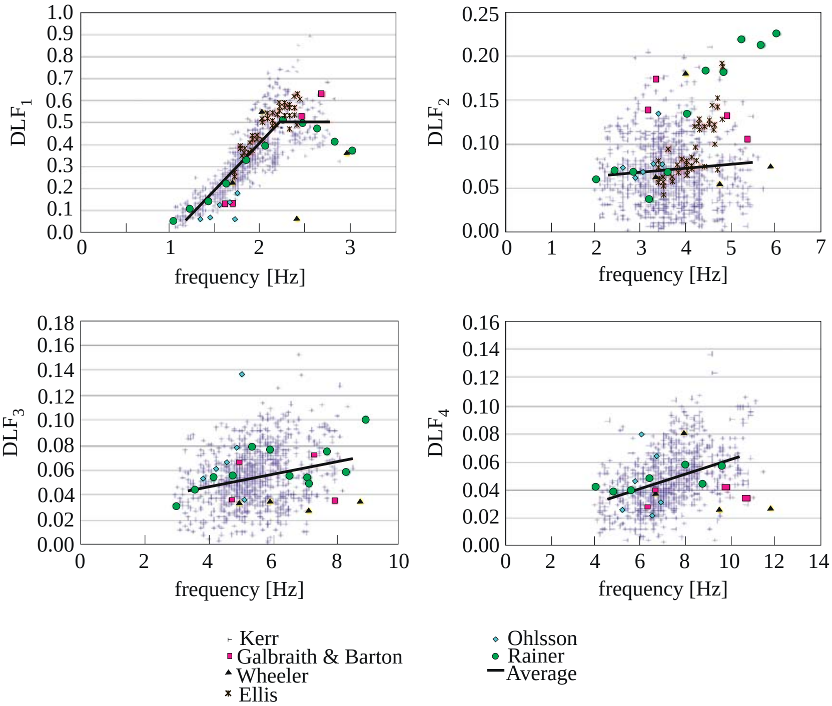

Fig. 20. DLFs of the walking force for the first four harmonics collected from different authors (after Young [131]).

All mentioned studies clearly indicate that people acting in a group cannot achieve perfect synchronization of their movement and therefore reduce total DLF [138,139]. In a study on footbridge crowd loading, Matsumoto et al. [140] estimated vertical forces due to normal pedestrian traffic as the force due to a single person multiplied by a factor

Table 1
DLFs for single person force models after different authors (after Zivanovic et al. [1]).

Author(s)	DLFs for considered harmonics	Comment	Type of activity and its direction
Blanchard et al. [50]	$\alpha_1 = 0.257$	DLF is lessen for frequencies from 4 to 5 Hz	Walking—vertical
Bachmann and Ammann [7]	$\alpha_1 = 0.4{-}0.5$	Between 2.0 Hz and 2.4 Hz	Walking—vertical
	$\alpha_2 = \alpha_3 = 0.1$	At approximately 2.0 Hz	
Schulze (after Bacmann and Ammann [7])	$\alpha_1 = 0.37\alpha_2 = 0.10\alpha_3 = 0.12\alpha_4 = 0.04\alpha_5 = 0.08$	At 2.0 Hz	Walking—vertical
	$\alpha_1 = 0.039\alpha_2 = 0.01\alpha_3 = 0.043\alpha_4 = 0.012\alpha_5 = 0.015$	At 2.0 Hz	Walking—lateral
	$\alpha_{1/2} = 0.037\alpha_1 = 0.204\alpha_{3/2} = 0.026\alpha_2 = 0.083\alpha_{5/2} = 0.024$	At 2.0 Hz	Walking—longitudinal
Rainer et al. [51]	α_1, α_2, α_3 and α_4	DLFs are frequency dependent (Fig. 10)	Walking, running, jumping—vertical
Bachmann et al. [5]	$\alpha_1 = 0.4/0.5\alpha_2 = \alpha_3 = 0.1/-$	At 2.0/2.4 Hz	**Walking—vertical**
	$\alpha_1 = \alpha_3 = 0.1$	At 2.0 Hz	Walking—lateral
	$\alpha_{1/2} = 0.1\alpha_1 = 0.2\ \alpha_2 = 0.1$	At 2.0 Hz	Walking—longitudinal
	$\alpha_1 = 1.6\ldots\alpha_2 = 0.7\alpha_3 = 0.2$	At 2.0–3.0 Hz	Running—vertical
Kerr [44]	α_1, $\alpha_2 = 0.07\alpha_3 \approx 0.06$	α_1 is frequency dependent (Fig. 11)	Walking—vertical
Young [131]	$\alpha_1 = 0.37(f-0.95)\leqslant 0.5$ $\alpha_2 = 0.054 + 0.0044f$ $\alpha_3 = 0.026 + 0.0050f$ $\alpha_4 = 0.010 + 0.0051f$	These are mean values for DLFs	Walking—vertical
Bachmann et al. [5]	$\alpha_1 = 1.8/1.7\alpha_2 = 1.3/1.1\alpha_3 = 0.7/0.5$	Normal jump at 2.0/3.0 Hz	Jumping—vertical
	$\alpha_1 = 1.9/1.8\alpha_2 = 1.6/1.3\alpha_3 = 1.1/0.8$	High jump at 2.0/3.0 Hz	Jumping—vertical
	$\alpha_1 = 0.17/0.38\alpha_2 = 0.10/0.12\alpha_3 = 0.04/0.02$	At 1.6/2.4 Hz	Bouncing—vertical
	$\alpha_1 = 0.5$	At 0.6 Hz	Body swaying while standing—lateral
Yao et al. [92]	$\alpha_1 = 0.7\alpha_2 = 0.25$	Free bouncing on a flexible platform with natural frequency of 2.0 Hz	Bouncing—vertical

$\sqrt{N} = \sqrt{\lambda T_0}$. Here, N is number of people on the bridge at any time instant, λ is a mean arrival rate expressed as the number of pedestrian per second, and T is the time needed to cross the bridge in seconds. This relationship was derived using the sum of responses of individual pedestrians who arrived on the bridge following the Poisson distribution and inducing the walking forces with equal resonant frequencies and random phases. However, when Fujino et al. [72] utilized Matsumoto's formula on the laterally vibrating *T*-footbridge in Tokyo, they found that the formula significantly underestimated (almost nine times) the measured vibration response. Similarly, Matsumoto's formula could not predict the vibration level on the Millennium Bridge [141], suggesting that the approach is not viable for bridges prone to strong lateral vibration due to synchronized crowd. Synchronization phenomenon is a significant subject on its own and will be discussed in Section 5 in more detail.

4.1.1.2. Force models for high-frequency structures. When subjected to footfall forces generated by pedestrians, the response of structures having natural frequencies above approximately 10 Hz (i.e. more than four times the walking pace) typically take the form of a transient response, as illustrated in Fig. 21. The initial peak can be associated with a heel impact followed by vibration at the natural frequency of the structure having a decaying rate associated with the structural damping. As each following heel strike is made, another transient decay is generated, but no build-up of vibration can be developed due to the damping. Willford and Young [8] recognized the analogy between dynamic response of a high-frequency structure when subjected to pedestrian movement and a decaying vibration of a single degree of freedom (SDOF) system under a series of successive impulses. This provided a walking force model for prediction of the vibration of high-frequency structures based on the analytical solution for the decay of the impulsive response, assuming that the magnitude of initial velocity peak can be determined [8].

In effect, the initial and hence maximum velocity under an impulsive action can be calculated as magnitude of the impulse divided by the mass. Moreover, for the unit mass the initial velocity becomes numerically equal to the impulse applied. Based on this relation, Willford and Young [8] proposed a method to determine the so-called 'effective impulse' of a particular force–time history. They applied the continuous walking forces derived from approximately 1000 Kerr's single footfall force records to a series of SDOF systems having unit modal mass and different natural frequencies and damping to calculate the velocity response. The peak response values generated in each SDOF system were then extracted to account for numerical values of the effective impulse for a particular force measurement as the natural frequency and damping vary. This is conceptually identical to the derivation of the response spectra for a large number of seismograms [142].

The results of the analysis are presented in Fig. 22. It can be seen that the effective impulse decreases as natural frequency of the structure increases and as footfall rate decreases. For design purposes and to account for the variation of the effective impulse value between the different footfalls, an empirical formula was proposed as [8]

$$I_{\text{eff}} = 54f^{1.43}/f_n^{1.30} \tag{4}$$

where I_{eff} is the effective impulse in Ns, f is the footfall rate in Hz and f_n is the natural frequency of the structure in Hz. This model provides impulse values having 25 percent chance to be exceeded.

The model can generate vibration response such as shown in Fig. 23. The simulated response is based on a representative effective impulse which is identical for each footfall and therefore shows a uniform repeating vibration

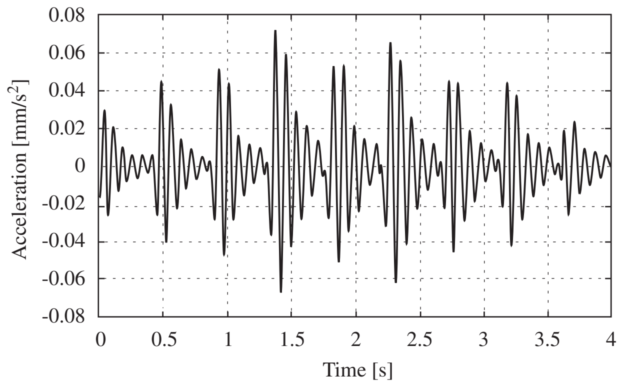

Fig. 21. Acceleration response of a high-frequency floor due to a single person walking at 2.2 Hz.

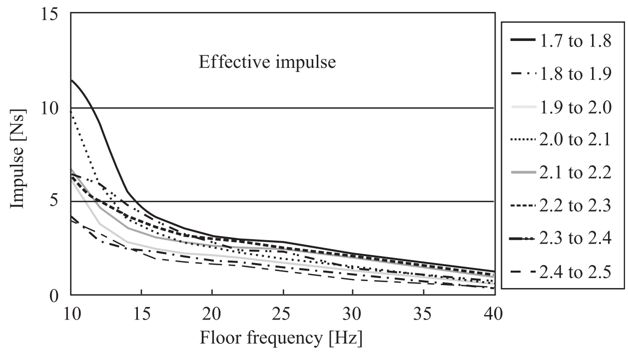

Fig. 22. Effective impulse derived from Kerr's footfall measurements as a function of the natural frequency of the structure and the footfall rate (after Willford and Young [8]).

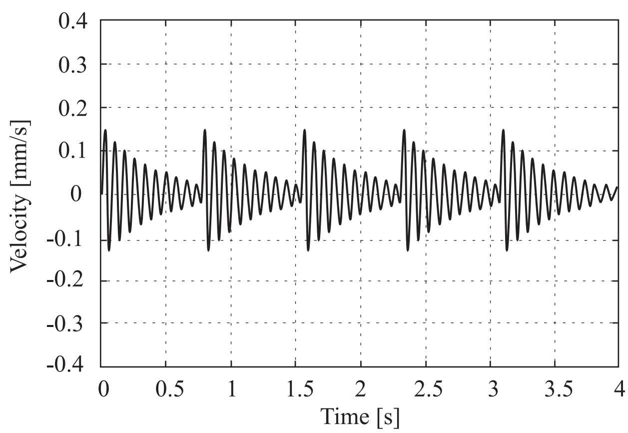

Fig. 23. Simulated vibration response using the effective impulse model (after Willford et al. [128]).

pattern. Compared to the prediction of footfall-induced vibrations (Fig. 23), measured vibrations of a real full-scaled high-frequency structure show considerable variability between effects of individual footfalls, both in magnitudes and timing (Fig. 21). These irregularities are due to natural variability between successive footfall impacts induced by a single person walking (i.e. intra-subject variability). Therefore, further improvement in the model is required to account for this variability. However, the current version is used extensively within Arups's consultancy practice [143] and has been independently validated on floors, footbridges and staircases constructed of steel and concrete for the past decade [128]. Moreover, it is incorporated into two footfall-induced vibration guidelines: the Concrete Society Technical Report 43, Appendix G [9] and the Concrete Centre [132].

4.1.2. *Probabilistic force models*

A random or stochastic process is one whose behaviour is non-deterministic in the way that a current state does not fully determine its next state [144]. As shown in Section 3.5, human walking forces are characterized by considerable variability and uncertainty, so their mathematical characterization can be seen from the probabilistic and statistical perspective. This section thus first provides an overview of probability density functions and basic statistics (mean value and standard deviation) of key design parameters related to the pedestrian loading, such as step frequency, walking speed, step length and forcing amplitude. Next, a relevant model will be presented to put this knowledge into practice.

Matsumoto et al. [140,145] were the first to report reliable statistics of step frequencies based on a sample of 505 persons walking at self-selected speeds. Collected data show a normal distribution with a mean pacing rate of 1.99 Hz and standard deviation of 0.173 Hz (Fig. 24). More recently, Zivanovic et al. [80] monitored nearly 2000 people crossing the Podgorica footbridge in the capital of Montenegro to estimate probability density functions of various time–distance parameters, including step frequency. Although the normal distribution was confirmed, they identified mean value of 1.87 Hz and standard deviation of 0.186 Hz, which differ considerably from the statistics reported by Matsumoto et al. [140,145]. However, these results were close to data reported by other researchers: 1.9 Hz measured by Kerr and Bishop [3], 1.8 Hz measured by Pachi and Ji [78] and 1.82 Hz reported by Sahnaci and Kasperski [79]. Zivanovic [146] later explained the discrepancy between reported statistics by being due to the different ethnic populations studied, for example Japanese or Caucasians. This clearly suggests that a random sample of people with mixed sex, race and geographical diversity should be collected to ensure uniformity of measurements.

Pachi and Ji [78] reported that frequency and velocity of walking may even vary depending on location and environment. They collected 800 measurements for 100 men and 100 women who walked across two footbridges and two shopping floors. Statistical analysis revealed that people walked faster on the shopping floors, with average frequency of 2 Hz and velocity of 1.4 m/s, compared with footbridges, where the average frequency measured was 1.8 Hz and velocity of 1.3 m/s. Distributions for walking frequency on both footbridges and floors followed a normal distribution, with standard deviations of 0.11 and 0.13 Hz, respectively. Moreover, they found a linear relationship between the velocity v (m/s) of the

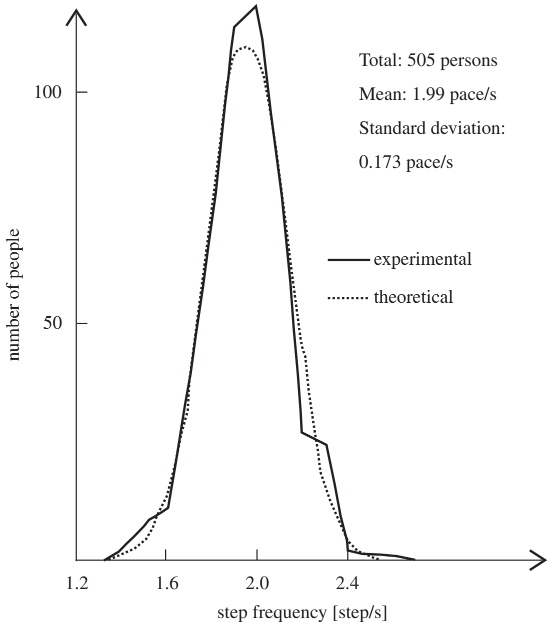

Fig. 24. Normal distribution of step frequencies for level walking (after Matsumoto et al. [145]).

pedestrian and the corresponding pacing rate f (Hz), expressed as

$$v = L_s f = \begin{cases} 0.75f & \text{for males} \\ 0.67f & \text{for females} \end{cases} \quad (5)$$

or for both groups together:

$$v = L_s f = 0.71f \quad (6)$$

where coefficient 0.71 represents the average step length L_s expressed in metres. Using the data collected by Pachi and Ji [78], Zivanovic [146] reported that walking speeds at a certain frequency are also normally distributed (Fig. 25).

Zivanovic et al. [80] further analysed data collected on Podgorica footbridge. A total of 1976 pedestrians were observed and it was found that their step length varied between 0.479 and 0.923 m. The data fitted a normal distribution having mean value of 0.71 m and standard deviation of 0.071 m, independently of the walking frequency.

Yamasaki et al. [120] conducted a comprehensive biomechanical study designed to investigate the effects of sex and speed on the variation of the time–distance parameters such as step length (L_s) and step duration (ΔT) during treadmill walking. They showed that relationship between L_s and walking speed (v) was not linear (Fig. 26) as previously reported elsewhere [30,78,147–149]. Deviation from linearity became apparent at faster walking speeds, i.e. 120 in males and 110 m/min in females (Fig. 26), while differences in L_s between the two groups were statistically significant at walking speeds above 90 m/min. Regression analysis suggested that the step length increased approximately in proportion to the square root of v (Fig. 26). Interestingly, the study also indicated that females walked with shorter L_s than the males, especially at fast walking speeds. This was entirely consistent with results reported by other investigators [30,32,149–151] who claimed that females had a tendency to increase speed by increasing their pacing rate, while males increased their step length. However, the walking speed at which the variation of L_s showed minimum was about 90 m/min in both genders (Fig. 27). This speed was in the range of usual self-selected speeds of about 88 m/min measured for Japanese population [120], and 80–90 m/min reported for Caucasians [123,124] when allowed to walk freely. As previously mentioned in Section 3.5.2, these free walking speeds were commonly established to yield optimal energy expenditure during walking [125]. There is also some evidence from both measurements of oxygen consumption [152] and mechanical simulations of bodies in motion [153–155] that people select unconsciously gait style in order to optimize energy cost of locomotion. Indeed, walking feels easiest when going slowly and running feels easiest when going faster [156]. Hence people switch from a walk to run at speeds close to the boundary at which walking ceases to be optimal [155,157,158]. The same mechanism can possibly explain why people alter their gait and hence the corresponding GRFs when walking on perceptible moving structures. A good starting point can be a study by Anderson and Pandy [159] where they forced a mechanics-based model of the body to optimize walking performance on a rigid ground given only the states of the model (i.e. the positions and velocities of all body segments) at the beginning and end of the walking cycle. As a result, the predicted GRFs were similar to those directly measured. Energetics of human motion is the biomechanical area from which valuable knowledge might form the basis for a new generation of walking force models in civil structural engineering.

Probability density functions presented can be used as building blocks to develop a modelling procedure which can estimate the probability of occurrence of a particular walking loading scenario and therefore a certain level of vibration response. Based on this, a probability that the vibration response will not exceed predefined limiting values can be found. In this way, Zivanovic [146] proposed a novel probability-based framework for predicting vertical vibration response of footbridges to a single pedestrian excitation. The main goal of her research was to model a statistically described harmonic force taking into account as many as possible independent gait parameters relevant to a single person. The method proposed therefore takes into account probability distributions of walking frequency, step length, forcing amplitude and imperfections in human walking (i.e. intra-subject variability). Moreover, when including these distributions in the

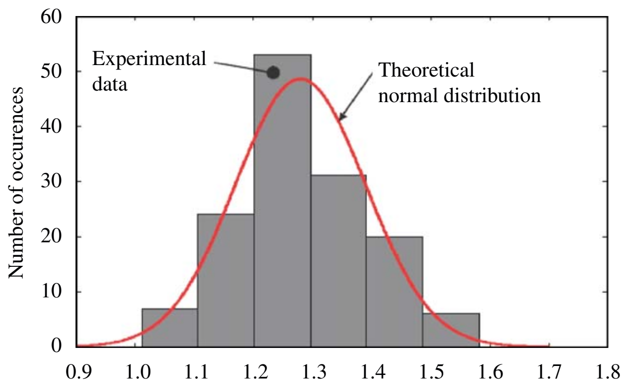

Fig. 25. Normal distribution of walking speed when walking with step frequency around 1.8 Hz (after Zivanovic [146]).

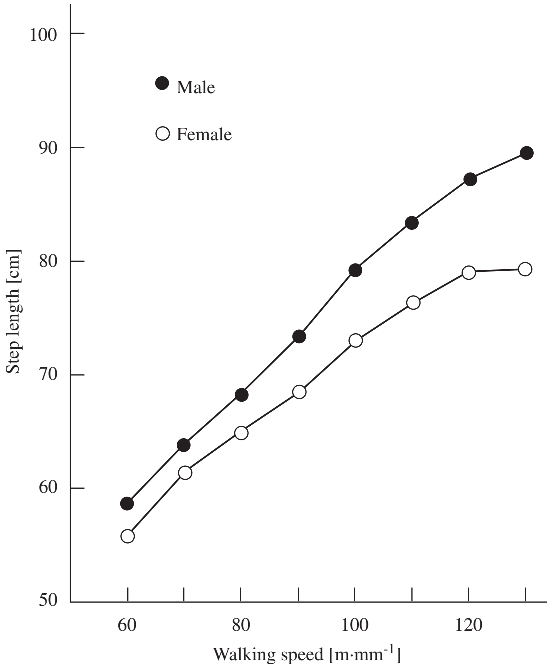

Fig. 26. Relationship between the walking speed and the mean step length (after Yamasaki et al. [120]).

dynamic analysis of a particular footbridge, the cumulative probability that the response will not exceed a certain peak acceleration level could be obtained. This information can be used further as a key design criterion when making decision about vibration serviceability of the footbridge. As recommended by Zivanovic [146], this probability procedure can be utilized in design of footbridges that are not exposed to heavy pedestrian traffic and where a single person loading scenario is the most likely. However, having a good mathematical model of a single pedestrian as provided in this study is a necessary prerequisite for developing a similar probability-based model for multi-pedestrian excitation in the future.

4.2. Frequency-domain force models

Many of the basic concepts in analysis of the frequency content of human-induced excitation were formulated by Ohlsson [43] in the early 1980s. He analysed the auto-spectral density (ASD) of the walking force treating it as a stationary random process. Supervised by Ohlsson, Eriksson [70] spent a better part of his doctoral studies developing further this method. A typical ASD of the walking force in the frequency range below 6 Hz is shown in Fig. 28. He emphasized that each peak around the main harmonics has some 'leaking' of the excitation energy (i.e. some width in the spectrum) provide a clear evidence that human walking forces are not periodic, but in fact a narrow-band random process [160].

Further, Brownjohn et al. [16] reported that the effect of energy spread was more dominant for higher harmonics, indicating their greater randomness. Moreover, using direct measurements of the continuous vertical GRF for three subjects walking on an instrumented treadmill, the authors suggested a more realistic frequency domain model for calculation of a bridge vertical response under large numbers of pedestrians based on theory of a turbulent wind on linear structures. When applying the Gaussian probability distribution of mean pacing rates (with mean value of 2 Hz and standard deviation of 0.2 Hz), the ASD of the response in a particular mode $S_x(f)$ in a degree of freedom (DOF) defined by the coordinate x can be calculated as [16]

$$S_x(f) = \psi_z^2 |H(f)|^2 S_{P,1}(f) \int_0^L \int_0^L \psi_{z_1} \psi_{z_2} \,\mathrm{coh}(f, z_1, z_2)\, \mathrm{d}z_1\, \mathrm{d}z_2 \tag{7}$$

where ψ_z is the ordinate of the mode shape at the same location, $H(f)$ is the frequency response function for acceleration response, $S_{P,1}(f)$ is the ASD of the pedestrian loads per unit length of the bridge span for the fundamental harmonic, while ψ_{z_1} and ψ_{z_2} are mode shape ordinates related to the location of each two pedestrians on the bridge at coordinates z_1 and z_1. Additionally, coherence function $0 \leqslant \mathrm{coh}(f, z_1, z_2) \leqslant 1$ takes account for correlation among pedestrians at different locations on the structure. As pointed out by the authors, more research work is required to determine the likely form of the coherence function as a measure of synchronization among pedestrians and verify it against results from experiments on real full-scale structures. This issue will be discussed in Section 5 in some detail.

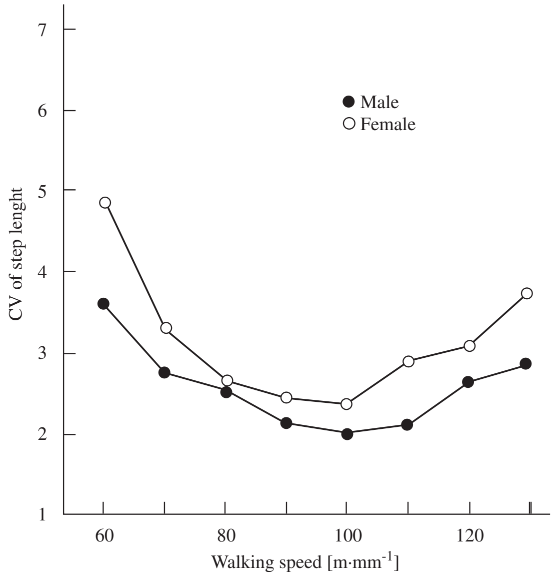

Fig. 27. Coefficient of variation (CV) calculated for 200 step lengths vs. walking speed (after Yamasaki et al. [120]).

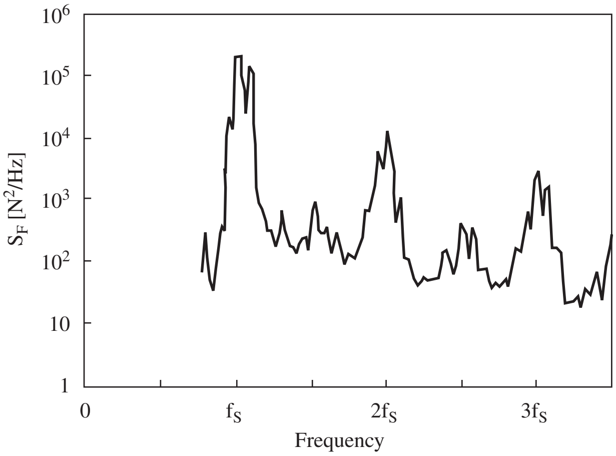

Fig. 28. ASD of a walking force (after Eriksson [70]).

More recently, Sahnaci and Kasperski [79] demonstrated that imperfections in individual human walking pattern generate subharmonics (also called intermediate harmonic load amplitudes) having energies between the bands corresponding to the main harmonics in the ASD plot. The reason for this is slight differences in gait parameters for the left and right legs, such as step length and walking frequency. Some biomechanical research also recognized the phenomenon of so-called 'limb dominance' [111,161]. Therefore, the assumption of gait symmetry is generally considered old-fashioned nowadays [162]. Sahnaci and Kasperski [79] quoted an example where the response predicted without taking into consideration presence of subharmonics differed from the actual response by more than 50 percent. Therefore, Zivanovic et al. [80] made an extension of a force model formulated by Brownjohn et al. [16] to a multi-harmonic approach. They included complete frequency content of the force spectrum for the first five harmonics and corresponding subharmonics without any discontinuities. The model was then transformed to the time-domain assuming random phase shifts (i.e. time delays) between spectral lines. Vibrations generated under the reconstructed forces were successfully verified on a model of an as-built footbridge in operation.

There have been numerous attempts to provide reliable and practical descriptions of human walking forces for design of structures for which pedestrian dynamic excitation is a major concern. The basis and limitations of codes and guidelines most widely used in the UK are discussed in the next section.

4.3. Design codes and guidelines in UK

The UK is known as a country with a long standardization tradition in civil engineering practice. While British Standard Institution (BSI) regulated and formalized some subject areas in detail (e.g. earthquake resistance and wind loading), vibration serviceability design of civil engineering structures under human-induced excitation is not necessarily controlled by national codes of practice and even the codes are not legally enforced. More often it is based upon design manuals generally called ‘guidelines’. These publications are simply advisory and offer instructions to an engineer responsible for planning and designing of civil engineering structures, such as footbridges and floors, that are dominantly occupied and dynamically excited by humans. Guidelines describe steps in the design process and discuss alternative methodologies as well as their present limitations. Even when officially formalized, guidelines still include a certain freedom in their application. An engineer may therefore deviate from their recommendations whenever reasonable arguments are provided, such as implementation of new structural systems and materials.

The current UK design guideline for footbridges [134] uses a simple 30-year old walking model proposed by Blanchard et al. [50] involving a sinusoidal force assumed to be perfectly synchronized with the first vertical vibration mode of the footbridge. Numerous studies have shown this model to be inappropriate for real situations of single or multiple pedestrians generating in reality near-periodic forces [16] at normally distributed random frequencies [80,145].

There is also very limited codified provision for dynamic loads on footbridges occupied by light or heavy traffic of pedestrians. The exceptions are the limited British guidance resulting from the London Millennium Bridge experience and based on the obsolete frequency-tuning method [163] and French guidance [164] using a multiplication factor applied to single pedestrian response. The later procedure provides the best match with observations and suggests further development of the frequency domain random vibration model.

After it had been used and validated extensively worldwide within Arup’s design practice [143], their methodology for vibration serviceability design of floors was incorporated into the Concrete Society Technical Report 43, Appendix G [9], CCIP-016 [132] and the Steel Construction Institute P354 [165]. All three guidelines provide design values of dynamic loading factor (DLF) for single pedestrians (for low frequency floors) and equivalent impulse values (for high frequency floors), as presented in Section 4.1.1. The CSTR43 and CCIP-016 provision for vibration serviceability assessment is based on the most comprehensive data set available on footfall forces collected by Kerr [44] and well established methods for calculation of dynamic structural response [142]. Moreover, the SCI guide brought slightly different DLFs to account for Eurocode’s reliability factors [166]. However, as already pointed out in Section 4.1.1.1, the key problem with Kerr’s database is that GRF records were generated by individuals as they passed over a force plate and made a single footfall. Therefore, it cannot represent the inter-subject variability of real walking during one walking exercise. However, no successfully populated database of GRFs in the form of continuously recorded time series has yet been found that can be used for development of statistically reliable characterization of GRFs for application in a civil engineering practice. This means that there remains a requirement to establish a sufficiently large database of GRF time series to provide statistical reliability even for a rigid surface. The database also needs to include time series for multiple pedestrians as well as pedestrians moving on more or less perceptibly moving surfaces. Establishment of such a database is at the core of an overall strategy for developing a more realistic and reliable probability-based mathematical model of human walking forces.

The next section highlights two modelling tasks that are still serious challenges to the structural dynamics community worldwide. The first is the very specific but under-researched phenomenon of synchronization between people walking in groups. The second is the degree of synchronization between movement of the pedestrians and the structure whose motion is perceived. Although different in nature, they usually happen simultaneously and influence significantly GRFs generated on structures prone to human-induced vibrations [15]. In this way, synchronization is commonly considered as important aspect of the human–structure dynamic interaction affecting structural response.

5. Synchronization phenomenon in human–structure dynamic interaction

The phenomenon that occurs when people change their gait to adapt to excessive vibration of the structure is known as human–structure synchronization [7] or lock-in effect [167]. Broadly speaking, it can either be deliberate or subconscious (unintentional). The former type has been usually related to vandal loading. The latter has become an important side effect of new architectural trends towards using light materials to provide slender and aesthetic design. Architects sometimes fail to balance innovation and practicality, so many modern structures have become highly susceptible to vibrations induced by humans even when they perform normal daily activities such as walking or running.

Current understanding of the synchronization problem covers mainly theoretical aspects of the subject, with very little experimental verification. According to the popular belief, excessive structural vibrations under unintentional pedestrian–structure synchronization can be generated in two ways, as summarized in Fig. 29. The first occurs when the density of pedestrians δ present on a structure is lower than some critical value δ_c, i.e. the density great enough to influence motion of pedestrians within a group. In this case, occupants act on a structure as a non-synchronized group and GRFs are induced by each individual pedestrian independently [168]. Further, if the maximum amplitude of structural vibrations x induced by pedestrians is lower than a critical value x_c (i.e. the value great enough for humans to notice or become aware of it), pedestrians are not affected by the motion of the structure and no human–structure synchronization

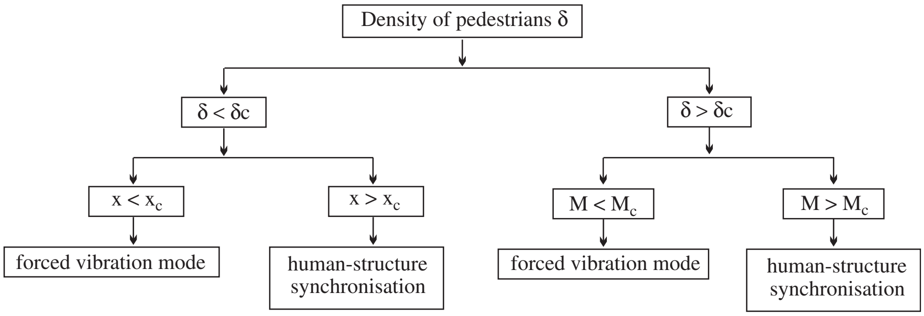

Fig. 29. Flow chart of unintentional pedestrian–structure synchronization.

occurs. However, in the case of perceptible vibrations ($x > x_c$), pedestrians unconsciously tend to adjust their gait and synchronize with motion of the structure they occupy [89].

Alternatively, excessive structural vibrations may occur under a dense crowd ($\delta > \delta_c$). In this case, unintentional synchronization becomes more likely because the limited space and the possibility to see each other subconsciously improve correlation of movements between occupants [76,169]. Thereupon, pedestrians somehow interact with each other and tend to walk with the same step frequency and phase, independently of the motion of the structure they occupy. The resultant force then approaches the sum of the forces exerted by each pedestrian in the synchronized group [168]. Moreover, structural vibrations may become unstable when the live load, represented by mass of pedestrians, is too great a proportion of the bridge's dead load [160]. In this case, the total mass M of the synchronized pedestrians is greater than the critical value M_c, i.e. the mass which inertial force would induce amplitude of structural vibration x_c. Thereupon, this high vibration level leads to the lock-in effect.

The next two sections present an overview of the unintentional human–structure dynamic synchronization. Section 5.1 presents the synchronization between lateral structural motion and pedestrians in a dense crowd, whereas Section 5.2 discusses synchronization between single pedestrians and a structure they occupy. Section 5.3 presents the Scruton number adapted and modified from wind engineering (i.e. vortex-induced oscillations of structures) as a tool to check both vertical and lateral lock-in of footbridges.

5.1. Synchronization between structure and dense crowd

Synchronization of a group of pedestrians to structural movements has been observed in the past on several footbridges [72,170], open-plan floors [70] and staircases [3]. However, a significant interest in the field was prompted by problem of excessive lateral vibration of the London Millennium Bridge during the opening day on 10 June 2000 [163]. Analysis of video records indicated that up to 2000 people (i.e. as many as 1.3–1.5 pedestrians per square metre of the deck) were present at any time on that day. Measured lateral accelerations were in the range of 0.20–0.25g corresponding to lateral displacement amplitudes up to 7 cm [73,167]. At this level of acceleration a significant number of pedestrians began to have difficulty in walking and held onto the balustrade for support [163]. The bridge was subsequently closed and research into this phenomenon was launched.

As part of this research, Dallard et al. [73,167] conducted a series of walking tests with a gradually increasing number of pedestrians on the bridge. Assuming that each of up to 275 participants contributed equally to the structural response, they calculated the amplitude of the modal lateral force per person (Fig. 30a) and its dependence on the footbridge velocity (Fig. 30b). Excessive vibration did not occur continuously, but built up when a large number of pedestrians were on the affected spans. Interestingly, peak amplitude of the lateral modal force in Fig. 30a showed that the synchronization started at about 900 s, but also clearly revealed that lock-in was not triggered two times between 600 and 800 s although the same level of vibrations was achieved. However, Dallard and co-investigators did not offer any possible explanation of this. Based on the plot given in Fig. 30b, the same authors proposed that people, after they synchronized movement with the structural swaying, started producing a dynamic force $F(t)$ proportional to the deck lateral velocity $v(t)$:

$$F(t) = kv(t) \quad (8)$$

where k is an empirically determined lateral walking force coefficient. This reveals that human occupants act as highly effective negative dampers amplifying the structural response. The tests on the Millennium Bridge indicated the value of k to be approximately 300 N s/m over the frequency range 0.5–1 Hz. Typically, the excessive swaying occurs on bridges with lateral natural frequencies near 1 Hz which is the predominant frequency of the first harmonic of the pedestrian lateral force [1]. Similarly, Brownjohn et al. [171,172] did a series of crowd loading tests on Changi Mezzanine Bridge at Singapore's Changi Airport and the value of the coefficient k was determined to be 188 N s/m before accounting for lateral mode shape effect. However, for modal force the value would be very close to the value 300 N s/m for London Millennium Bridge.

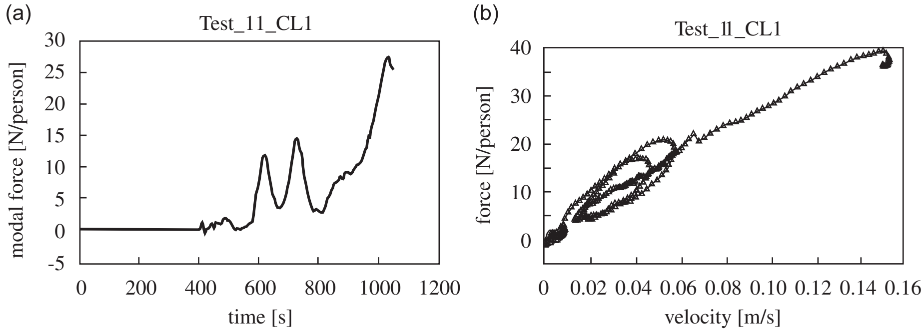

Fig. 30. (a) The lateral modal force per person per vibration cycle and (b) lateral force per person per vibration cycle as a function of deck velocity (after Dallard et al. [167]).

More recently, Macdonald et al. [173] reported k value 270 N s/m derived from heavy pedestrian traffic measurements of Clifton Suspension Bridge.

In effect, Dallard et al. [73,141,167] found that pedestrian–structure synchronization is theoretically possible on every bridge prone to human-induced vibrations when occupied with sufficient number of pedestrians. For a given level of damping c, the limiting (critical) number of people N_L likely to induce lock-in can be predicted by

$$N_L = \frac{8\pi cfM}{k} \tag{9}$$

where f is the lateral frequency of the bridge and M is the corresponding modal mass expressed in kg. This theoretical model has been derived assuming that pedestrians are uniformly distributed over the whole span and the lateral mode shape is sinusoidal and has been normalized to unity. Caetano et al. [174] showed quite recently that this relationship could estimate well the number of pedestrians for lateral dynamic instability of the Coimbra footbridge, being approximately 70.

To account for a loading case when the pedestrians are not uniformly distributed over the span, Roberts [175] used a simple analytical model, based on differential equations of motion of the bridge under pedestrian excitation, and predicted the critical number of people (N_p) as

$$N_p = \frac{\rho\alpha L}{m_p \Omega^2 Dk} \tag{10}$$

where ρ is mass of the bridge per unit length, α is loaded proportion of the span, m_p is average mass of a single pedestrian, Ω relates frequency of pedestrian loading to natural frequency of the n-th mode of the bridge (known as frequency ratio f_p/f_n), and D is dynamic amplification factor [142]. Here, pedestrian distribution over the span is considered via the k factor. With regard to all this, Eq. (10) accounts not only for any form of distribution of pedestrians (e.g. symmetric or antisymmetric) but also for the increased tendency of pedestrians to synchronize their motion with the lateral sway of the bridge when and where the vibration amplitudes are very large (such as the middle span of a simply supported bridge). Roberts pointed out that there was a practical lower limit for α which depends upon the crowd density at which pedestrians were still able to walk freely (i.e. up to 1.5 persons/m^2). Theoretical predictions were verified, and showed reasonably close agreement, by comparison with the results of the full-scale tests on the Millennium Bridge published by Dallard et al. [73,141,167]. However, for simplicity the analysis presented was based on a simply supported bridge with sinusoidal lateral mode shape, similar to the solution proposed by Dallard et al. [141]. The analysis thus should be generalized to include various structural systems when the actual modes of vibration of the bridge are not necessarily sinusoidal.

There are three other studies worth mentioning. Strogatz et al. [176] carried out a study motivated and supported by the analogy between human walking and rhythms of other biological processes, such as operation of neurons and behaviour of fireflies, being affected by weak periodic stimuli. In this case the rhythm is pacing and the weak stimulus is the lateral motion of the bridge to random pedestrian excitation. The result is a critical crowd size for ‘wobbling’ and synchrony to occur simultaneously. In the relation to the Solferino Bridge, Blekherman [177] alternatively proposed that the mechanism is autoparametric resonance when a mainly lateral mode frequency occurs at the half the frequency of mainly vertical or torsional mode. However, full-scaled measurements showed a lack of correlation between lateral and vertical vibrations [172,173]. Piccardo and Tubino [178] critically reviewed reported models describing the phenomena of large lateral vibrations caused by crowds walking across footbridges, classified as direct resonance [72], dynamic interaction [167,179–181] and internal resonance [177,182]. They then proposed a parametric excitation model covering the cases where modes are 1 and 0.5 times pacing rates. However, the authors noted that the model is not applicable when a footbridge was sufficiently ‘stiff’ in the lateral direction, i.e. its first lateral mode is around 1 Hz. They also admit that the model is based on an uncertain forcing function adopted in the study due to lack of the actual experimental measurements concerning pedestrian–structure dynamic interaction. Therefore, the authors highlighted the necessity of conducting free-field measurements on flexible footbridges, recording simultaneously the bridge response and the pedestrian motion, in order to provide reliable models of pedestrian-induced excitation of such structures.

Some of the most recent site measurements showed a lack of evidence of pedestrian lock-in to a single mode, indicating that this is not necessarily the triggering mechanism of dynamic instability. On the Changi Mezzanine Bridge, Brownjohn et al. [172] noted that a hardly evident peak in the spectra of vertical responses at twice the lateral frequency, for which the bridge lateral amplitude increased significantly under the pedestrian crowd, cast doubt that the synchronization had occurred. In other words, if there was synchronization to the lateral frequency, there would also be synchronization of vertical forces at twice this frequency. This is because the period of the medial–lateral force is two times longer than the period of the corresponding vertical force, as explained in Section 3.1 and also illustrated in Fig. 12. The results are in line with recent findings for crowd excitation observed on the Cliffton Suspension Bridge [173]. Despite the absence of synchronization, in both studies data analysis showed that the pedestrian behaviour could be reliably described by the negative damping model proposed by Dallard et al. [167] in developing a solution for the Millennium Bridge where lock-in clearly happened in the lateral direction. Additionally, an Eq. (9) was found to estimate quite well the critical crowd size. This provides further evidence that underlying mechanism of human–structure dynamic interaction remains unclear, pointing instead to models such as proposed by Barker [183] and Macdonald [184]. These will be reviewed in the next section.

5.2. Synchronization between structure and individuals

Dallard and co-investigators went further and continued experiments in an artificial laboratory environment involving single pedestrians walking on a moving platform [141,167]. The results revealed that the fundamental component of lateral force increases with the amplitude of the platform movement, but were apparently insensitive to the shaking frequency (Fig. 31a). Also shown in the Fig. 31b is the estimated mean probability that individuals will synchronize their pacing rate to the swaying rate of the platform. Willford [185] later added that the tests indicated 40 percent probability of people adapting their movement to the lateral swaying of the bridge at 1 Hz with amplitude of 5 mm.

Studies on pedestrians trying to walk on a moving surface having large amplitudes of lateral vibration (up to 100 mm) were done by McRobie et al. [14]. A common response of humans to the platform motion was to spread feet apart and to walk at the pacing rate such that feet and deck maintained a constant phase relation. Other walking patterns involved crossing the feet or walking in 'undulating lines'. However, there were subjects who did not show a clear change of gait. They tended to adjust their walking pattern in the way that absorbed energy leading to attenuation of vibrations and bringing the experimental rig to an effective halt [14]. For walkers whose motion led to a build-up of vibrations, lateral forces were approaching 300 N amplitude towards the end of the experiment. The authors pointed out that this was around four times the proposed Eurocode 5 [186] design value of 70 N for normal walking. In contrast, measurements on lateral walking forces carried out by Pizzimenti and Ricciardelli [89] using an instrumented treadmill vibrating in the lateral direction with fixed amplitude and frequency reported that Eurocode 5 tends to overestimate the force amplitude by factor 2.5. It seems that the treadmill walkers could adapt quickly to the specified vibration level in an effort to minimize discomfort and save energy. Moreover, this relaxing walk synchronized by the treadmill lateral sway is the most likely explanation for the lower force amplitude. Here, it becomes apparent that greater insight into the complexity of human motion is necessary to understand how human activities affect vibrations of structures. It is important to link biomechanical understanding on human gait and civil engineering knowledge on dynamics of structures to solve the problem whose solution is beyond the scope of civil engineering domain alone.

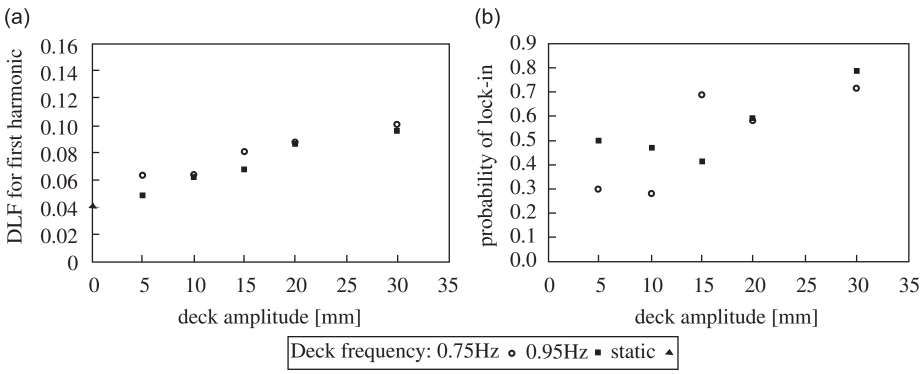

Fig. 31. (a) DLF and (b) probability of human–structure synchronization for a single person as a function of the moving platform amplitude and frequency (after Dallard et al. [167]).

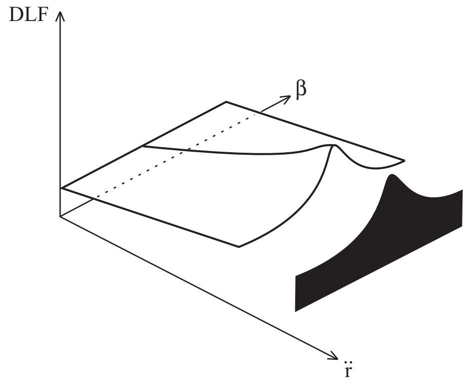

Fig. 32. 3D illustration of the lateral dynamic load factor (DLF_L) as a function of structural acceleration $\ddot{r}$ and the frequency ratio β (after Rönnquist [90]).

In a study of large lateral sway, Rönnquist [90] carried out experiments designed to record time series of lateral dynamic load and corresponding structural response induced by pedestrians crossing a section model of a footbridge in horizontal lateral motion. He showed that the magnitude of the increase of a pedestrian-induced excitation depends on the actual horizontal acceleration of a bridge deck $\ddot{r}$ and the frequency ratio $\beta = f/f_n$, where f is a pedestrian pacing rate and f_n is lateral natural frequency of the structure. This means that for a constant pacing rate, the walking load varies for each footstep depending on the structural response $\ddot{r}(t)$ at the position of a pedestrian along a bridge. When β was close to 1, the walking frequency gradually synchronized with the natural frequency of the structure and then remained more or less constant in resonance (Fig. 32). Moreover, the resonant effect was at its highest around lateral deck acceleration of $1\,\mathrm{m/s^2}$. On the other hand, at non-resonant pacing rate the magnitude of lateral walking forces followed a lower and more linear increase with increasing deck acceleration, as illustrated in Fig. 32. The sampled data were passed through curve fitting process, thus the first four lateral DLFs could be analytically described as

$$\mathrm{DLF}_L^{1\mathrm{st}} = 0.14 - 0.095\mathrm{e}^{-(0.45+1.5\mathrm{e}^{-(1/2)(f-f_n/0.07)^2})\ddot{r}^{1.35}} \tag{11}$$

$$\mathrm{DLF}_L^{2\mathrm{nd}} = 0.010 + 0.008\ddot{r} \tag{12}$$

$$\mathrm{DLF}_L^{3\mathrm{rd}} = 0.015 \tag{13}$$

$$\mathrm{DLF}_L^{4\mathrm{th}} = 0.005 \tag{14}$$

where $\mathrm{DLF}_L^{1\mathrm{st}}$ of 0.14 is its absolute upper limit value. The author also suggested these predictions should be restricted to the range of lateral bridge acceleration between 0 and $2\,\mathrm{m/s^2}$. The main drawback of this study is the lack of statistical reliability. Although the lateral walking force model was validated successfully on the Larder Bridge in Norway, the study still needs validation on different full-scale bridges with different structural systems and with and without problems of excessive lateral vibrations. The study also lacks detail on the synchronization mechanism. There are uncertainties of how this delicate mechanism is actually triggered off and what drives the pedestrian pacing rate towards the frequency of perceptible structural vibrations.

Various authors have proposed models of the lateral dynamic instability, based on lock-in [167,176,179–181] or certain frequency ratios [177]. Baker [183] went further and adapted a mechanism of swinging pendulum-like walking from the biomechanics field. The model assumes that humans continue movement by transferring from one pendulum-like stance leg to the next without the double support phase, alternatively left and right, and unaffected by the bridge motion. The pedestrian is modelled as a point mass, placed at the body centre of the mass which is approximately in the pelvic area [125], that moves in a straight line forwards supported by an inclined rigid massless leg. He showed that the work done on the bridge in the lateral direction as a result of the weight resolved along an inclined leg is an asymmetric function, even when the pedestrian walks at a different frequency to the bridge motion. This is because the lateral force increases as the bridge moves away from the mass, but decreases as the bridge moves towards it. Hence even uncorrelated pedestrians put energy into the lateral mode leading to excessive lateral bridge motions which had previously only been expected from strongly synchronized crowd. This works for any pacing rate at or above the lateral mode frequency. However, the major shortcoming of the model is that the inertia of the BCOM contributing to the lateral force has been neglected.

Inspired by this approach, Macdonald [184] recently developed a more refined model to describe pedestrian–structure dynamic interaction, based on the control of whole body balance in lateral plane during walking. In this, balance is achieved most effectively by the control of the position, rather than the timing, of foot placement for each step, based only on the final position and velocity of the BCOM from the previous step. As a result, without altering their pacing rate (unsynchronized with the lateral bridge sway), the pedestrian generates additional lateral force components due to inertia of the BCOM, which may be at any walking frequency. These additional forces were found equivalent to the pedestrian effectively acting as a negative damper to the bridge motion. Hence, without synchronization, this mechanism can explain the empirical negative damping model derived from tests on the Millennium Bridge [163,167]. It is also in line with the measurements on the Changi Mezzanine Bridge [172] and Cliffton Suspension Bridge, where uncorrelated crowd behaviour resulted in large vertical responses. However, Macdonald noted that the present version of the model cannot provide the numerical results which can match accurately the full-scale measurements. Moreover, the model does not account for large lateral sway for which pedestrians might change their gait, such as to synchronize with the bridge or stopping walking.

5.3. Lock-in and Scruton number

An entirely different approach to those considered so far was given by McRobie et al. [14]. They recognized the analogy between the wind excitation of flexible structures and crowd loading of lively footbridges. In wind engineering, the tendency for vortex shedding to cause wind-induced structural oscillations is measured by the dimensionless Scruton number which is a product of damping and the ratio of representative structural and fluid masses [187]. Similarly, for each vertical mode of a footbridge, the vertical pedestrian Scruton number (vPSN) may be defined as [14]

$$\mathrm{vPSN} = k_1 k_2 m \tag{15}$$

where $k_1 = \zeta/0.005$ relates the damping ratio of the empty structure to that of a typical mode in a lightly damped steel structure of 0.5 percent, and $k_2 = 0.6/n$ takes account (if desired) the possibility that crowd density n could be different from the typical value of 0.6 persons/m^2, and m is mass per unit deck area for an equivalent simply supported beam having constant cross section expressed in kg/m^2. As for the case of wind excitation, to have a structure which will meet vibration serviceability requirements, a large Scruton number is generally preferred.

For the purpose of analysis of lateral bridge oscillations, Newland [187] defined lateral Scruton number as

$$S_{\mathrm{cp}} = 2\zeta M/m \tag{16}$$

where M is modal mass, or, for a uniform deck, bridge mass per unit length. Similarly, m is modal mass of pedestrians, or, for a uniform bridge deck with evenly spaced pedestrians, pedestrian mass per unit length. Also, he determined that the limiting value of structural damping ratio ζ needed to prevent build-up of lateral vibrations must satisfy the following equation:

$$\zeta > \frac{\alpha\beta m}{2M} \tag{17}$$

where the coefficient β reduces the effective pedestrian mass m due to imperfections in synchronization between pedestrians themselves, whereas parameter α relates the amplitude of lateral body movement of pedestrians to the amplitude of the structural lateral sway. Substituting from Eq. (16), Newland's stability criterion (17) becomes [187]:

$$S_{\mathrm{cp}} > \alpha\beta \tag{18}$$

A novelty proposed in Newland's model is the factor α which accounts for changes in lateral body movement due to lateral deck motion. In this way, this model includes body motion inertia forces, assuming that the movement of the body centre of mass is a fraction of the movement of the feet, therefore $\alpha \leqslant 1$. However, the model is limited to small amplitude of structural movement (up to 10 mm), where it is reasonable to expect that humans behave as rigid masses and can counteract the body inertia forces by identical lateral force generated against the deck. At larger displacements the upper body parts would not follow the feet and legs, but are expected to move less to keep the lateral balance. As pointed out by Newland himself, the movement of the centre of mass of the pedestrian would then be significantly different from movement of the bridge deck. Thereupon, the lateral force a person generates against the flexible structure must react against inertia of their body, so the sum of products of masses and accelerations for all body parts must equal the lateral GRF at all times [187]. Here, the vibration serviceability issue is stretched to breaking point where the need for interdisciplinary research involving biomechanical studies of human gait becomes absolutely indispensable. Namely, contribution of body motion to GRFs is essentially a biomechanical problem, generally referred to as 'inverse dynamics', and will come under the spotlight later in Section 8. To help in understanding better its principles, the next two sections provide background knowledge on how motion of the body (or bodies) can be measured (Section 6) and how masses of different body parts can be estimated (Section 7).

6. Kinematics of human body motion

As opposed to kinetics, kinematics is the study of bodies in motion without considering the forces (both internal and external) that cause the body movement [188]. It is focused on description and quantification of linear and angular positions of bodies in space and their time derivatives: linear and angular velocities and accelerations.

6.1. Motion analysis techniques

Modern motion analysis dates back to 1836 when the Weber brothers carried out extensive observations of people walking [30]. During the second half of the nineteen century Marey et al. [189] and Muybridge [190] performed pioneering research in the assessment of human locomotion making photographs of a man walking. Finally, by a more detailed approach to imaging techniques, Bernstein [191] initiated the formal study of kinematics. Early methods also involved the use of electrogoniometers [192–195] which were designed to convert electrical signals from transducers attached to the adjacent limb segments into continuous measurements of the joined angle. Additionally, accelerometers were used for measuring body acceleration directly [196–198].

Broadly speaking, the current state-of-the-art procedure for human movement analysis typically involves several discrete steps [199]:

(1) The motion of tracking markers attached to the subject is recorded using video-based optoelectronic technology such as cameras or sensors [200]. If device is optoelectronic, it means that it interacts with light. General principles, known as stereophotogrammetry, apply to majority of video-based systems, and will be discussed in Section 6.2.
(2) A biomechanical model of human body is defined to represent selected characteristics of a test subject such as the number of body segments, their inertial properties (e.g. mass and centre of mass) and number of degrees of freedom (DOF). Overview of different biomechanical models will be presented in Section 7.
(3) The kinematics of the model is calculated by determining the transformation from the recorded trajectories of tracking markers to the motion of the biomechanical model. Section 6.3 explains this issue in more detail.
(4) The application of 'inverse dynamics analysis' to the kinematics of the biomechanical model and to the location, magnitude, and direction of externally applied forces (e.g. GRFs acting on the foot). This biomechanical technique will be described thoroughly in Section 8 and finally put into civil engineering context to estimate GRFs when the body kinematics is measured.

6.2. General approach to optoelectronic systems

The key objective of optoelectronic stereophotogrammetry is to estimate instantaneous 3D position and orientation of the body segments using reconstructed trajectories of markers placed on the body [200]. The most common way is to segment the body between the joints [201]. For example, the thigh is defined as a part of the body between the knee and the hip joint. Furthermore, if assumed that the body segments are non-deformable, the human body can be described as a kinematic chain of rigid links hypothetically joined with spherical hinges [202]. Not all body joints are spherical hinges, but for the purposes here, there is no loss of generality assuming spherical hinges. In addition, although each body segment represents a portion of the human body referred to a bony part and corresponding soft tissue, in this case the body segment represents a single bone only.

The 3D representation of the movement is reconstructed from optical sources attached to the skin and serve as markers (therefore also called skin-markers), as illustrated in Fig. 33. Motion analysis markers can be retroreflective (passive) and light-emitting (active). Passive markers are illuminated by an external power source, exposed to stroboscopic rays of light produced by light emitting diodes (LED). Markers reflect light impulses recognized by a multi-camera system, also called a

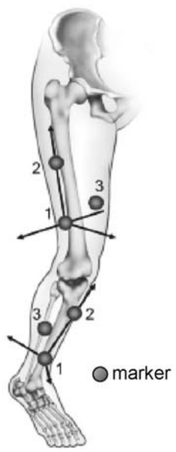

Fig. 33. SCSs for the shank and thigh reconstructed from skin markers (after Cappozzo et al. [200]).

multi-sensor system, which then records position of the each marker in form of video frames. The video frames (also known as video images) need additional processing using pattern recognition software [203] or specialized hardware [204] to identify positions of each marker. Conversely, active optoelectronic systems utilize self-illuminated markers. Each active marker in the set has a LED that pulses sequentially and is activated at slightly different instants of time in the order of microseconds [205]. This time shift enables sensors to detect positions of markers independently (i.e. each marker is given a unique identity), so no software processing is required to identify individual marker positions. Between two consecutive pulses, marker position can be determined using interpolation. Although passive marker systems, such as VICON [18], have the advantage of using lightweight reflective markers without wires and batteries on the body of the test subject [206], their accuracy usually cannot reach the standards of their active marker counterparts [207]. Even if markers are temporarily lost from a field of view, active marker systems, such as CODA [19] can maintain the identification of markers automatically by interpolation and optimization algorithms [208]. Also, contrary to passive systems, virtual merging of markers when their trajectories pass across each other cannot occur with active system, so the markers can be placed close together [209] which is their very important advantage.

The core technology of passive marker systems is a set of cameras. In the case of active marker systems they are called sensors instead. Both calibrated cameras and sensors track each skin-marker while it moves with a test subject. However, the two technologies have nothing in common. Each of the cameras can provide only a set of 2D passive marker coordinates placed in the plane perpendicular to its optical axes [200]. If at least two cameras identify the same marker, 3D coordinates can be estimated using the geometrical properties of central projection from multi-camera observations and mathematical triangulation method [202]. This is similar to the human brain which uses input from both eyes to perceive depth in the field of vision [210]. On the other hand, a single sensor is enough to measure the locations of active markers in 3D with high resolution and accuracy. This is because a single unit (sensor) has multiple cameras built-in (e.g. a CODA sensor has three cameras). Multiple units may be combined to give even greater capture volume (so-called '3D volume') and to maximize visibility of active markers [211].

The markers are placed in a manner to satisfy technical requirements, such as high visibility from cameras or sensors and to minimize relative displacement between them and underlying bone during walking [200]. The latter is important since the assumption of rigid body segments has been made. Markers should therefore be placed on special locations on the body (Fig. 33), so-called anatomical landmarks (AL), where the thickness of the soft tissue between skin surface and bone is negligible [200]. Palpable bony prominences on the skin, also called bony landmarks, are commonly chosen for ALs. These can be identified easily in a repeatable fashion among humans. However, the choice of where and how to place target markers is a significant subject on its own.

A comprehensive review on optoelectronic stereophotogrammetry published recently in four parts by Cappozzo et al. [200], Chiari et al. [207], Leardini et al. [212], and Della Croce et al. [213] is recommended for further reading.

6.3. Tracking body segments in 3D space

Motion capture analysis involves typically two kinds of coordinate systems: global and local. Despite the International Society of Biomechanics (ISB) investing a great deal of time and effort in setting up standardization in the reporting of kinematics data [214], there is no standard coordinate system used within the international motion analysis community. However, researchers defined the global coordinate system (GCS), also called global frame, as an orthogonal right-handed Cartesian coordinate system with the X-axis pointing along the direction of progression, the Z-axis pointing vertically upward and the Y-axis pointing to the left (Fig. 34). This frame with arbitrary origin defines a fixed laboratory coordinate system from which positions of all markers are ultimately defined in space [34].

Generally speaking, the motion of rigid segments in space can be described fully by measuring three independent translations and three independent rotations with respect to the GCS [199]. Stereophotogrammetric procedures for measuring all six DOFs require that at least three non-collinear markers should be stuck to each segment (Fig. 33). These non-collinear markers are used to define local segment coordinate systems (SCSs), also known as local frames, rigidly fixed within each of the body segments (Figs. 33 and 34). Located independently, these orthogonal right-handed coordinate systems move with the segments as the segments move through space during gait (Fig. 34). Therefore, measurements of the instantaneous position and orientation of all SCSs with respect to the GCS can be used to calculate the whole body motion in real time and space. It can be done based on a principle of analytic geometry referred to as 'coordinate transformation' [34].

When using optoelectronic stereophotogrammetry, there are some principal sources of error which propagate to the kinematics data measured. Model calibration [213], soft tissue artefact [212] and instrumentation errors are highlighted in the next section as the most important to affect accuracy of a method to estimate GRFs indirectly from human body kinematics. Principles behind the method and potential for utilization in the civil engineering dynamics will be explained fully in Section 8.

6.4. Sources of error in optoelectronic analysis

Model calibration deals with the difficulty in determining anthropometry of individuals from two aspects: placing markers accurately with respect to specific anatomical landmarks (AL) and determining the location of the joint centres

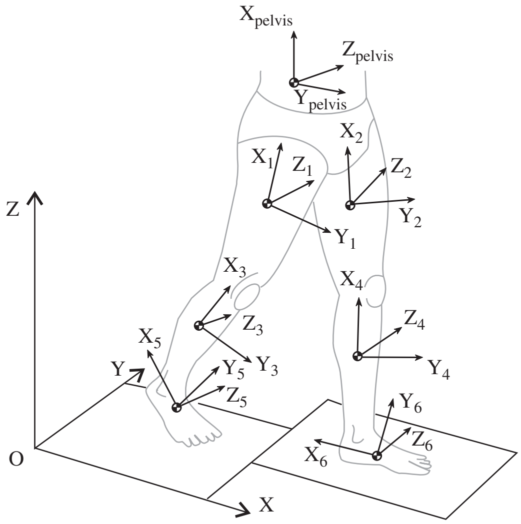

Fig. 34. Global (*X*,*Y*,*Z*) and segment (*x*,*y*,*z*) coordinate systems for lower extremities (after Vaughan et al. [237]).

[215]. Anatomical landmarks are palpable bony prominences such as hip, elbow, and ankle, which can be easily identified for diverse human population. However, many of them might be inaccurately defined in overweight test subjects. In this case, bony landmarks are not sharply defined points on the skin but surfaces, sometimes large and irregular, so a considerable thickness of underlying fat tissue makes their position difficult to locate [213]. Because of this, Riley et al. [65] suggested all subjects with a body mass index higher than 30 should be excluded from measurements. Here, the body mass index $\mathrm{BMI} = m/h^2$ was defined as the ratio of body mass m versus square of a subject's height h. However, including a higher number of markers [213] and advanced biomechanical software (e.g. Visual 3D by C-Motion, Inc [199]) can gain better accuracy in tracking anatomical landmarks for obese test subjects. Viewed from the perspective of civil engineering, this is of great importance because occupants of civil engineering structures are not only fit athletes, but also people with various body conditions.

Many researchers assumed that body segments are rigid. However, in recent years several studies have showed that ignoring soft tissue deformability relative to underlying bone may affect significantly the reliability of kinematic measurements [216–218]. This deformability, known as 'soft tissue artefact', is dominant during highly accelerated movements such as the heel impacts (see Section 2.3). This is because soft tissue wobbles significantly when the heel abruptly hits the ground. Skin markers thus oscillate considerably with respect to the underlying bone inducing noisy kinematic data [219]. Fuller et al. [220] measured displacements of the individual markers relative to the bone of up to 20 mm, whereas Reinschmidt et al. [221] reported values up to 40 mm. Early techniques designed to minimize the contribution of and compensate for the effects of this artefact include tissue fixators [222], markers mounted on bone pins [220] and Roentgen photogrammetry [223].While these methods provide direct measurements of the skeletal movement, they are invasive, painful or expose the test subject to radiation [212]. However, low-pass filtering of raw kinematic data seems to be the only appropriate (it is cheap and highly effective) method suitable for civil engineering [44].

To the best knowledge of the authors of this review, there is no study published so far which has utilized the optoelectronic systems described above in measurements of outdoor activities. With regard to this, there may be a problem with the application of the passive marker systems for monitoring people in their natural environments such as sport facilities, offices and footbridges. The reason for this is that stroboscopic light impulses generated by external power sources in passive marker systems might be hard to distinguish in daylight. Consequently, the multi-camera system might not be able to detect the reflected light from markers and thus provide adequate video images. Hence there is no alternative but to do the experiments during night. Also, the reflected light from passive markers cannot be detected if markers are outside the optimal distance from the cameras (usually <6 m). Alternative active marker systems do not struggle so much to detect a marker position in daylight, but the infra-red signal can easily become very noisy when the marker is far away from the sensors thus creating the same problem. Since the cameras/sensors must be at fixed positions to ensure that they do not move relative to the markers, monitoring people on long-span structures, typically lively footbridges for which the only fixed points are at the nearby ground, seems impossible using marker-based technology which is commercially available today.

Eliminating the need for markers would considerably reduce the subject's preparatory time and enable simple, time-efficient, and potentially more meaningful assessments of human movement [224]. Moreover such a system could allow tracking human motion in natural environments. Therefore, a new technique for human body kinematics estimation that does not require markers or sensors placed on the body would greatly expand the applicability of human motion capture in numerous fields of science, including structural dynamics. The terms markerless and marker-free are used interchangeably in this review for motion capture system without markers, and will be explained briefly in the next section.

6.5. Markerless motion capture systems

Markerless systems are typically divided into two categories, active and passive vision systems. Active systems, such as laser scanners and structured light systems, emit light in the visible or infra-red spectrum in the form of laser rays, light patterns or modulated light pulses [225]. They provide generally very accurate 3D measurements, but require a controlled laboratory environment and often are limited to static measurements (e.g. a full body laser scan to capture the surface of a human body). On the other hand, passive systems are advantageous as they only rely on capturing video images and thus provide an ideal framework for tracking subjects in their natural environment [226]. This is the reason why the main direction in development of marker-free motion capture technology is focused currently on employing passive systems.

Passive systems vary in the number of cameras used, the representation of captured data, types of algorithms, use of various human-body models, and the application to specific body regions or whole body [226]. The camera configurations range from using a single camera to multiple camera systems. Similarly to marker-based systems, multi-camera configurations utilize algorithms that can reconstruct 3D kinematics of various body parts from single 2D image planes. These algorithms usually employ image processing techniques for automatic identification of subject's boundaries based on pixel brightness [225,227]. Here the human form can be separated from the background in the image sequence of each camera using intensity and colour threshold identification [225–227]. When the body silhouette is identified, the body kinematics data can be extracted taking a model-based or model-free approach [224]. The most popular is the model-based approach in which a predetermined human body model with relevant anatomic and kinematic information is tracked or matched to the video images [226]. On the other hand, the model-free approaches attempt to determine the body features and its kinematics in the absence of an a priori generated model. It aims to represent morphology of each body segment by a relevant mathematical model, such as a cylinder or sphere, which should match the shape of the segment the best. Alternatively, a simple stick-figure can be used as a satisfactory approximation of the trunk and lower and upper limbs [226]. Unfortunately, due to technical limitations and errors in the shape and/or size of body whose motion is investigated, markerless systems still cannot reach the accuracy of their marker-based counterparts [225]. Moreover, the application of markerless technology in civil engineering to monitoring pedestrian crowd is still difficult because the algorithms to determine the body anthropometry cannot distinguish between the body segments of different individuals when they are huddled together.

After introducing basic methodology and application of kinetics (Section 3) and kinematics (Section 6) of human gait, the next section describes methods for estimating human anthropometry. This is necessary to achieve physically meaningful relationship between measurements of body motion and corresponding GRFs. Those relationships will be the final subject for discussion in Section 8 where all this biomechanical knowledge will be put together into the civil engineering context.

7. Anthropometry: body segment parameters

The anthropometry refers to measurement of a human body in terms of physical properties of body segments, such as mass and centre of mass, generally known as body segment inertial parameters (BSIP). This section contains a brief introduction and notes to estimating BSIP through the most prominent techniques that have been used to date. General descriptions of cadaver studies, mathematical modelling of human anthropometry and imaging and scanning techniques are included. For more detailed explanation on the subject, the reader should be referred to papers by Drillis et al. [228], Reid and Jansen [229], Nigg and Herzog [230], and Pearsal and Reid [231].

7.1. Cadaver studies

The first notable achievements in estimating segment inertia parameters date back to the nineteen century, when Harless [232] and Braune and Fischer [233] carried out detailed analyses on adult male cadavers. After being frozen, the cadavers were dismembered at each of the primary joints such as knees and elbows. Each segment was then weighed and the centre of mass was estimated using, for example, a specially designed balance plate.

In a more comprehensive study of eight male cadavers, Dempster [234] estimated the mass and centre of mass (Tables 2 and 3, respectively), volume, density and mass moments of inertia for the body segments. Similarly to Broune and Fischer [233], he described the segmental masses as proportions of the total body mass, and the locations of the centres of gravity as ratio of the segment's length. Dempster [234] defined the segment's length as distance between proximal and distal joint centres of rotation. This definition is still considered as a gold standard in biomechanics [214,235]. For example, estimated mass of the thigh is 10 percent of total body mass, located at 43.3 percent along the distance between hip to knee joint centre (see Fig. 35 for comparison).

In 1969, Clauser and coworkers [236] conducted a study designed to supplement the existing knowledge of the anthropometry of body segments and to permit more accurate estimation (Tables 2 and 3). The study was based on 13 male

Table 2
Segmental mass as percentage of total body mass after different authors.

Source	Dempster [235]	Clauser et al. [237]	De Leva [252]
Hand	0.0060	0.0065	0.0061
Forearm	0.0160	0.0161	0.0016
Upper arm	0.0280	0.0263	0.0027
Foot	0.0145	0.0147	0.0013
Shank	0.0465	0.0435	0.0433
Thigh	0.1000	0.1027	0.1416
Trunk	0.4970	0.5070	0.4346
Head	0.0810	0.0728	0.0694

Table 3
Locations of segmental centre of mass after various authors.

Source	Dempster [235]		Clauser et al. [237]		de Leva [252]	
	Proximal	Distal	Proximal	Distal	Proximal	Distal
Hand	0.506	0.494	0.1802	0.8198	0.7900	0.2100
Forearm	0.430	0.570	0.3896	0.6104	0.4574	0.5426
Upper arm	0.436	0.564	0.5130	0.4870	0.5772	0.4228
Foot	0.500	0.500	0.4485	0.5515	0.4415	0.5585
Shank	0.433	0.567	0.3705	0.6295	0.4459	0.5541
Thigh	0.433	0.547	0.3719	0.6281	0.405	0.5905
Trunk	0.495	0.505	0.3803	0.6197	0.5514	0.4486
Head	1.00	0.000	0.4642	0.5358	0.4024	0.5976

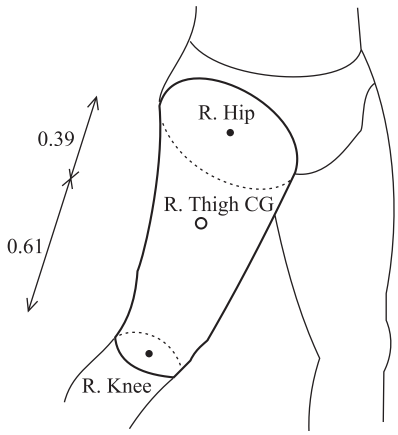

Fig. 35. The location of the centre of gravity of the right thigh, with the joint centres (hip and knee) and corresponding body segment parameters (0.39, 0.61) (after Vaughan et al. [237]).

cadavers, which each were dissected into 14 body segments. Not only the mass, volume and centre of mass for the each segment were collected, but also anthropometric measurements such as the length, circumference and segmental breadth or depth. Based on these measurements, a series of regression equations were defined for estimating the BSIPs on living subjects.

For practical reasons, the main criterion for selection of regression parameters should be a limited number of anthropometric measurements that can be gathered easily and quickly [201]. A good example is nonlinear regression by Vaughan et al. [237] for estimating the masses and centre of masses of the lower extremities (Fig. 36). For example, an equation for prediction of the thigh mass is given as [237]:

$$\text{mass of thigh} = (0.1032)(\text{total body mass}) + (12.76)(\text{thigh length})(\text{midthigh circumference})^2 + (-1.023) \tag{19}$$

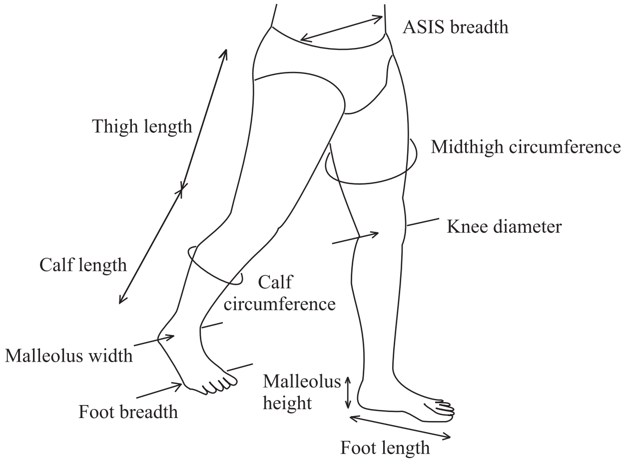

Fig. 36. The anthropometric measurements of the lower extremity required for prediction of body segment parameters (after Vaughan et al. [237]).

where masses are expressed in kg and lengths and circumferences in *m*. It should be stressed that regression equations can be used successfully in BSIP estimation, but under the assumption that all individuals have the same body proportions [238]. However, this cannot be true in general and might lead to significant errors in estimates for those individuals that differ significantly from the average of group from which regressions were derived. Moreover, cadaver studies are typically based on a limited number of elderly males, and with a very few exceptions [239,240] the vast majority of these studies examined a Caucasian population only. In this way, the cadaver-based studies seem to be inappropriate for BSIP estimation of women, children, young adults, and non-Caucasians [231]. Therefore, alternative methods for more direct assessment of body inertial characteristics that account for differences in morphology, age, gender and race should be utilized in future studies.

7.2. Mathematical modelling

One method of estimating the BSIP of a human body is to develop a mathematical model that approximates the body segments as fairly simple [241–243] or complex [244] geometric solids. Such models vary in the number and shapes of the segments, from unsegmented rigid body [245], 15-segment model with standard geometric shapes [242], 16 segments composed of elliptical zones [246–248], and finally complex 17-segment human body model [244]. Two of these models are illustrated in Fig. 37.

According to Reid et al. [229], among a number of mathematical models proposed to date the most accurate is the anthropometrico-computational model (so-called hominoid given in Fig. 37b) developed by Hatze [244]. It is able to distinguish between male and female subjects taking into account the actual shape fluctuations and asymmetry of the individual segments, including all changes in body morphology due to obesity, pregnancy, and age [249]. Moreover, this is the only mathematical model which accounts for varying tissue densities both across and along the body segments using a ‘subcutaneous-fat indicator value’ capable to adjust the density of specific segmental sub-elements (e.g. bones and fat). Experimentally confirmed on a large number of subjects, the overall accuracy of the model is better than 3 percent [249]. Despite the high accuracy, the model has not gained widespread popularity. This is because collecting the model input parameters from test subjects is complicated and time-consuming. The original version required 242 measurements while a new modified version requires ‘only’ 133 anthropometric measurements.

7.3. Scanning and imaging techniques

Since medical imaging techniques have become available to investigators worldwide, anthropometric measurements have reached high standards enabling assessment of living individuals. Using advanced technology, such as gamma-mass scanning, computerized tomography (CT), magnetic resonance imaging (MRI), ultrasound and dual energy X-ray absorbtiometry (DEXA), it is possible to include variations in morphology, physical fitness, age, gender and race diversity into BSIP estimations.

Zatsiorsky and Seluyanov [250] carried out an extensive study on the BSIPs of 100 male and 15 female Caucasian students using a gamma scanner. They determined density distribution of underlying tissues based on the intensity of absorption of the gamma radiation, and then, using the gamma scanner images, calculated the volume of each segment. Having these data, they could estimate the mass, centre of mass and principal moments of inertia in 3D space for a 15-segment body model. Moreover, they applied linear regression and developed equations to assess individual BSIPs based on total body mass, segment length and circumference [250].

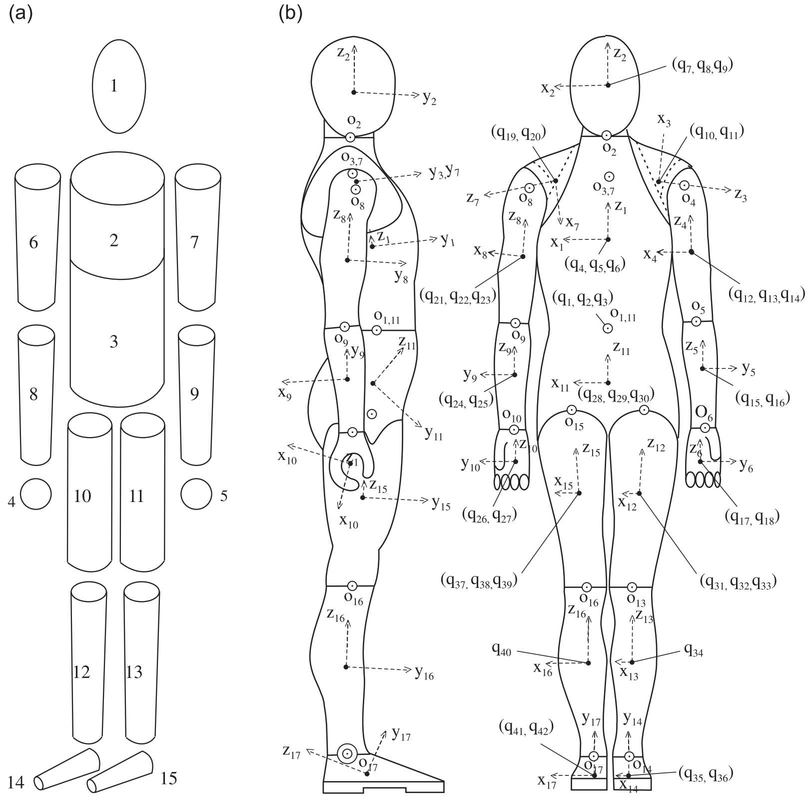

Fig. 37. Mathematical modelling of human body: (a) 15-segment model of Hanavan [242] and (b) lateral and frontal view of the 17-segment hominoid of Hatze [244].

de Leva [251] went further and adjusted the original data from Zatsiorsky and Seluyanov [250] to define centre of mass locations relative to the joint centres (as Dempster did) instead of anatomical landmarks. The scaling equations of de Leva [251] represent the most complete and practical series of predictive equations to date [252]. This work typically produces errors of only 1 percent on centre of mass locations.

Several studies [253–255] used X-ray computerized tomography (CT) to reconstruct 3D representations of the segments. Knowing densities of various tissues and contours of the segments, it is possible to estimate BSIPs [256]. However, both conventional X-ray and CT are not widely used because of high radiation doses. On the other hand, magnetic resonance imaging (MRI) and dual energy X-ray absorptiometry (DEXA or DXA) appeared recently as new non-invasive techniques commonly used in medical research for measuring bone mineral density and the body composition in general [257]. Although its use as a gold standard has been questioned [258,259], when compared with a number of BSIP estimation techniques, DEXA can be regarded as a precise method for measuring anthropometric data with error under 3.2 percent [260–263]. In spite of the fact that numerous studies verified that both MRI and DEXA technology can provide reliable estimations of segmental inertial properties, current research can offer estimations of upper and lower limbs only.

Although scanning techniques provide very precise BSIP measurements, the high cost of instrumentation and need for qualified personnel have not gained them popularity among the biomechanical community. Moreover, in the last years biomechanical researchers have faced a growing need for a method that could determine BSIP more rapidly, but still accurately enough. To meet these criteria, Hatze and Bacca [264] suggested a video-based system for BSIP estimation. Their algorithm uses a set of anthropometric dimensions obtained from video images and then employs the anthropometrico-computational model by Hatze [244] explained in previous section. More recently, Bacca [265] improved this image processing method applying techniques for automatic identification of subject boundaries with sub-pixel accuracy. With application in both markerless capture kinematics and non-invasive estimation of inertial properties of body segments, the video image processing might perhaps become the leading method in near future.

8. Indirect measurement of human loading

This section essentially evolves from biomechanical research in kinetics (Section 3), kinematics (Section 6) and human anthropometry (Section 7) previously covered in this review.

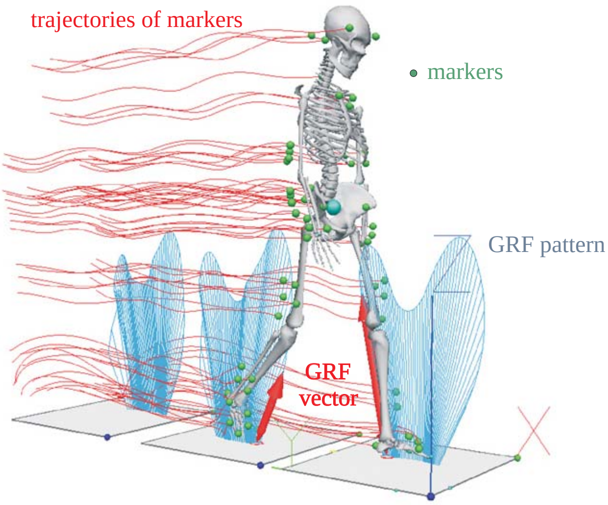

Fig. 38. Typical experimental setup for a 3D kinematic and kinetic analysis of a walking stride (courtesy of C-Motion, Inc. [199]).

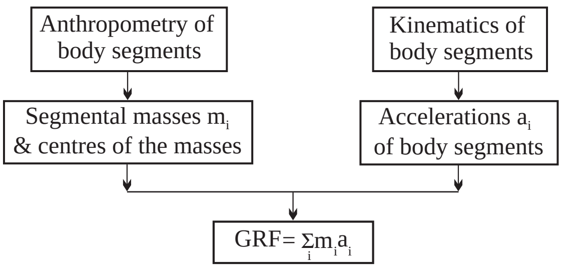

Fig. 39. Flow chart of indirect measurements of human-induced loading.

In biomechanical applications, motion tracking systems are traditionally used together with force plate measurements (Fig. 38) and information on the BSIP to estimate values of internal forces in patients. This method is referred to as inverse dynamics, a field of mechanics that bridges the areas of kinematics and kinetics based on Newton's laws of motion [266]. On the other hand, for application in the civil engineering context a slightly different approach to inverse dynamics may be more powerful. It offers excellent potential for indirect measurements of the GRFs via combination of visual motion tracking data (Section 6) and known body mass distribution (Section 7), as summarized in Fig. 39. It therefore presents great potential for a novel method, in the context of a civil engineering application, to estimate continuous human-induced forces applied directly to structures under a wide range of conditions.

8.1. Theoretical background

When applied to the human body, Newton's second law states that external force acting upon the body (i.e. ground reaction force vector $\mathbf{F_{GR}}$) is equal to product of the body mass m concentrated at a single point referred to the body centre of mass (BCOM), and its acceleration $\mathbf{a_{CoM}}$:

$$\mathbf{F_{GR}} = m\mathbf{a_{CoM}} + m\mathbf{g} = m(\mathbf{a_{CoM}} + \mathbf{g}) \tag{20}$$

where $\mathbf{g}$ is gravity. The BCOM actually represents the mean position of the total mass of the human body as a multi-segment system. Taking the mass distribution into account (Section 7), Eq. (20) becomes

$$F_{GR} = \sum_{i=1}^{s} m_i(\mathbf{a_i} + \mathbf{g}) \tag{21}$$

where m_i and $\mathbf{a_i}$ are mass and acceleration vector of the centre of the mass of the i-th body segment, and s is the total number of segments.

8.2. Experimental verification

Since about 1970, development of the modern force plate and motion capture technology has resulted in several attempts to estimate contributions of various body segments to ground reaction forces. Among the first was the study by Thornton-Trump and Daher [31]. They gathered kinematic data from the published research of Bresler and Frankel [267], Murray et al. [124,268] and Murray [30], while mass and centre of mass of various body segments were adopted from Dempster's regression equations [234]. The upper part of the body, called the head-arm-trunk (HAT) complex, was modelled as one rigid segment. On the other hand, thighs, shanks and feet were considered separately and hypothetically hinged by hip, knee and ankle spherical joints. Fig. 40 presents a plot of estimated vertical GRFs using Eq. (21), compared with data measured by Cunningham [269]. The results were not very accurate and did not show the force spike at the beginning of the gait cycle (Fig. 9), but the characteristic M-shape of the vertical GRF pattern was confirmed. Although the authors did not directly quote the sampling rate of the kinematic data, it is most likely that such an imprecision appeared due to a low sampling rate which missed the high frequency sharp peak due to heel strikes. Also, the predicted and measured GRFs were not collected from the same test subject, so differences in body morphology and gait style in different studies certainly affected the results. As the same authors suggested, more detailed model of the upper body, which would consider head, trunk and arms as individual segments, could also result in further improvement.

Miller and Nissinen [270] carried out a series of experiments designed to predict vertical GRF for gymnasts turning a forward somersault. Although they analysed neither walking nor running, this study is worth mentioning because it raised many important questions. Kinematic data were collected using a single camera system operating at approximately 197 Hz, whereas the impact force was recorded simultaneously by a force plate at a sampling rate of 1000 Hz. The displacements recorded were first low-pass filtered at cut off frequencies of 7–9 Hz, then differentiated twice with respect to time to obtain accelerations of body segments. They concluded that only the low-frequency components of the GRF could be predicted accurately (Fig. 41). The failure to estimate high-frequency components almost certainly resulted from using too low a cut off frequency.

More recently, Bobbert et al. [271] calculated segmental contributions to the vertical GRF during running (Fig. 42). Bodies of each of the three participants were modelled as a kinematic chain of seven segments, as in the study of Thornton-Trump and Daher [31]. Positions of motion tracking markers attached on the segments were recorded as a function of time using four video cameras operating at 200 Hz. These were filtered and finally differentiated twice to obtain accelerations of corresponding mass centres. To evaluate the accuracy of the model given by Eq. (21), the GRFs were also directly measured with a force plate, sampled at 1000 Hz and synchronized with the video system. Special care was taken to reproduce the high frequency transient loading that occurs when a heel strikes the ground. This was quite difficult to achieve since the markers, especially those attached to the lower extremities, oscillated at high frequencies during initial heel impact due to soft tissue artefact as explained in Section 6.4. Despite special precautions taken to minimize these unwanted effects (e.g. mounting limbs rigidly on wooden rods), time histories of the marker positions still remained too noisy. As an alternative, Bobbert et al. showed that a good correlation between directly measured force signals and calculated force signals could be obtained if displacements of individual segments were filtered with different cut off frequencies. The best result was obtained when time histories of foot, ankle and knee markers were filtered at 50 Hz low pass cut off frequency, 20 Hz for hip markers, and at 15 Hz cut off for the markers on the HAT complex (Fig. 42c). The magnitude of the heel impact force was estimated with <10 percent error, whereas the time occurrence of the peak was estimated with <5 percent error. Bobbert and colleagues emphasized that the fluctuations which caused the errors were not noise, but represented real acceleration of the markers. This is because the human body is not assembled of rigid segments, hence marker accelerations could not reflect accelerations of the segmental centre of mass, as explained in Section 6.4. Moreover, markers

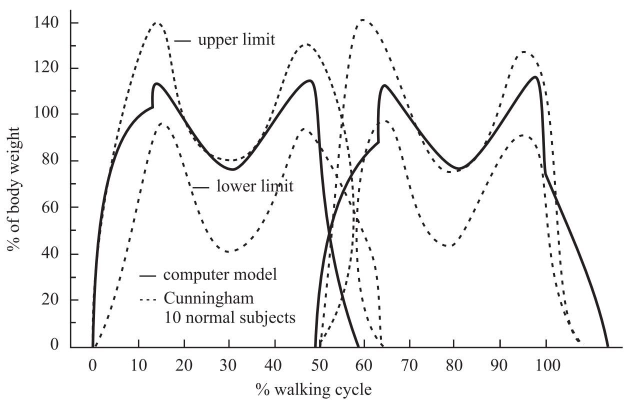

Fig. 40. Vertical reaction forces estimated from kinematic data (after Thornton-Trump and Daiher [31]).

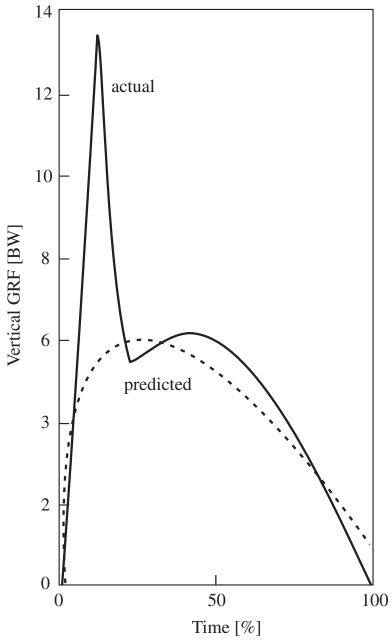

Fig. 41. Actual and predicted vertical GRF (after Miller and Nissinen [270]).

were placed on neither the soft tissue mass nor the bony structure, but on the skin which may have large oscillations during impacts, especially in the case of overweight test subjects.

8.3. Reconstruction of walking forces

Following biomechanical studies of his predecessors [31,270,271], in his doctoral thesis Kerr [44] demonstrated the Newtonian approach to predict vertical GRFs of level walking and both ascending and descending stairs. The study included equipment for direct force measurement comprising a force plate set up to 1000 Hz and CODA system [19] for visual motion tracking operating at 200 Hz. To estimate the BSIP, he used a 12-segment anthropometric model by Clauser et al. [236]. Kerr confirmed that if the same low-pass filter were applied to all marker displacements, there would be a trade-off between the benefits of smoothing out the noise due to the skin artefact and losing the initial peak. Moreover, the same combination of cut off frequencies for various body parts proposed by Bobbert et al. [271] in the study of running forces led to the best estimation of level walking GRF. Predicting trace and the peak force value almost completely fell within ± 10 percent error bands on the actual GRF records measured by a force plate (Fig. 43). Conversely, poor correlation was found for stair walking.

One way to improve the accuracy of inverse dynamics method is to apply various optimization criteria, such as minimal energy expenditure already mentioned in Sections 3.5.2 and 4.1.2. Much research has also been done in domain of cybernetics and artificial intelligence to provide an analogy between human gait and locomotion of bipedal robots. A prime example of implementation of such research in medical biomechanics is a method developed by Chou et al. [119] based on combination of robotics and 'multi-state optimization algorithm' to generate the energy efficient motion of the swing limb for a patient with abnormalities in the gait cycle. The method was validated on six healthy subjects and the predicted GRF was not significantly different from those directly measured (Fig. 44). It seems that similar approach might be a powerful tool for development of future load models in civil structural engineering.

Practically all studies described here, disregarding the activity investigated, were dealing with recovering only vertical GRF on rigid surfaces induced by a single test subject. This creates a considerable potential for future research of three-component forces generated by single and multiple pedestrians on more or less perceptibly moving structures.

9. Summary and conclusions

This paper has reviewed 250 references dealing with different experimental and analytical characterizations of human walking forces and their application in vibration serviceability design of civil engineering structures when subjected to pedestrian movement such as footbridges, floors and staircases. The state-of-the-art was found to be fragmented and under-researched, so the main aim of this review was to provide consistent background information and to indicate major gaps in the subject signifying directions for future research.

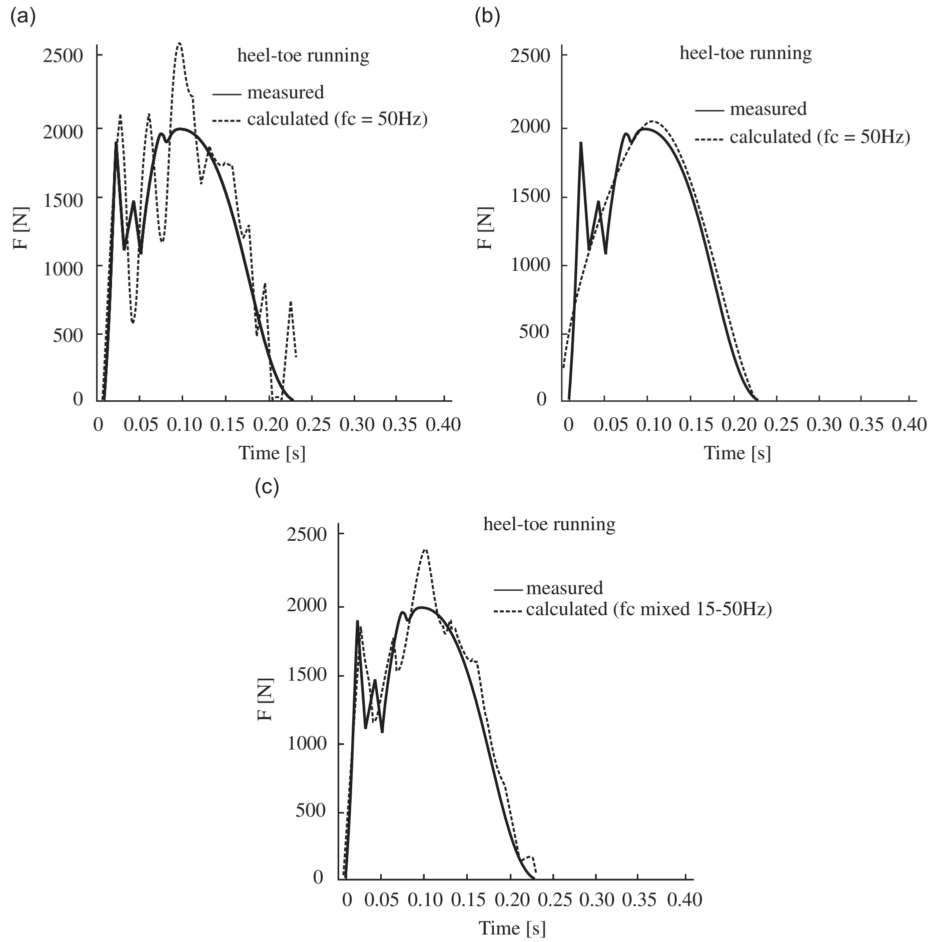

Fig. 42. Effect of lowering the low-pass cut off frequency on time histories of the vertical GRF calculated from positional data: (a) all marker position histories were filtered using; (b) they were filtered using; and (c) was 15 Hz for the markers on the HAT, 20 Hz for the hip markers, and 50 Hz for leg segments (after Bobbert et al. [271]).

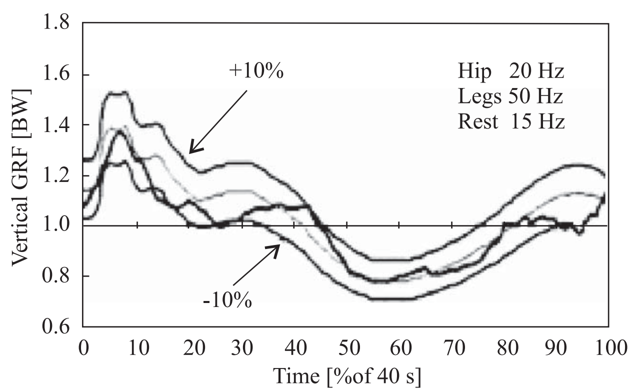

Fig. 43. Predicted GRF trace and 10 percent error bands placed on the actual trace (after Kerr [44]).

Contrary to common belief, it was found that human walking forces are not periodic but, as recently demonstrated [16], are narrow-band random phenomena. Therefore, they require experimental and analytical treatment similar to other random forces dynamically exciting civil engineering structures, such as wind, waves or earthquakes. Such comprehensive

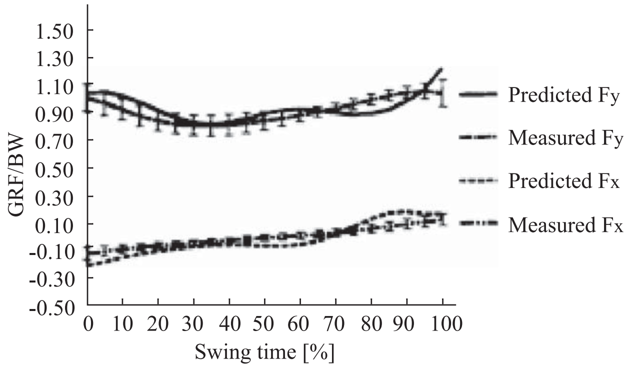

Fig. 44. Measured and predicted GRF based on optimization algorithm. F_x is antero-posterior, and F_y is vertical GRF (after Chou et al. [119]).

statistical and probabilistic treatment of moving human-induced excitation currently does not exist. Therefore, gathering a large number of time-varying records of walking forces, establishing a viable database of them and using it directly for various forms of probability-based dynamic calculations of real-life structures presents a timely opportunity to advance the whole field of vibration serviceability assessment of relevant structures.

It is now widely accepted that visual contact between people improves the degree of synchronization of individuals [76,169]. This is also the case if people are synchronized by prompting provided by metronome or music [169], or by perceptible movements of the structure they occupy [163,171,172]. Moreover, synchronization between people themselves becomes more likely in a dense crowd, since constrains in free body movement and possibility to see each other would subconsciously improve correlation of their pacing rates [168]. Unfortunately, there is no known mechanism that accounts for pedestrian synchronization in crowds.

In the case of light and slender civil engineering structures, pedestrian synchronization can further trigger perceptible structural vibrations and thereupon affect significantly pedestrian dynamic loading [163]. However, the dependency of the nature and magnitude of induced forces on the size of the active crowd and perceptible motion of the structure is currently not clear. Research achievements reported so far in this field have been found very fragmented and incoherent.

In experimental civil engineering dynamics, the present state-of-the-art facilities include equipment for direct measurement of the contact forces between pedestrians and a rigid laboratory floor comprising a force plate and an instrumented treadmill. Unfortunately, the artificial laboratory environment and constraints imposed by the direct measurement system (e.g. treadmill handrails or targeting footsteps on a force plate) can exert a strong influence on ability of humans to walk naturally and therefore may alter walking forces [26]. However, when dealing with issues like vibration serviceability of real full-scaled structures, there is a need to estimate walking loads applied directly by occupants under a wider range of conditions in their natural environments, such as office or a footbridge. Available data on pedestrian GRFs is conspicuously deficient in quantity, fullness, and extent, particularly for moving surfaces. Also, there is no convincing study on alteration in both vertical and lateral GRFs with structure motion.

The origin of dynamic human excitation is in motion of the body present on the structure. Recent development of the motion capture technology has resulted in several biomechanical studies designed to estimate contributions of various body segments to ground reaction forces [31,270,271]. Inverse procedures have been developed to measure indirectly human-induced forces from the motion of the body and information about distribution of body mass. When compared with the present international state-of-the-art, there are two key novel advances in this experimental approach:

(1) utilization of ‘free field’ measurement of three-component continuous walking forces without artificial restrictions imposed on human movement, and
(2) establishing a database of time-varying traces of walking forces to simulate dynamic response of real-life structures thereby assessing serviceability convincingly at the design stage. This can be done in a manner similar to using numerous existing earthquake and wind records to predict dynamic response of structures for which such dynamic excitations are relevant.

It will thus be possible to study areas of significant interest and uncertainty, specifically human–structure dynamic interaction and pedestrian coordination when walking on more or less perceptibly moving structures. Moreover, the so established database could be used to develop and calibrate a new generation of probability based pedestrian load models for groups whose development for individuals has already began [16,80].

Acknowledgements

The authors would like to acknowledge the financial support provided by the UK Engineering and Physical Sciences Research Council (EPSRC) for grant reference EP/E018734/1 ('Human Walking and Running Forces: Novel Experimental Characterization and Application in Civil Engineering Dynamics').

References

[1] S. Zivanovic, A. Pavic, P. Reynolds, Vibration serviceability of footbridges under human-induced excitation: a literature review, *Journal of Sound and Vibration* 279 (2005) 1–74.
[2] P. Reynolds, A. Pavic, Vibration performance of a large cantilever grandstand during an international football match, *ASCE Journal of Performance of Constructed Facilities* 20 (2006) 202–212.
[3] S.C. Kerr, N.W.M. Bishop, Human induced loading on flexible staircases, *Engineering Structures* 23 (2001) 37–45.
[4] A. Pavic, P. Reynolds, Vibration serviceability of long-span concrete building floors. Part 1: review of background information, *Shock and Vibration Digest* 34 (2002) 191–211.
[5] H. Bachmann, *Vibration Problems in Structures: Practical Guidelines*, Birkhäuser Verlag, Basel, Boston, Berlin, 1995.
[6] H. Bachmann, Vibration upgrading of gymnasia, dance halls and footbridges, *Structural Engineering International* 2 (1992) 118–124.
[7] H. Bachmann, W. Ammann, *Vibrations in Structures Induced by Man and Machines*, International Association of Bridge and Structural Engineering, Zürich, Switzerland, 1987.
[8] M.R. Willford, P. Young, Improved methodologies for the prediction of footfall-induced vibration, *Sixth European Conference on Structural Dynamics EURODYN*, Paris, France, September 2005.
[9] A. Pavic, M. Willford, Vibration serviceability of post-tensioned concrete floors, *Appendix G in Post-Tensioned Concrete Floors Design Handbook—Technical Report* 43, 2005, pp. 99–107.
[10] M.W. Whittle, Generation and attenuation of transient impulsive forces beneath the foot: a review, *Gait and Posture* 10 (1999) 264–275.
[11] S. Zivanovic, A. Pavic, P. Reynolds, Human–structure dynamic interaction in footbridges, *Proceedings of ICE, Bridge Engineering* 158 (2005) 165–177.
[12] M.J. Griffin, *Handbook of Human Vibration*, Academic Press, London, 1996.
[13] A. Forner Cordero, Human gait, stumble, and … fall? Mechanical Limitations in the Recovery from a Stumble, Ph.D. Thesis, University of Twente, Enschede, The Netherlands, 2003.
[14] A. McRobie, G. Morgenthal, J. Lasenby, M. Ringer, Section model tests on human–structure lock-in, *Bridge Engineering* 156 (2003) 71–79.
[15] R. Sachse, A. Pavic, P. Reynolds, Human–structure dynamic interaction in civil engineering dynamics: a literature review, *The Shock and Vibration Digest* 35 (2003) 3–18.
[16] J.M.W. Brownjohn, A. Pavic, P. Omenzetter, A spectral density approach for modelling continuous vertical forces on pedestrian structures due to walking, *Canadian Journal of Civil Engineering* 31 (2004) 65–77.
[17] C. Sahnaci, M. Kasperski, Excitation of buildings and pedestrian structures from walking and running, *Experimental Vibration Analysis for Civil Engineering Structures EVACES*, Porto, Portugal, October 2007.
[18] *Vicon Motion Systems Product Manuals*, Vicon Motion Systems, Oxford, UK, 2008.
[19] *Codamotion User Manuals*, Charnwood Dynamics Ltd., Leicestershire, UK, 2009.
[20] N. Messenger, Moving the human machine: understanding the mechanical characteristics of normal human walking, *Physics Education* 29 (1994) 352–357.
[21] R.B. Davis, S. Ounpuu, D. Tybursky, J.R. Gage, A gait analysis data collection and reduction technique, *Human Movement Science* 10 (1991) 575–578.
[22] E. Ayyappa, Words about words: the terminology of human walking, bipedal exchange, *Monograph of the American Academy of Orthotists and Prosthetists Gait Society*, Vol. 1–2, American Academy of Orthotists and Prosthetists Gait Society, Alexandria, USA, 1994.
[23] E. Ayyappa, Gait and pathomechanics syllabus, Certificate Program in Professional Development—Final Report, American Academy of Orthotists and Prosthetists Gait Society, 1996.
[24] S. Ounpuu, Terminology for clinical gait analysis, *Proceedings of North American Clinical Gait Lab Conference*, Portland, USA, April 1994.
[25] V.T. Inman, H.J. Ralston, F. Todd, *Human Walking*, Williams & Wilkins, Baltimore, USA, 1981.
[26] J. Perry, *Gait Analysis: Normal and Pathological Function*, Thorofare, New York, 1992.
[27] J. Rose, J.G. Gamble, *Human Walking*, Williams & Wilkins, Baltimore, USA, 1994.
[28] M.W. Whittle, *Gait Analysis: An Introduction*, Butterworth Heinemann, Edinburgh, 2004.
[29] E. Ayyappa, Normal human locomotion, part 1: basic concepts and terminology, *Journal of Prosthetics and Orthotics* 9 (1997) 1–10.
[30] M.P. Murray, Gait as a total pattern of movement, *American Journal of Physical Medicine* 46 (1967) 290–333.
[31] A.B. Thonrton-Trump, R. Daher, The prediction of reaction forces from gait data, *Journal of Biomechanics* 8 (1975) 173–178.
[32] F.R. Finley, K. Cody, R. Finizie, Locomotive characteristics of urban pedestrians, *Achieves of Physical Medicine and Rehabilitation* 51 (1970) 423–426.
[33] R. Seliktar, L. Bo, The theory of kinetic analysis in human gait, in: R.L. Craik, C.A. Oatis (Eds.), *Gait Analysis. Theory and Application*, Mosby, St. Louis, Missouri, USA, 1995, pp. 223–238.
[34] J. Hamill, W.S. Selbie, Three-dimensional kinetics, in: D.G.E. Robertson, D.W. Caldwell, J. Hamill, G. Kamen, S.N. Whittlesey (Eds.), *Research Methods in Biomechanics*, Human Kinetics, Champaign, IL, USA, 2004.
[35] F. Beely, Zur Mechanik des Stehens. Über die Bedeutung des Fussgewölbes beim Stehen, *Langenbecks Archiv für Klinische Chirurgie* 27 (1882) 457.
[36] D.J. Morton, *The Human Foot*, Columbia University Press, New York, 1935.
[37] E.J. Marey, *Le Mouvement*, Masson, Paris, 1894.
[38] J. Amar, Energetique biologique-Trottoir dynamographique, *French Academy of Sciences* 163 (1916) 132.
[39] W.O. Fenn, Direct determination of the work associated with changes in velocity of the body by means of a recording platform, *American Journal of Physiology* 93 (1930) 447–462.
[40] G. Caldwell, D.G.E. Robertson, S.N. Whittlesey, Forces and their measurement, in: D.G.E. Robertson, G.E. Caldwell, J. Hamill, S.N. Whittlesey (Eds.), *Research Methods in Biomechanics*, Human Kinetics, Champaign, IL, USA, 2004.
[41] F.C. Harper, The forces applied to the floor by the foot in walking, in: W.J. Warlow, B.L. Clarke (Eds.), Department of Scientific and Industrial Research (DSIR), HMSOr, 1961.
[42] F.W. Galbraith, M.V. Barton, Ground loading from footsteps, *Journal of Acoustic Society of America* 48 (1970) 1288–1292.
[43] S.V. Ohlsson, *Floor Vibrations and Human Discomfort*, Chalmers University of Technology, Göteborg, 1982.
[44] S.C. Kerr, Human Induced Loading on Staircases, Ph.D. Thesis, University College London, Mechanical Engineering Department, London, UK, 1998.
[45] J.E. Wheeler, Prediction and control of pedestrian induced vibration in footbridges, *Journal of the Structural Division ASCE* 108 (1982) 2045–2065.
[46] D.A. Winter, *Biomechanics and Motor Control of Human Movement*, John Wiley & Sons, Toronto, 1990.
[47] S.S. Hasan, M.A. Edmondstone, T.J. Limbird, R.G. Shiavi, S.W. Peterson, Reaction force patterns of injured and uninjured knees during walking and pivoting, *Journal of Electromyography and Kinesiology* 1 (1991) 218–228.
[48] G. Giakas, V. Bultzopoulos, A comparison of automatic filtering techniques applied to biomechanical walking data, *Journal of Biomechanics* 30 (1997) 847–850.

[49] S.R. Simon, I.L. Paul, J. Mansour, M. Munro, P.J. Abernethy, E.L. Radin, Peak dynamic force in human gait, *Journal of Biomechanics* 14 (1981) 817–822.
[50] J. Blanchard, B.L. Davies, J.W. Smith, Design criteria and analysis for dynamic loading of footbridges, *Proceedings of the DOE and DOT TRRL Symposium on Dynamic Behaviour of Bridges*, Crowthorne, UK, May 1977.
[51] J.H. Rainer, G. Pernica, D.E. Allen, Dynamic loading and response of footbridges, *Canadian Journal of Civil Engineering* 15 (1988) 66–71.
[52] S.A. Gard, S.C. Miff, A.D. Kuo, Comparison of kinematic and kinetic methods for computing the vertical motion of the body center of mass during walking, *Human Movement Science* 22 (2004) 597–610.
[53] F. Dierick, M. Penta, D. Renaut, C. Detrembleur, A force measuring treadmill in clinical gait analysis, *Gait and Posture* 20 (2004) 299–303.
[54] R. Kram, Force Treadmill for measuring vertical and horizontal ground reaction forces, *Journal of Applied Physiology* 85 (1998) 764–769.
[55] R. Kram, A.J. Powell, A treadmill-mounted force platform, *Journal of Applied Physiology* 67 (1989) 1692–1698.
[56] J.B. Dingwell, B.L. Davis, A rehabilitation treadmill with software for providing real-time gait analysis and visual feedback, *Journal of Biomechanical Engineering* 118 (1996) 253–255.
[57] G. Paolini, U. Della Croce, P.O. Riley, F.K. Newton, D.C. Kerrigan, Testing of a tri-instrumented-treadmill unit for kinetic analysis of locomotion tasks in static and dynamic loading conditions, *Medical Engineering & Physics* 29 (2007) 404–411.
[58] A. Belli, P. Bui, A. Berger, J.R. Lacour, A treadmill for measurements of ground reaction forces during walking, *The XVth Congress of the International Society of Biomechanics*, Jyväskylä, Finland, July 1995, pp. 100–101.
[59] A. Belli, P. Bui, A. Berger, A. Geyssant, J.R. Lacour, A treadmill ergometer for three-dimensional ground reaction forces measurement during walking, *Journal of Biomechanics* 34 (2001) 105–112.
[60] G.J. van Ingen Schenau, Some fundamental aspects of biomechanics of overground versus treadmill locomotion, *Medicine & Science in Sports & Exercise* 12 (1980) 257–261.
[61] W.C. Scott, H.J. Yack, C.A. Tucker, H.Y. Lin, Comparison of vertical ground reaction forces during overground and treadmill walking, *Medicine & Science in Sports & Exercise* 30 (1998) 1537–1542.
[62] J.B. Dingwell, J.P. Cusumano, P.R. Cavanagh, D. Sternad, Local dynamic stability versus kinematic variability of continuous overground and treadmill walking, *Journal of Biomechanical Engineering* 123 (2001) 27–32.
[63] R.C. Nelson, C.J. Dillman, P. Lagasse, P. Bickett, Biomechanics of overground versus treadmill running, *Medicine and Science in Sports* 4 (1972) 233–240.
[64] M. van de Putte, N. Hagemeister, N. St-Onge, G. Parent, J.A. de Guise, Habituation to treadmill walking, *Bio-Medical Materials and Engineering* 16 (2006) 43–52.
[65] P.O. Riley, G. Paolini, U. Della Croce, K.W. Paylo, D.C. Kerrigan, A kinematic and kinetic comparison of overground and treadmill walking in healthy subjects, *Gait and Posture* 26 (2007) 17–24.
[66] H.H. Savelberg, A.L. de Lange, Assessment of the horizontal, fore-aft component of the ground reaction force from insole pressure patterns by using artificial neural networks, *Clinical Biomechanics* 14 (1999) 585–592.
[67] A. Forner Cordero, H.J.F. Koopman, F.C.T. van der Helm, Use of pressure insoles to calculate the complete ground reaction forces, *Journal of Biomechanics* 37 (2004) 1427–1432.
[68] S. Barnett, J.L. Cunningham, S. West, A comparison of vertical force and temporal parameters produced by an in-shoe pressure measuring system and a force platform, *Clinical Biomechanics* 16 (2000) 353–357.
[69] M. Lord, Spatial resolution in plantar pressure measurement, *Medical Engineering and Physics* 19 (1997) 140–144.
[70] P.-E. Eriksson, Vibration of Low-Frequency Floors—Dynamic Forces and Response Prediction, Ph.D. Thesis, Chalmers University of Technology, Göteborg, Sweden, 1994.
[71] R.L. Pimentel, Vibrational Performance of Pedestrian Bridges Due to Human-Induced Loads, Ph.D. Thesis, University of Sheffield, UK, 1997.
[72] Y. Fujino, B.M. Pacheo, S.-I. Nakamura, P. Warnitchai, Synchronisation of human walking observed during lateral vibration of a congested pedestrian bridge, *Earthquake Engineering and Structural Dynamics* 22 (1993) 741–758.
[73] P. Dallard, A. Fitzpatrick, A. Flint, A. Low, R. Ridsll Smith, The Millennium Bridge, London: problems and solutions, *The Structural Engineer* 79 (2001) 15–17.
[74] P. Dziuba, G. Grillaud, O. Flamand, S. Sanquier, Y. Tetard, La passerelle Solferino: comportement dynamique (Solferino bridge: dynamic behaviour), *Bulletin Ouvrages Metalliques* (2001) 34–57.
[75] A. Ebrahimpour, R.L. Sack, W.N. Patten, A. Hamam, Experimental measurements of dynamic loads imposed by moving crowds, *Structures Congress* XII (1994) 1385–1390.
[76] A. Ebrahimpour, A. Hamam, R.L. Sack, W.N. Patten, Measuring and modelling dynamic loads imposed by moving crowds, *Journal of Structural Engineering* 122 (1996) 1468–1474.
[77] C.R. James, J.A. Herman, J.S. Dufek, B.T. Bates, Number of trials necessary to achieve performance stability of selected ground reaction force variables during landing, *Journal of Sports Science and Medicine* 6 (2007) 126–134.
[78] A. Pachi, T. Ji, Frequency and velocity of people walking, *The Structural Engineer* 83 (2005) 36–40.
[79] C. Sahnaci, M. Kasperski, Random loads induced by walking, *Sixth European Conference on Structural Dynamics EURODYN*, Paris, September 2005.
[80] S. Zivanovic, A. Pavic, P. Reynolds, Probability-based prediction of multi-mode vibration response to walking excitation, *Engineering Structures* 29 (2007) 942–954.
[81] J.E. Zachazewski, P.O. Riley, D.E. Krebs, Biomechanical analysis of body mass transfer during stair ascent and descent of healthy subjects, *Journal of Rehabilitation Research and Development* 30 (1993) 412–422.
[82] R. Riener, M. Rabufetti, C. Frigo, J. Quintern, G. Schmidb, Instrumented staircase for ground reaction measurement, *Medical and Biological Engineering and Computing* 37 (1999) 529.
[83] E. Savvidis, C.B. von der Decken, Forces acting on foot soles during stair climbing in healthy probands and in patients with coxarthrosis, *Biomedical Technology (Berlin)* 44 (1999) 98–103.
[84] K.A. Christina, P.R. Cavanagh, Ground reaction forces and frictional demands during stair descent: effects of age and illumination, *Gait and Posture* 15 (2002) 153–158.
[85] R. Riener, M. Rabufetti, C. Frigo, Stair ascent and descent at different inclinations, *Gait and Posture* 15 (2002) 32–44.
[86] A. Stacoff, C. Diezi, G. Luder, E. Stüssi, I.A. Kramers-de Quervain, Ground reaction forces on stairs: effects of stair inclination and age, *Gait and Posture* 21 (2005) 24–38.
[87] M.S. Redfern, J. DiPasquale, Biomechanics of descending ramps, *Gait and Posture* 6 (1997) 119–125.
[88] A.S. McIntosh, K.T. Beatty, L.N. Dwan, D.R. Vickers, Gait dynamics on an inclined walkway, *Journal of Biomechanics* 39 (2006) 2491–2502.
[89] A.D. Pizzimenti, F. Ricciardelli, Experimental evaluation of the dynamic lateral loading of footbridges by walking pedestrians, *Sixth European Conference on Structural Dynamics EURODYN*, Paris, France, September 2005.
[90] A. Ronnquist, *Pedestrian Induced Lateral Vibrations of Slender Footbridges*, Norwegian University of Science and Technology, Trondheim, Norway, 2005.
[91] T.A. McMahon, P.R. Greene, The influence of track compliance on running, *Journal of Biomechanics* 12 (1979) 893–904.
[92] S. Yao, J.R. Wright, A. Pavic, P. Reynolds, Experimental study of human-induced dynamic forces due to jumping on a perceptibly moving structure, *Journal of Sound and Vibration* 296 (2006) 150–165.
[93] C.T. Farley, Mechanism of leg stiffness adjustment for hopping on surfaces of different stiffnesses, *Journal of Applied Physiology* 85 (1998) 1044–1055.
[94] J.K. DeWitt, R.L. Cromwell, R.D. Hagan, The effect of manipulating subject mass on ground reaction force during locomotion, *American Society of Biomechanics Annual Meeting*, Blacksburg, USA, September 2006.

[95] M. Fritz, K. Peikenkamp, Simulation of the influence of surfaces on measured vertical ground reaction forces during fast movements, in: D. de Waard, K.A. Brookhuis, S.M. Sommer, W.B. Verwey (Eds.), *Human Factors in the Age of Virtual Reality*, Shaker Publishing, Maastricht, The Netherlands, 2003, pp. 233–235.
[96] K.J. Simpson, P. Jiang, Foot landing position during gait influences ground reaction forces, *Clinical Biomechanics* 14 (1999) 396–402.
[97] T.E. Clarke, E.C. Frederick, L.B. Cooper, Effect of shoe cushioning upon ground reaction forces in running, *International Journal of Sports Medicine* 4 (1983) 247–251.
[98] B.M. Nigg, S.M. Bahlsen, S.M. Luethi, S. Stokes, The influence of running velocity and midsole hardness on external impact forces in heel–toe running, *Journal of Biomechanics* 20 (1987) 951–959.
[99] M.A. Nurse, M. Hulliger, J.M. Wakeling, B.M. Nigg, D.J. Stefanyshyn, Changing the texture of footwear can alter gait patterns, *Journal of Electromyography and Kinesiology* 15 (2005) 496–506.
[100] T.A. McMahon, G. Valiant, E.C. Frederick, Groucho running, *Journal of Applied Physiology* 62 (1987) 2326–23337.
[101] J.E. Bertram, A. Ruina, Multiple walking speed-frequency relations are predicted by constrained optimization, *Journal of Theoretical Biology* 209 (2001) 445–453.
[102] T.P. Andriacchi, J.A. Ogle, J.O. Galante, Walking speed as a basis for normal and abnormal gait measurements, *Journal of Biomechanics* 10 (1977) 261–268.
[103] J. Hamill, S.L. McNiven, Reliability of selected ground reaction force parameters during walking, *Human Movement Science* 9 (1990) 117–131.
[104] T.S. Keller, A.M. Weisberger, J.L. Ray, S.S. Hasan, R.G. Shiavi, D.M. Spengler, Relationship between vertical ground reaction force and speed during walking, slow jogging, and running, *Clinical Biomechanics* 11 (1996) 253–259.
[105] P. DeVita, B.T. Bates, Intraday reliability of ground reaction force data, *Human Movement Science* 7 (1988) 73–85.
[106] J.M. Hausdorff, C.K. Peng, Z. Ladin, J.Y. Wei, A.L. Goldberger, Is walking a random walk? Evidence for long-range correlations in stride interval of human gait, *Journal of Applied Physiology* 78 (1995) 349–358.
[107] D.A. Winter, Kinematic and kinetic patterns in human gait: variability and compensating effects, *Human Movement Science* 3 (1984) 51–76.
[108] M.P. Kadaba, H.K. Ramakrishnan, M.E. Wootten, J. Gainey, G. Gorton, G.V. Cochran, Repeatability of kinematic, kinetic, and electromyographic data in normal adult gait, *Journal of Orthopaedic Research* 7 (1989) 849–860.
[109] T.M. Owings, M.D. Grabiner, Measuring step kinematic variability on an instrumented treadmill: how many steps are enough?, *Journal of Biomechanics* 36 (2003) 1215–1218.
[110] R. White, I. Agourisa, R.D. Selbie, M. Kirkpatrick, The variability of force platform data in normal and cerebral palsy, *Clinical Biomechanics* 14 (1999) 185–192.
[111] G. Giakas, V. Bultzopoulos, Time and frequency domain analysis of ground reaction forces during walking: an investigation of variability and symmetry, *Gait and Posture* 5 (1997) 189–197.
[112] R.F. Woolson, W.R. Clarke, *Statistical Methods for the Analysis of Biomedical Data*, John Wiley & Sons, Inc., New York, 2002.
[113] E.A. Haggard, *Intraclass Correlation and the Analysis of Variance*, Dryden Press, New York, 1958.
[114] B.T. Bates, L.R. Ostering, J.A. Sawhill, S.L. James, An assessment of subject variability, subject–shoe interaction, and the evaluation of running shoes using ground reaction force data, *Journal of Biomechanics* 16 (1983) 181–191.
[115] S.C. Wearing, S.R. Urry, J.E. Smeathers, The effect of visual targeting on ground reaction force and temporospatial parameters of gait, *Clinical Biomechanics* 15 (2000) 583–591.
[116] R. Rodano, R. Squadrone, Stability of selected lower limb joint kinetic parameters during vertical jump, *Journal of Applied Biomechanics* 18 (2002) 83–89.
[117] M.D. Grabiner, J.W. Feurebach, T.M. Lundin, B.L. Davis, Visual guidance to force plates does not influence ground reaction force variability, *Journal of Biomechanics* 28 (1995) 1115–1117.
[118] E.R.C. Draper, A treadmill-based system for measuring symmetry of gait, *Medical Engineering and Physics* 22 (2000) 215–222.
[119] L.S. Chou, S.M. Song, L.F. Draganich, Predicting the kinematics and kinetics of gait based on the optimum trajectory of the swing limb, *Journal of Biomechanics* 28 (1995) 377–385.
[120] M. Yamasaki, T. Sasaki, M. Torii, Sex difference in the pattern of lower limb movement during treadmill walking, *European Journal of Applied Physiology* 62 (1991) 103.
[121] N. Sekiya, H. Nagasaki, H. Ito, T. Furuna, Optimal walking in terms of variability in step length, *Journal of Orthopaedic and Sports Physical Therapy* 26 (1997) 266–272.
[122] K. Masani, M. Kouzaki, T. Fukunaga, Variability of ground reaction forces during treadmill walking, *Journal of Applied Physiology* 92 (2002) 1885–1890.
[123] H.J. Ralston, Energy-speed relation and optimal speed during level walking, *Internationale Zeitschrift für Angewandte Physiologie Einschliesslich Arbeitsphysiologie* 17 (1958) 277–283.
[124] M.P. Murray, R.C. Kory, B.H. Clarkson, S.B. Sepic, Comparison of free and fast speed walking patterns of normal men, *American Journal of Physical Medicine and Rehabilitation* 45 (1966) 8–24.
[125] J.B. Saunders, V.T. Inman, H.D. Eberhart, Major determinants in normal and pathological gait, *Journal of Bone and Joint Surgery* 35 (1953) 543–558.
[126] M. Willford, P. Young, C. Field, Predicting footfall-induced vibration: part 1, *Structures & Buildings* 160 (2007) 65–72.
[127] M. Willford, P. Young, C. Field, Predicting footfall-induced vibration: part 2, *Structures & Buildings* 160 (2007) 73–79.
[128] M. Willford, C. Field, P. Young, Improved methodologies for the prediction of footfall-induced vibration, *Architectural Engineering National Conference*, 2006.
[129] K. Baumann, H. Bachmann, *Dynamic Loads Caused by Humans and their Effect on Beam Structures*, Institute of Structural Engineering (IBK), Swiss Federal Institute of Technology (ETH), Zürich, Switzerland, 1988.
[130] H. Bachmann, *Vibration Problems in Structures*, Birkhäuser, Basel, Boston, Berlin, 1995.
[131] P. Young, Improved floor vibration prediction methodologies, *Proceedings of Arup Vibration Seminar on Engineering for Structural Vibration—Current Developments in Research and Practice*, London, UK, 2001.
[132] M. Willford, P. Young, *A Design Guide for Footfall Induced Vibrations of Structures*, The Concrete Centre, Slough, 2006.
[133] The Highway Engineering Division, *Ontario Highway Bridge Design Code*, The Highway Engineering Division, Ontario, Toronto, Canada, 1983.
[134] BSI, Steel, concrete and composite bridges. Part 2: specification for loads, *Appendix C: Vibration Serviceability Requirements for Foot and Cycle Track Bridges* (BS 5400: Part 2: 1978), British Standards Institution, London, 1978.
[135] B.R. Ellis, On the response of long-span floors to walking loads generated by individuals and crowds, *The Structural Engineer* 10 (2000) 17–25.
[136] B.R. Ellis, The influence of crowd size on floor vibrations induced by walking, *The Structural Engineer* 81 (2003) 20–27.
[137] G. Pernica, Dynamic load factors for pedestrian movements and rhythmic exercises, *Canadian Acoustics* 18 (1990) 3–18.
[138] D.E. Allen, Floor vibrations from aerobics, *Canadian Journal of Civil Engineering* 17 (1990) 771–779.
[139] M.R. Willford, An investigation into crowd-induced vertical dynamic loads using available measurements, *The Structural Engineer* 79 (2001) 21–25.
[140] Y. Matsumoto, T. Nishioka, H. Shiojiri, K. Matsuzaki, Dynamic design of footbridges, *IABSE Proceedings* (1978) 1–15.
[141] P. Dallard, T. Fitzpatrick, A. Flint, A. Low, R. Ridsdill Smith, M.R. Willford, M. Roche, London Millennium Bridge: pedestrian-induced lateral vibration, *ASCE Journal of Bridge Engineering* 6 (2001) 412–417.
[142] R.W. Clough, J. Penzien, *Dynamics of Structures*, McGraw-Hill, New York, 1993.
[143] Arup Consulting Engineers Ltd. 〈www.arup.com〉.
[144] H.S. Strogatz, *Nonlinear Dynamics and Chaos: With Applications to Physics, Biology, Chemistry and Engineering*, Westview Press, Cambridge, MA, USA, 2000.

[145] Y. Matsumoto, A study on dynamic design of pedestrian over-bridges, *Transaction of JSCE* 4 (1972) 50–51.
[146] S. Zivanovic, Probability-Based Estimation of Vibration for Pedestrian Structures due to Walking, Ph.D. Thesis, University of Sheffield, UK, 2006.
[147] D.W. Grieve, R.J. Gear, The relationships between length of stride, step frequency, time of swing and speed of walking for children and adults, *Ergonomics* 5 (1966) 379–399.
[148] L.A. Lamoreux, Kinematic measurements in the study of human walking, *Bulletin of Prosthetic Research* 10 (1971) 3–84.
[149] P. Rosenrot, J.C. Wall, J. Charteris, The relationship between velocity, stride time, support time and swing time during normal walking, *Journal of Human Movement Studies* 6 (1980) 323–335.
[150] J. Booyens, W.R. Keatinge, The expenditure of energy by men and women walking, *The Journal of Physiology* 138 (1957) 165–171.
[151] S. Hirokawa, Normal gait characteristics under temporal and distance constrains, *Journal of Biomedical Engineering* 11 (1989) 449–456.
[152] H.J. Ralston, Energetics of human walking, in: R.M. Herman, S. Grillner, P.S.G. Stein, D.G. Stuart (Eds.), *Neural Control of Locomotion*, Plenum Press, New York, 1976, pp. 77–98.
[153] J.M. Donelan, R. Kram, A.D. Kuo, Mechanical and metabolic determinants of the preferred step width in human walking, *Proceedings of the Royal Society B* 268 (2001) 1985–1992.
[154] A.D. Kuo, Energetics of actively powered locomotion using the simplest walking model, *Journal of Biomechanical Engineering* 124 (2002) 113–120.
[155] M. Srinivasan, A. Ruina, Computer optimisation of a minimal biped model discovers walking and running, *Nature* 439 (2006) 72–75.
[156] R. Margaria, *Biomechanics and Energetics of Muscular Exercise*, Clarendon, Oxford, 1977.
[157] A. Thorstensson, H. Robertson, Adaptations to changing speed in human locomotion: speed of transition between walking and running, *Acta Physiology Scandinavia* 131 (1987) 211–214.
[158] A.E. Minetti, L.P. Ardigo, F. Saibene, The transition between walking and running in humans: metabolical aspects at different gradients, *Acta Physiology Scandinavia* 150 (1994) 315–323.
[159] F.C. Anderson, M.G. Pandy, Dynamic optimisation of human walking, *Journal of Biomechanical Engineering* 123 (2001) 381–390.
[160] D.E. Newland, *An Introduction to Random Vibrations and Spectral Analysis*, Longman Group Ltd., Harlow, Essex, UK, 1993.
[161] W. Herzog, B.M. Nigg, L.J. Read, E. Olsson, Asymmetries in ground reaction force patterns in normal human gait, *Medicine and Science in Sports Exercise* 21 (1989) 110–114.
[162] H. Sadeghi, P. Paul Allard, F. Prince, H. Labelle, Symmetry and limb dominance in able-bodied gait: a review, *Gait and Posture* 12 (2000) 34–45.
[163] A. Fitzpatrick, P. Dallard, S. le Bourva, A. Low, R. Ridsill Smith, M. Willford, *Linking London: The Millennium Bridge*, The Royal Academy of Engineering, London, 2001.
[164] Setra, Guide méthodologique passerelles piétonnes (Technical guide Footbridges: assessment of vibrational behaviour of footbridges under pedestrian loading), Setra, 2006.
[165] A.L. Smith, S.J. Hicks, P.J. Devine, *Design of Floors for Vibration: A New Approach (SCI P354)*, SCI, Ascot, Berkshire, 2007.
[166] Eurocode BS EN 1990:2002—Basis of Structural Design, British Standard Institution, 2002.
[167] P. Dallard, A.J. Fitzpatrick, A. Flint, B.S. le, A. Low, R. Ridsdill Smith, M. Willford, The London Millennium footbridge, *The Structural Engineer* 79 (2001) 17–33.
[168] F. Ricciardelli, D. Pizzimenti, Lateral walking-induced forces on footbridges, *Journal of Bridge Engineering* 12 (2007) 677–688.
[169] A. Ebrahimpour, L.L. Fitts, Measuring coherency of human-induced rhythmic loads using flat force plates, *Journal of Structural Engineering (ASCE)* 122 (1996) 829–831.
[170] H. Bachmann, "Lively" footbridges—a real challenge, *International Conference on the Design and Dynamic Behaviour of Footbridges*, 2002.
[171] J.M.W. Brownjohn, P. Fok, M. Roche, P. Moyo, Long span steel pedestrian bridge at Singapore Changi Airport—part 1: prediction of vibration serviceability problems, *The Structural Engineer* 82 (2004) 21–27.
[172] J.M.W. Brownjohn, P. Fok, M. Roche, P. Omenzetter, Long span steel pedestrian bridge at Singapore Changi Airport—part 2: crowd loading tests and vibration mitigation measures, *The Structural Engineer* 82 (2004) 28–34.
[173] J.H.G. Macdonald, Pedestrian-induced vibrations of the Clifton suspension bridge, *Proceeding of the Institution of Civil Engineers, Structures and Buildings* 161 (2008) 69–77.
[174] E. Caetano, A. Cunha, C. Moutinho, Implementation of passive devices for vibration control at Coimbra footbridge, *Experimental Vibration Analysis for Civil Engineering Structures EVACES*, Porto, Portugal, October 2007, pp. 43–54.
[175] T.M. Roberts, Synchronised pedestrian excitation of footbridges, *Bridge Engineering* 156 (2003) 155–160.
[176] S.H. Strogatz, D.M. Abrams, A. McRobie, B. Eckhardt, E. Ott, Crowd synchrony on the Millennium Bridge, *Nature* 438 (2005) 43–44.
[177] A.N. Blekherman, Swaying of pedestrian bridges, *ASCE Journal of Bridge Engineering* 10 (2005) 142–150.
[178] G. Piccardo, F. Tubino, Parametric resonance of flexible footbridges under crowd-induced lateral excitation, *Journal of Sound and Vibration* 311 (2008) 353–371.
[179] S. Nakamura, Model for lateral excitation of footbridges by synchronous walking, *Journal of Structural Engineering* 130 (2004) 32–37.
[180] D.E. Newland, Pedestrian excitation of bridges, *Journal of Mechanical Engineering Science* 218 (2004) 477–492.
[181] T.M. Roberts, Lateral pedestrian excitation of footbridges, *ASCE Journal of Bridge Engineering* 10 (2005) 107–112.
[182] Y. Fujino, P. Warnitchai, B.M. Pacheco, An experimental and analytical study of autoparametric resonance in a 3 DOF model of a cable-stayed beam, *Nonlinear Dynamics* 4 (1993) 111–138.
[183] C. Barker, Some observations on the nature of the mechanism that drives the self-excited lateral response of footbridges, *International Conference on the Design and Dynamic Behaviour of Footbridges*, Paris, France.
[184] J.H.G. Macdonald, Lateral excitation of bridges by balancing pedestrians, *Proceedings of the Royal Society A* 16 (2008).
[185] M. Willford, Dynamic actions and reactions of pedestrians, *International Conference on the Design and Dynamic Behaviour of Footbridges*, Paris, 2002.
[186] Eurocode 5: Design of Timber Structures, 1995, pp. 1–6.
[187] D. E. Newland, Pedestrian excitation of bridges-recent results, *10th International Congress on Sound and Vibration*, Stockholm, Sweden, 2003.
[188] V.M. Zatsiorsky, *Kinematics of Human Motion*, Human Kinetics, Champaign, IL, USA, 1998.
[189] E.J. Marey, *Développement de la Methode Graphique Par L'emploi de la Photographie*, Masson, Paris, 1885.
[190] E. Muybridge, *Complete Human and Animal Locomotion*, Dover Publishers, New York, 1887.
[191] N. Bernstein, *The Co-ordination and Regulation of Movements*, Pergamon Press, New York, 1967.
[192] R.C. Johnson, G.L. Smidt, Measurement of hip joint motion during walking, *Journal of Bone and Joint Surgery* 15A (1969) 1083–1094.
[193] G.L. Kinzel, B.M. Hillberry, A.S. Hall, V. Sickle, W.M. Harvey, Measurement of the total motion between two body segments, II. Description of application, *Journal of Biomechanics* 5 (1972) 283–293.
[194] P.C. McLeod, D.B. Kettelkamp, V. Srinivasan, O.L. Henderson, Measurement of repetitive activities of the knee, *Journal of Biomechanics* 8 (1975) 369–373.
[195] Y.S. Chao, Justification of triaxial goniometer for the measurement of joint rotation, *Journal of Biomechanics* 13 (1980) 989–1006.
[196] G.L. Smidt, R.H. Deusinger, J. Arora, J.P. Albright, An automated accelerometry system for gait analysis, *Journal of Biomechanics* 10 (1977) 367–375.
[197] W.C. Hayes, J.D. Gran, M.L. Nagurka, J.M. Feldman, C. Oatis, Leg motion analysis during gait by multiaxial accelerometry: theoretical foundations and preliminary validations, *Journal of Biomechanical Engineering* 105 (1983) 283–289.
[198] R.E. Mayagoitia, A.V. Nene, P.H. Veltnik, Accelerometer and rate gyroscope measurement of kinematics: an inexpensive alternative to optical motion analysis systems, *Journal of Biomechanics* 35 (2002) 542.
[199] C-Motion, Inc. ⟨www.c-motion.com⟩, 2008.

[200] A. Cappozzo, A. Leardini, U. Della Croce, L. Chiari, Human movement analysis using stereophotogrammetry. Part 1: theoretical background, *Gait and Posture* 21 (2005) 186–196.
[201] D.G.E. Robertson, Body segment parameters, in: D.G.E. Robertson, G.E. Caldwell, J. Hamill, G. Kamen, S.N. Whittlesey (Eds.), *Research Methods in Biomechanics*, Human Kinetics, Champaign, IL, USA, 2004.
[202] W. Braune, O. Fischer, *The Human Gait*, Springer, Berlin, 1987.
[203] K.M. Taylor, F.M. Mottier, D.W. Simmons, W. Cohen, R. Pavlak Jr., D.P. Cornell, G.B. Hawkins, An automated motion measurement system for clinical gait analysis, *Journal of Biomechanics* 15 (1982) 505–516.
[204] G. Ferrigno, N.A. Borghese, A. Peddoti, Pattern-recognition in 3-D automatic human motion analysis, *ISPRS Journal of Photogrammetry and Remote Sensing* 45 (1990) 227–246.
[205] A. Esquenazi, B. Hiari, Assessment of gait and orthotic prescription, *Medicine and Rehabilitation Clinics of North America* 2 (1991) 473–485.
[206] H. Furnée, Real-time motion capture systems, in: P. Allard, A. Cappozzo, A. Lumberg, K. Vaughan (Eds.), *Three-dimensional Analysis of Human Locomotion*, Wiley, New York, 1997, pp. 85–108.
[207] L. Chiari, U. Della Croce, A. Leardini, A. Cappozzo, Human movement analysis using stereophotogrammetry. Part 2: instrumental errors, *Gait and Posture* 21 (2005) 197–211.
[208] V. Medved, *Measurement of Human Locomotion*, CRC Press, Boca Raton, 2001.
[209] E.L. Bontrager, Instrumented gait analysis systems, in: J.A. De Lisa (Ed.), *Gait Analysis in the Science of Rehabilitation*, Department of Veterans Affairs, Baltimore, 1998, pp. 11–32.
[210] A. Esquenazi, M. Talaty, Gait analysis: technology and clinical application, in: R.L. Braddom (Ed.), *Physical Medicine and Rehabilitation*, W. B. Saunders Company, Philadelphia, USA, 2000, pp. 93–108.
[211] Charnwood Dynamics Ltd. 〈http://www.charndyn.com/〉.
[212] A. Leardini, L. Chiari, U. Della Croce, A. Cappozzo, Human movement analysis using stereophotogrammetry. Part 3: soft tissue artifact assessment and compensation, *Gait and Posture* 21 (2005) 212–225.
[213] U. Della Croce, A. Leardini, L. Chiari, A. Cappozzo, Human movement analysis using stereophotogrammetry. Part 4: assessment of anatomical landmark misplacement and its effect on joint kinematics, *Gait and Posture* 21 (2005) 226–237.
[214] G. Wu, P.R. Cavanagh, ISB recommendations for standardization in the reporting of kinematic data, *Journal of Biomechanics* 28 (1995) 1257–1261.
[215] R. Baker, Gait analysis methods in rehabilitation, *Journal of Neuroengineering and Rehabilitation* 3 (2006).
[216] L. Lucchetti, A. Cappozzo, A. Cappello, U. Della Croce, Skin movement artefact assessment and compensation in the estimation of knee-joint kinematics, *Journal of Biomechanics* 31 (1998) 977–984.
[217] T.W. Lu, J.J. O'Connor, Bone position estimation from skin marker coordinates using global optimization with joint constraints, *Journal of Biomechanics* 32 (1999) 129–134.
[218] E. Alexander, T.P. Andriacchi, Correcting for deformation in skin-based marker systems, *Journal of Biomechanics* 34 (2001) 355–361.
[219] H. Hatze, The fundamental problem of myoskeletal inverse dynamics and its implications, *Journal of Biomechanics* 35 (2002) 109–115.
[220] J. Fuller, L.J. Liu, M.C. Murphy, R.W. Mann, A comparison of lower-extremity skeletal kinematics measured using skin- and pin-mounted markers, *Human Movement Science* 16 (1997) 242.
[221] C. Reinschmidt, A.J. vam den Bogert, A. Lundberg, B.M. Nigg, N. Murphy, A. Stacoff, A. Stano, Tibiofemoral and tibiocalcaneal motion during walking: external vs. skeletal markers. Gait posture, *Gait and Posture* 6 (1997) 98–109.
[222] A. Cappozzo, F. Cantani, A. Leardini, M.G. Benedetti, U. Della Croce, Position and orientation of bones during movement: experimental artefacts, *Clinical Biomechanics* 11 (1996) 90–100.
[223] M. Sati, J.A. de Guise, S. Larouche, G. Drouin, Quantitative assessment of skin-bone movement at the knee, *The Knee* 3 (1996) 121–138.
[224] S. Corazza, L. Mündermann, T. Andriacchi, Markerless motion capture methods for the estimation of human body kinematics, Valenciennes, France, 28–30 June.
[225] G. Moeslund, E. Granum, A survey of computer vision-based human motion capture, *Computer Vision and Image Understanding* 81 (2001) 231–268.
[226] L. Mündermann, S. Corazza, A.M. Chaudhari, T.P. Andriacchi, A. Sundstrand, R. Chellappa, Measuring human movement for biomechanical applications using markerless motion capture, *Proceedings of SPIE*, January 2006.
[227] L. Wang, W. Hu, T. Tan, Recent developments in human motion analysis, *Pattern Recognition* 36 (2003) 585–601.
[228] R. Drillis, R. Contini, M. Bluestein, *Body Segment Parameters: A Survey of Measurement Techniques, Selected Articles from Artificial Limbs*, Robert E. Krieger Publishing Co. Inc., New York, 1964.
[229] J.G. Reid, R.K. Jensen, Human body segment inertia parameters: a survey and status report, *Exercise and Sport Sciences Reviews* 18 (1990) 225–241.
[230] B.M. Nigg, W. Herzog, *Biomechanics of Musculo-Skeletal System*, John Wiley & Sons, Toronto, 1994.
[231] D.J. Pearsall, J.G. Reid, The study of human body segment parameters in biomechanics: an historical review and current status report, *Sports Medicine* 18 (1994) 126–140.
[232] E. Harless, Die statischen momente der menschlichen gliedmassen (The static moments of the component masses of the human body), *Abhandl Mathematische-Physikalischen Classe Konigl Bayerischen Akad Wissenschaft* 8 (1860) 69–96.
[233] W. Braune, O. Fisher, Über den Schwerpunkt des menschlichen Körpers, mit Rücksicht auf die Aüsrustung des deutschen Infanteristen (The center of gravity of the human body as related to the equipment of the German infantry), *Abhandlungen der mathematisch-physichen Klasse der Königlich-Sächsischen Gesellschaft der Wissenschaften* 26 (1889) 561–672.
[234] W.T. Dempster, *Space Requirements of the Seated Operator, Geometrical, Kinematic, and Mechanical Aspects of the Body with Special Reference to the Limbs*, Wright Air Development Centre, Wright-Petterson Air Force Base, Ohio, USA, 1955.
[235] G. Wu, F.C.T. van der Helm, H.E.J. Veeger DirkJan, M. Makhsouse, P. van Roy, C. Anglin, J. Nagels, A.R. Karduna, K. McQuadej, X. Wang, F.W. Werner, B. Buchhoz, ISB recommendation on definitions of joint coordinate systems of various joints for the reporting of human joint motion—part II: shoulder, elbow, wrist and hand, *Journal of Biomechanics* 38 (2005) 981–982.
[236] C.E. Clauser, J.T. McConville, J.W. Young, *Weight, Volume and Centre of Mass of Segments of the Human Body*, Aerospace Medical Research Laboratory, Wright-Petterson Air Force Base, Ohio, USA, 1969.
[237] C.L. Vaughan, B.L. Davis, J.C. O'Connor, *Dynamics of Human Gait*, Kiboho Publishers, Cape Town, 1999.
[238] M.R. Yeadon, M. Morlock, The appropriate use of regression equations for estimation of segmental inertia parameters, *Journal of Biomechanics* 22 (1989) 683–689.
[239] M. Mori, T. Yamamoto, Die Massenanteile der einzelnen Korperabschmitte der Japaner, *Acta Anatomica (Basel)* 37 (1959) 388.
[240] K. Fujikawa, The centre of gravity in the parts of the human body, *Okajimas Folia Anatomica Japonica* 39 (1963) 117–125.
[241] C.E. Whitsett, *Some Dynamic Response Characteristics of Weightless Man*, Aerospace Medical Research Laboratory, Wright-Petterson Air Force Base, Ohio, USA, 1963.
[242] E.P. Hanavan, *A Mathematical Model of the Human Body*, Aerospace Medical Research Laboratory, Wright-Petterson Air Force Base, Ohio, USA, 1964.
[243] R. Drillis, R. Contini, *Body Segment Parameters*, School of Engineering and Science, New York University, New York, 1966.
[244] H. Hatze, A mathematical model for the computational determination of parameter values of anthropometric segments, *Journal of Biomechanics* 13 (1980) 833–843.
[245] H. Hemami, F.C. Weimer, S.H. Koozekanani, Some aspects of the inverted pendulum problem for modelling locomotion systems, *IEEE Transactions on Automatic Control* 18 (1973) 658–661.
[246] R.K. Jensen, Estimation of the biomechanical properties of three body types using a photogrammetric method, *Journal of Biomechanics* 11 (1978) 349–358.
[247] R.K. Jensen, P. Fletcher, Distribution of mass to the segments of elderly males and females, *Journal of Biomechanics* 27 (1994) 89–96.

[248] R.K. Jensen, G. Nassas, Growth of segment principal moments between four and twenty years, *Medicine & Science in Sports & Exercise* 20 (1988) 594–604.
[249] H. Hatze, Parameter identification for human body segment models, *Theoretical Issues in Ergonomics Science* 6 (2005) 331–334.
[250] V. Zatsiorsky, V. Seluyanov, The mass and inertia characteristics of the main segments of the human body, in: H. Matsui, K. Kobayashi (Eds.), *Biomechanics VIII-B*, Human Kinetics, Champaign, IL, USA, 1983, pp. 1152–1159.
[251] P. De Leva, Joint center longitudinal position computed from a selected subset of Chandler's data, *Journal of Biomechanics* 29 (1996) 1231–1233.
[252] R. Dumas, L. Chèze, J.-P. Verriest, Adjustments to McConville et al. and Young et al. body segment inertial parameters, *Journal of Biomechanics* 40 (2006) 543–553.
[253] H.K. Huang, F.R. Suarez, Evaluation of cross-sectional geometry and mass density distributions of humans and laboratory animals using computerized tomography, *Journal of Biomechanics* 16 (1983) 821–832.
[254] H.K. Huang, S.C. Wu, The evaluation of the mass densities of the human body in vivo from CT scans, *Computers in Biology and Medicine* 6 (1976) 337–343.
[255] D.J. Pearsall, J.G. Reid, L.A. Livingston, Segmental inertial parameters of the human trunk as determined from computed tomography, *Annals of Biomedical Engineering* 24 (1996) 198–210.
[256] P.E. Martin, M. Mungiole, M.W. Marzke, J.M. Longhill, The use of magnetic resonance imaging for measuring segment inertial properties, *Journal of Biomechanics* 22 (1989) 367–376.
[257] M. Mungiole, P.E. Martin, Estimating segment inertial properties: comparison of magnetic resonance imaging with existing methods, *Journal of Biomechanics* 23 (1990) 1039–1046.
[258] R. Roubenoff, J.J. Kehayias, B. Dawson-Hughes, S.B. Heymsfield, Use of dual-energy X-ray absorbtiometry in body-composition studies: not yet a 'gold standard', *American Journal of Clinical Nutrition* 58 (1993) 589–591.
[259] O.L. Svendsen, J. Haarbo, C. Hassenger, C. Christiansen, Accuracy of measurements of body composition by dual energy X-ray absorptiometry in vivo, *American Journal of Clinical Nutrition* 57 (1993) 605–608.
[260] J.L. Durkin, J.J. Dowling, Analysis of body segment parameter differences between four human populations and the estimation errors of four popular mathematical models, *Journal of Biomechanical Engineering* 125 (2003) 515–522.
[261] J.L. Durkin, J.J. Dowling, Body segment parameter estimation of the human lower leg using an elliptical model with validation from DEXA, *Annals of Biomedical Engineering* 34 (2006) 1483–1493.
[262] J.L. Durkin, J.J. Dowling, D.M. Andrews, The measurement of body segment inertial parameters using dual energy X-ray absorptiometry, *Journal of Biomechanics* 32 (2002) 1575–1580.
[263] G.J. Ganley, C.M. Powers, Anthropometric parameters in children: a comparison of values obtained from dual energy X-ray absorptiometry and cadaver-based estimates, *Gait and Posture* 19 (2004) 133–140.
[264] H. Hatze, A. Bacca, Contact-free determination of human body segment parameters by means of videometric image processing of an anthropomorphic body model, *International SPIE Congress on Image Processing*, San Diego, USA.
[265] A. Bacca, Precise determination of anthropometric dimensions by means of image processing methods for estimating human body segment parameter values, *Journal of Biomechanics* 29 (1996) 563–567.
[266] S.N. Whittlesey, D.G.E. Robertson, Two-dimensional inverse dynamics, in: D.G.E. Robertson, G.E. Caldwell, J. Hamill, G. Kamen, S.N. Whittlesey (Eds.), *Research Methods in Biomechanics*, Human Kinetics, Champaign, IL, USA, 2004.
[267] B. Bresler, J.P. Frankel, The forces and moments in the leg during level walking, *Transactions of the American Society of Mechanical Engineers (ASME)* 72 (1950) 27–36.
[268] M.P. Murray, A.B. Drought, R.C. Kory, Walking patterns of normal man, *Journal of Bone and Joint Surgery (American ed)* 46 (1964) 335–360.
[269] D.M. Cunningham, *Components of floor reactions during walking*. Prosthetic Devices Research Project I.E.R. Rept. Ser. II Issue 14, University of California, Berkeley, USA, 1950.
[270] D.I. Miller, M.A. Nissinen, Critical examination of ground reaction force in the running forward Somersault, *International Journal of Sport Biomechanics* 3 (1987) 189–206.
[271] M.M. Bobbert, H.C. Schamhardt, B.M. Nigg, Calculation of vertical ground reaction force estimates during running from positional data, *Journal of Biomechanics* 24 (1991) 1095–1105.